

Electronic Thesis and Dissertation Repository

---

11-23-2020 2:30 PM

## Self-immolative Polymers as a Degradable and Triggerable Class of Surfactants

Siamak Keshtpour, *The University of Western Ontario*

Supervisor: Gillies, Elizabeth R., *The University of Western Ontario*

A thesis submitted in partial fulfillment of the requirements for the Master of Science degree in Chemistry

© Siamak Keshtpour 2020

Follow this and additional works at: <https://ir.lib.uwo.ca/etd>

 Part of the [Polymer Chemistry Commons](#)

---

### Recommended Citation

Keshtpour, Siamak, "Self-immolative Polymers as a Degradable and Triggerable Class of Surfactants" (2020). *Electronic Thesis and Dissertation Repository*. 7510.  
<https://ir.lib.uwo.ca/etd/7510>

This Dissertation/Thesis is brought to you for free and open access by Scholarship@Western. It has been accepted for inclusion in Electronic Thesis and Dissertation Repository by an authorized administrator of Scholarship@Western. For more information, please contact [wlsadmin@uwo.ca](mailto:wlsadmin@uwo.ca).

## Abstract

Self-immolative polymers (SIPs) are degradable polymers that undergo end-to-end depolymerization upon triggering. They have potential for the development of degradable surfactants addressing human and environmental toxicity concerns associated with non-degradable surfactants, but they have not yet been investigated as surfactants. Herein, polyglyoxylamide SIPs with different pendent groups and end-caps were synthesized, envisioning they could serve as depolymerizable analogues of poly(vinyl alcohol) and its derivatives. Polyglyoxylamides with pendent hydroxyls stabilized both PEA and PLA particle suspensions. They showed the potential to undergo triggered degradation, resulting in destabilization of the suspensions. However, untriggered suspensions exhibited poor long-term stability, so further structural tuning will be needed to optimize their properties for applications. Additionally, poly(ethylene glycol)-poly(ethyl glyoxylate) block copolymers were synthesized as potential emulsifiers of oil-in-water emulsions. Triggering depolymerization of the SIPs led to loss of emulsion stability, showing the promise of SIP block copolymers as a degradable and triggerable class of surfactants.

## Keywords

Self-immolative polymer, stimuli-responsive, degradation, depolymerization, polyglyoxylate, polyglyoxylamide, surfactant, emulsifying agent, emulsifier, particle preparation, poly(ester amide), poly(lactic acid).

## Summary for Lay Audience

Self-immolative polymers (SIPs) are a relatively recent class of degradable polymers that convert back to small molecules when exposed to stimuli such as heat, light, or reducing and oxidizing agents. They are of interest for a variety of applications.

Surfactants are molecules containing water-liking and oil-liking groups. They may solubilize a water-liking molecule in an organic (oil-liking) solvent or solubilize an oil-liking molecule in an aqueous (water-liking) solution. Surfactants have been widely used in a variety of areas such as agricultural, pharmaceutical, cosmetics, and food-processing industries.

It was envisioned that SIPs could serve as degradable versions of conventional non-degradable surfactants. This work investigates the properties of different SIPs as surfactants. The first class of synthesized SIP had a water-soluble group in its structure. Four different SIPs were investigated in this section, each with a specific speed of breakdown. The second class of synthesized SIP was attached to a water-soluble polymer, to make a polymer containing two different parts, a water-soluble and a water-insoluble parts. The synthesized SIPs were then used to prepare stable emulsions. Afterwards, they were exposed to the appropriate stimuli to investigate the effects of polymer breakdown on the stability of the emulsions. The breakdown of the SIPs led to changes in the stabilities of these systems.

## Co-Authorship Statement

The work described here is a result of a collaboration between the author, Prof. Elizabeth R. Gillies, and the individual contributions, as listed below.

Chapter one was written by the author and edited by Prof. Elizabeth R. Gillies.

Chapter two describes a study designed by the author and Prof. Elizabeth R. Gillies. Aneta Borecki and Dr. Xiaoli Liang carried out the SEC analyses. The PEA was synthesized by Dr. Ian Villamagna. **PEtG<sub>T</sub>**, **PEtG<sub>MMT</sub>**, and **PEtG<sub>AMT</sub>** were synthesized by Dr. Amir Rabiee Kenaree and Dr. Xiaoli Liang. All other experimentation was performed by the author. The chapter was written by the author and revised by Prof. Elizabeth R. Gillies.

Chapter 3, was written by the author and edited by Prof. Elizabeth R. Gillies.

## Acknowledgments

First, I would like to express my sincere gratitude and appreciation to my supervisor, Prof. Elizabeth R. Gillies for the great opportunity to be a member of her research group, her patience and continuous support throughout my program. Through Prof. Gillies guidance and during the past 2 years, I have become not only a better chemist but also a better person.

I want to also thank all the members of the Gillies group. Special thanks to Dr. Amir Rabiee Kenaree for his support and all the techniques he taught me during my first year. Thanks to Quinton Sirianni who was always helpful whenever I needed help.

I also want to express my gratitude to my committee members, Dr. James Wisner, Dr. Leonard Luyt, and Dr. Ying Zheng for taking the time to read my thesis and providing important and helpful feedback.

Thanks a lot to my best friend, Shayan Falah, who is always supportive and for all the fun and unforgettable memories we had during our graduate studies. Thanks to Afshion Marani and my great friends at Western university.

Last but not least, my wholehearted appreciation and gratitude to my parents and my brother, Babak. Thank you for always believing in me and your unconditional love. To my parents, you both have sacrificed a lot in your lives, so that I wouldn't have to sacrifice anything in mine. Everything I am today and everything I may become tomorrow, is for your sacrifices and support. You two are the best parents in the world. To my brother, Babak, my childhood has been special, my teenage years were joyously memorable, my grown-up years were unforgettable because I had you as my elder brother. I have never felt the need to ask for your help because you have always been there before I even had to ask. Thanks for being born.

# Table of Contents

Abstract.....	ii
Summary for Lay Audience.....	iv
Co-Authorship Statement.....	v
Acknowledgments.....	vi
Table of Contents.....	vii
List of Tables.....	x
List of Figures.....	xii
List of Schemes.....	xix
List of Appendices.....	xx
List of Abbreviations.....	xxii
Chapter 1.....	1
1 Introduction.....	1
1.1 Introduction to Polymers.....	1
1.1.1 Polymerization Mechanisms.....	2
1.1.2 Copolymers.....	3
1.1.3 Physical Properties of Polymers.....	4
1.1.4 Non-degradable Polymers.....	5
1.2 Degradable Polymers.....	5
1.2.1 Natural Degradable Polymers.....	6
1.2.2 Synthetic Degradable Polymers.....	7
1.2.3 Stimuli-responsive Degradable Polymers.....	7
1.3 Self-immolative Polymers (SIPs).....	8
1.3.1 Reversible SIPs.....	10
1.3.2 Polyglyoxylates (PGs).....	10

1.3.3	Polyglyoxylamides (PGAm)s .....	11
1.4	Surfactants.....	12
1.4.1	Classification and Applications of Surfactants .....	12
1.4.2	Hydrophilic-lipophilic Balance (HLB).....	16
1.4.3	Polymeric Surfactants .....	17
1.5	Thesis Scope and Objectives .....	20
Chapter 2	.....	22
2	Investigation of Polyglyoxylamides (PGAm)s and PEtG-based Block Copolymers as Degradable Surfactants .....	22
2.1	Experimental.....	22
2.1.1	General Materials and Procedures .....	22
2.1.2	General Methods.....	23
2.1.3	Synthetic Procedures.....	24
2.1.4	Degradation Studies of PGAm)s .....	31
2.1.5	Particle Suspension Preparation and Triggered Destabilization of the Suspensions.....	32
2.1.6	Oil-in-water and Water-in-oil Preparation and Triggered Destabilization of the Suspensions .....	33
2.2	Results and Discussion .....	34
2.2.1	Syntheses and Characterization of Poly(ethyl glyoxylate)s (PEtGs).....	34
2.2.2	Syntheses and Characterization of Polyglyoxylamides (PGAm)s.....	37
2.2.3	Reaction of PGAm <sub>UV</sub> with Acid Chlorides.....	38
2.2.4	Partially Acylated PGAm)s.....	39
2.2.5	Degradation Studies of PGAm)s .....	40
2.2.6	PGAm)s as Emulsifiers .....	43
2.2.7	Nile Red as a Probe for PEA Particle Aggregation .....	56



2.2.8 Oil-in-water and Water-in-oil Emulsions .....	68
2.2.9 Synthesis and Characterization of a Poly(ethylene glycol)- poly(ethyl glyoxylate) (PEG-PEtG) Block Copolymer.....	71
Chapter 3.....	78
3 Conclusions and Future Work.....	78
References.....	81
Appendices.....	94
Curriculum Vitae .....	103

## List of Tables

Table 2.1 SEC results of the synthesized PEtGs representing all four PEtGs had similar molar masses and relatively low dispersities. ....	35
Table 2.2 Targeted and actual conversions of partially acylated PGAMs. ....	40
Table 2.3 DLS results for PEA particle suspensions prepared using PGAM <sub>ac-5</sub> and PGAM <sub>ac-10</sub> as the emulsifying agents. Ratio of water:CH <sub>2</sub> Cl <sub>2</sub> was 3:1 (% V/V). The mass of PEA was fixed at 10 mg. ....	45
Table 2.4 DLS results for PEA particles prepared using PGAM <sub>ac-5</sub> and PGAM <sub>ac-10</sub> as the emulsifying agents. Ratio of water:CH <sub>2</sub> Cl <sub>2</sub> was 2:1 (% V/V). The mass of PEA was fixed at 10 mg. ....	46
Table 2.5 DLS results for PEA particle suspensions prepared at various ratios of water:CH <sub>2</sub> Cl <sub>2</sub> . The mass of PEA was fixed at 10 mg. ....	49
Table 2.6 DLS results for PEA particles prepared at two different ratios of emulsifying agent to PEA. ....	50
Table 2.7 DLS results for the particle suspensions prepared using PGAM <sub>T</sub> , PGAM <sub>MMT</sub> , and PGAM <sub>control</sub> as emulsifying agents. ....	52
Table 2.8 Preparation of oil-in-water emulsions at different concentrations of oil and PGAM <sub>UV</sub> . The volume of water was held constant at 3.0 mL. ....	69
Table 2.9 Preparation of toluene-in-water emulsions using different PGAMs. ....	70
Table 2.10 SEC results of PEG <sub>azide</sub> , PEtG <sub>AMT</sub> , and PEG-PEtG. The molar mass of PEG-PEtG is approximately the sum of the molar masses of PEtG <sub>AMT</sub> and PEG <sub>azide</sub> confirming the synthesis of PEG-PEtG. ....	73
Table 2.11 Preparation of water-in-toluene emulsions using PEG-PEtG as the emulsifier. ....	74

Table 2.12 Preparation of water-in-toluene emulsions using PEG-PEtG as the emulsifier.  
..... 76

## List of Figures

Figure 1.1 Global plastic consumption, from 1950 through 2015, measured in metric tonnes per year, showing the increase in plastic usage during the past few decades. <sup>9</sup> .....	2
Figure 1.2 Representation of (a) chain-growth and (b) step-growth polymerization. ....	3
Figure 1.3 Representation of a (a) homopolymer, (b) random copolymer, (c) alternating copolymer, (d) block copolymer, and (e) graft copolymer. X and Y represent the repeating units.....	4
Figure 1.4 Degradation of a polymer produces its starting monomer or other small molecules. ....	6
Figure 1.5 Various types of stimuli that can trigger the degradation of stimuli-responsive polymers.....	7
Figure 1.6 Chemical structures of pH-responsive polymers (a) poly(glutamic acid) and (b) poly(histidine). <sup>47</sup> .....	8
Figure 1.7 Depolymerization of SIPs. (a) The end-cap can be cleaved off of the polymer in the presence of a stimulus. (b) Removal of the end-cap results in end-to-end depolymerization. (c) The degradation products include the end-cap and small molecules. ....	9
Figure 1.8 (a) A reversible SIP depolymerizes to its starting monomers. (b) The depolymerization of the irreversible SIP results in products that differ from the starting monomers.....	10
Figure 1.9 Chemical structures of non-ionic surfactants (a) Triton X-100 (n= 9-10) (b) Cocodiethanolamide and (c) Tween 80 (w+x+y+z= 20). ....	14
Figure 1.10 Chemical structures of widely used cationic surfactants (a) hydroxyethyl laurdimonium chloride and (b) benzalkonium chloride, and anionic surfactants (c) ammonium lauryl sulfate solution and (d) sodium lauryl sulfate. ....	15

Figure 1.11 Schematic representation of a Gemini surfactant.....	15
Figure 1.12 Chemical structures of common amphiphilic diblock copolymers (a) PS- <i>b</i> -PAA (b) PCL- <i>b</i> -PAA and (c) PEO- <i>b</i> -PEtA.....	18
Figure 1.13 Chemical structure of PVA containing both acetate and alcohol groups.....	19
Figure 1.14 Chemical structures of (a) synthesized PGAMs as depolymerizable analogues of PVA and (b) synthesized PEtG-based block copolymers as depolymerizable analogues of surfactants such as PEO- <i>b</i> -PEA. ....	21
Figure 2.1 Comparison of the <sup>1</sup> H NMR spectra of (a) PEtG <sub>UV</sub> and (b) PGAM <sub>UV</sub> (400 MHz, CDCl <sub>3</sub> and D <sub>2</sub> O).....	36
Figure 2.2 Overlay of the FT-IR spectra of PEtG <sub>UV</sub> and PGAM <sub>UV</sub> . The peak around 1750 cm <sup>-1</sup> in PEtG <sub>UV</sub> spectrum disappears in the corresponding PGAM <sub>UV</sub> spectrum, and is instead replaced by the peaks around 1650 cm <sup>-1</sup> and 3300 cm <sup>-1</sup> .....	36
Figure 2.3 <sup>1</sup> H NMR spectra (400 MHz, D <sub>2</sub> O) of (a) PGAM <sub>ac-5</sub> and (b) PGAM <sub>ac-10</sub> .The conversions were calculated based on the peaks located at 2.1 ppm corresponding to the methyl protons on the acetyl group.....	40
Figure 2.4 An NMR spectral overlay (400 MHz, D <sub>2</sub> O) of the degradation of PGAM <sub>T</sub> at pH 7 as a representative sample of how degradation was monitored by <sup>1</sup> H NMR spectroscopy. ....	41
Figure 2.5 Degradation over time for (a) PGAM <sub>UV</sub> after 10, 20, 30, 45, and 60 minutes of irradiation with UV light (b) PGAM <sub>control</sub> at pH 7, pH 3 (citrate buffer), pH 3 (adjusted using acetic acid), and after 45 minutes of irradiation with UV light (c) PGAM <sub>T</sub> at pH 3 (citrate buffer) and 7 and (d) PGAM <sub>MMT</sub> at pH 3 (citrate buffer) and 7. ....	43
Figure 2.6 Structure of PEA that was used as the hydrophobic core for the preparation of particle suspensions. ....	44

Figure 2.7 Preparing PEA particle suspensions by the emulsification-evaporation method. (a) PGAm dissolved in water (b) organic phase containing PEA added to the first solution (c) solution subjected to sonication and then stirred for 4 hours to evaporate off CH<sub>2</sub>Cl<sub>2</sub> and (d) prepared particle suspensions by the emulsification-evaporation method. .... 44

Figure 2.8 Representative samples of how PEA particle suspensions were monitored qualitatively (a) unstable PEA particle suspensions (b) stable PEA particle suspensions. Stable particle suspensions were opaque and milky while unstable particles resulted in aggregation and eventually, sedimentation of PEAs. .... 46

Figure 2.9 Preliminary results of PEA particle suspensions using PGAm<sub>UV</sub> as the emulsifying agent. (a) DLS results and (b) the photo of the resulting suspension indicating the formation of PEA particles. .... 48

Figure 2.10 Representative samples of PEA particle suspensions from (a) experiment 1 (b) experiment 2 (c) experiment 3 and (d) experiment 4 in Table 2.6, showing that emulsions were effectively obtained for the 2:1,3:1, and 4:1 ratios but not for the 1:1 ratio. .... 50

Figure 2.11 (a) TEM image, (b) photo, and (c) DLS result of the PEA particle suspension that was prepared at the optimized conditions confirming the formation of PEA particles. .... 51

Figure 2.12 (a) size and (b) count rate results. DLS was conducted after particle preparation, 90 minutes of irradiation with UV light, and later on after 2.5 and 7 hours of the UV irradiation. No noticeable changes in the diameters were observed while increases in count rates were observed for all samples indicating that they were all likely aggregating. .... 54

Figure 2.13 Photos of PEA particle suspensions prepared using PGAm<sub>T</sub> as the emulsifying agent (a) after preparation (b) after the addition of buffer with pH 7 and (c) after the addition of buffer with pH 3. PEA particle suspensions prepared using PGAm<sub>MMT</sub> as the emulsifying agent (d) after preparation (e) after the addition of buffer with pH 7 and (f) after the addition of buffer with pH 3. Both sets of particles aggregated upon the addition of buffer. .... 55

Figure 2.14 DLS results for PEA particle suspensions prepared using PGAm<sub>control</sub>, PGAm<sub>T</sub>, and PGAm<sub>MMT</sub> as emulsifying agents. (a) Diameter and (b) count rate at pH 7; (c) diameter and (d) count rate at pH 3. Acetic acid (0.1 M) was added to adjust the pH values to 3. The PGAm<sub>MMT</sub> sample at pH 3 seemed to show the expected size increase followed by a decrease..... 56

Figure 2.15 Photos of PGAm-coated PEA particle suspensions using PGAm<sub>control</sub>, PGAm<sub>T</sub>, and PGAm<sub>MMT</sub> as their emulsifying agents. (a) PGAm<sub>control</sub> after preparation, (b) PGAm<sub>control</sub> after 2 days at pH 7, (c) PGAm<sub>control</sub> after 2 days at pH 3, (d) PGAm<sub>T</sub> after preparation, (e) PGAm<sub>T</sub> after 2 days at pH 7, (f) PGAm<sub>T</sub> after 2 days at pH 3, (g) PGAm<sub>MMT</sub> after preparation, (h) PGAm<sub>MMT</sub> after 2 days at pH 7, (i) PGAm<sub>MMT</sub> after 2 days at pH 3. Showing the destabilization of PGAm<sub>MMT</sub> coated PEA particle suspensions as a result of the degradation of PGAm<sub>MMT</sub>..... 58

Figure 2.16 Fluorescence intensity versus time for PGAm-coated PEA particles over time at (a) pH 7 and (b) pH 3 suggesting rapid destabilization and aggregation of the PGAm<sub>MMT</sub>-coated particle suspensions at pH 3. .... 59

Figure 2.17 DLS results for PEA particles after their preparation and over time. (a) Diameters of the particles at pH 7 (b) diameter of the particles at pH 3 (c) count rates of the particle suspensions at pH 7 and (d) count rates of the particle suspensions at pH 3. 59

Figure 2.18 Photos of PGAm-coated PEA particle suspensions (a) PGAm<sub>control-non-irrad</sub> after preparation, (b) PGAm<sub>control-non-irrad</sub> after 2 days, (c) PGAm<sub>UV-non-irrad</sub> after preparation, (d) PGAm<sub>UV-non-irrad</sub> after 2 days, (e) PGAm<sub>control-irrad</sub> after preparation, (f) PGAm<sub>control-irrad</sub> after 2 days, (g) PGAm<sub>UV-irrad</sub> after preparation, (h) PGAm<sub>UV-irrad</sub> after 2 days. No noticeable changes were observed except changes in the colours of particle suspensions after UV irradiation which was due to the photobleaching of Nile red during UV irradiation. .... 60

Figure 2.19 Fluorescence intensity versus time for PGAm-coated PEA particle suspensions. (a) Samples were kept in the dark and (b) samples irradiated with UV light for 90 minutes after their preparation, suggesting the photobleaching of Nile red during the 90 min of UV irradiation..... 61

Figure 2.20 DLS results for PGAm-coated PEA particle suspensions after their preparation and over 48 hours. (a) Diameter and (c) count rates for PGAm<sub>control-non-irrad</sub> and PGAm<sub>UV-non-irrad</sub>; (b) Diameter and (d) count rates for PGAm<sub>control-irrad</sub> and PGAm<sub>UV-irrad</sub>. Decreases in count rates were attribute to the general destabilization and sedimentation of the PEA particle suspensions. .... 62

Figure 2.21 Photos of PGAm-coated PLA particles: (a) PGAm<sub>control</sub> after preparation (b) PGAm<sub>control</sub> after 2 days at pH 7 (c) PGAm<sub>control</sub> after 2 days at pH 3 (d) PGAm<sub>T</sub> after preparation (e) PGAm<sub>T</sub> after 2 days at pH 7 (f) PGAm<sub>T</sub> after 2 days at pH 3 (g) PGAm<sub>MMT</sub> after preparation (h) PGAm<sub>MMT</sub> after 5 days at pH 7 (i) PGAm<sub>MMT</sub> after 2 days at pH 3. PGAm<sub>MMT</sub>-coated PLA particle suspensions showed the most destabilization at pH 3 as a result of the degradation of PGAm<sub>MMT</sub>..... 63

Figure 2.22 Fluorescence intensities of suspensions of Nile red-loaded PLA particles coated with PGAmS at (a) pH 7 and (b) pH 3 over 48 hours. Particle suspensions prepared using PGAm<sub>MMT</sub> at pH 3 underwent the most rapid decrease in fluorescence. .... 64

Figure 2.23 DLS results for suspensions of Nile red-loaded PLA particles coated with PGAmS over 48 hours. (a) Diameters and (c) count rates at pH 7, and (b) diameters and (d) count rates at pH 3. The large increase in count rates can likely be attributed to the gradual destabilization of the particles. PGAm<sub>MMT</sub>-coated particle suspensions at pH 3 underwent a rapid increase in particle diameter and a decrease in count rate due to the rapid degradation of PGAm<sub>MMT</sub> at pH 3. .... 65

Figure 2.24 Photos of PGAm-coated PLA particle suspensions: (a) PGAm<sub>control-non-irrad</sub> after preparation (b) PGAm<sub>control-non-irrad</sub> after 2 days (c) PGAm<sub>UV-non-irrad</sub> after preparation (d) PGAm<sub>UV-non-irrad</sub> after 2 days (e) PGAm<sub>control-irrad</sub> after preparation (f) PGAm<sub>control-irrad</sub> after 2 days (g) PGAm<sub>UV-irrad</sub> after preparation (h) PGAm<sub>UV-irrad</sub> after 2 days. No noticeable changes were observed except changes in the colours of particle suspensions after UV irradiation which was due to the photobleaching of Nile red during UV irradiation. .... 66

Figure 2.25 Fluorescence intensity versus time for PGAm-coated PLA particle suspensions. (a) Samples were kept in the dark and (b) samples irradiated with UV light



for 90 minutes after their preparation, suggesting the photobleaching of Nile red during the 90 min of UV irradiation..... 66

Figure 2.26 DLS results for suspensions of Nile red-loaded PLA particles coated with PGAMs over 48 hours. (a) Diameter and (c) count rates for PGAM<sub>control-non-irrad</sub> and PGAM<sub>UV-non-irrad</sub>, and (b) diameter and (d) count rates for PGAM<sub>control-irrad</sub> and PGAM<sub>UV-irrad</sub>. Increases in count rates were attribute to the general destabilization and sedimentation of the particle suspensions..... 67

Figure 2.27 Photos of emulsions described in Table 2.8 experiment (a) 1 (b) 2 (c) 3 (d) 4 (e) 5 (f) 6 and (g) 7 after preparation, experiment (h) 1 (i) 2 (j) 3 (k) 4 (l) 5 (m) 6 and (n) 7 after 15 hours, and experiment (o) 1 (p) 2 (q) 3 (r) 4 (s) 5 (t) 6 and (u) 7 after 2 days. All the emulsions started to show destabilization after 1 day..... 69

Figure 2.28 Photos of toluene-in-water emulsions after preparation using (a) PGAM<sub>control</sub> (b) PGAM<sub>UV</sub> (c) PGAM<sub>T</sub> (d) PGAM<sub>MMT</sub> (e) without an emulsifier, and after 6 hours (f) PGAM<sub>control</sub> (g) PGAM<sub>UV</sub> (h) PGAM<sub>T</sub> (i) PGAM<sub>MMT</sub> (j) without an emulsifier. All the emulsions started to show destabilization after 5-10 hours. The sample without emulsifier and sample using PGAM<sub>MMT</sub> showed the first and second destabilization rate as expected. .... 71

Figure 2.29 <sup>1</sup>H NMR spectrum of PEG-PEtG (400 MHz, CDCl<sub>3</sub>) confirming the synthesis of PEG-PEtG..... 73

Figure 2.30 Photos of water-in-toluene emulsions. Experiment 1 after (a) preparation (e) 3 days and (i) 5 days. Experiment 2 after (b) preparation (f) 3 days and (j) 5 days. Experiment 3 after (c) preparation (g) 3 days and (k) 5 days. Experiment 4 after (d) preparation (h) 6 hours and (l) 1 day, indicating the stability of prepared emulsions after days and showing the promise of PEG-PEtG as an emulsifier for such systems. .... 75

Figure 2.31 Photos of water-in-toluene emulsions. (a) After preparation (b) after 14 hours and (c) after 2 days. In photos, samples are arranged from experiment 1 to 8 (Table 2.12) from left to right. The emulsions were destabilized upon the addition of glacial acetic acid,

which triggered the depolymerization of the emulsifier, PEG-PEtG, while emulsions without glacial acetic acid remained stable and turbid over time. .... 77

## List of Schemes

Scheme 1.1 Depolymerization of PGs upon cleavage of the end-cap. ....	11
Scheme 1.2 Postpolymerization modification of PGs to synthesize PGAmS. ....	12
Scheme 2.1 Synthetic approaches for obtaining (a) PEtG <sub>control</sub> (b) PEtG <sub>UV</sub> (c) PEtG <sub>T</sub> and (d) PEtG <sub>MMT</sub> . ....	35
Scheme 2.2 Synthetic approaches for obtaining PGAmS via post-polymerization modifications of PEtGs. ....	37
Scheme 2.3 Acylation of PGAm <sub>UV</sub> with different acid chlorides. ....	38
Scheme 2.4 Syntheses of partially acylated PGAmS with different alkyl chain lengths. .	39
Scheme 2.5 General degradation scheme for PGAmS in D <sub>2</sub> O. The methine protons that were used to calculate the percent degradation by <sup>1</sup> H NMR spectroscopy are shown in blue. ....	41

## List of Appendices

Figure A1. $^1\text{H}$ NMR spectrum of PEtG <sub>control</sub> (400 MHz, $\text{CDCl}_3$ ).....	94
Figure A2. $^1\text{H}$ NMR spectrum of PEtG <sub>MMT</sub> (400 MHz, $\text{CDCl}_3$ ).....	94
Figure A3. $^1\text{H}$ NMR spectrum of PEtG <sub>UV</sub> (400 MHz, $\text{CDCl}_3$ ).....	95
Figure A4. $^1\text{H}$ NMR spectrum of PEtG <sub>T</sub> (400 MHz, $\text{CDCl}_3$ ).....	95
Figure A5. $^1\text{H}$ NMR spectrum of PGAm <sub>control</sub> (400 MHz, $\text{D}_2\text{O}$ ).....	96
Figure A6. $^1\text{H}$ NMR spectrum of PGAm <sub>MMT</sub> (400 MHz, DMSO).....	96
Figure A7. $^1\text{H}$ NMR spectrum of PGAm <sub>UV</sub> (400 MHz, $\text{D}_2\text{O}$ ).....	97
Figure A8. $^1\text{H}$ NMR spectrum of PGAm <sub>T</sub> (400 MHz, $\text{D}_2\text{O}$ ). Extra peaks at 3.3, 2.7, and 3.6 ppm denote residual methanol and ethanolamine signals.....	97
Figure A9. $^1\text{H}$ NMR spectrum of PGAm <sub>ac-100</sub> (400 MHz, $\text{D}_2\text{O}$ ). Extra peak at 3.3 ppm denotes residual methanol signal.....	98
Figure A10. $^1\text{H}$ NMR spectrum of PGAm <sub>buty-100</sub> (400 MHz, $\text{D}_2\text{O}$ ). Extra peak at 2.2 ppm denotes residual acetone signal.....	98
Figure A11. $^1\text{H}$ NMR spectrum of PGAm <sub>hex-100</sub> (400 MHz, $\text{D}_2\text{O}$ ).....	99
Figure A12. $^1\text{H}$ NMR spectrum of PGAm <sub>lau-100</sub> (400 MHz, $\text{D}_2\text{O}$ ). Extra peak at 2.2 ppm denotes residual acetone signal.....	99
Figure A13. $^1\text{H}$ NMR spectrum of PGAm <sub>ste-100</sub> (400 MHz, $\text{D}_2\text{O}$ ).....	100
Figure A14. $^1\text{H}$ NMR spectrum of PGAm <sub>hex-5</sub> (400 MHz, $\text{D}_2\text{O}$ ). Extra peaks at 2.2 and 3.3 ppm denote residual acetone and methanol signals.....	100
Figure A15. $^1\text{H}$ NMR spectrum of PGAm <sub>hex-10</sub> (400 MHz, $\text{D}_2\text{O}$ ). Extra peak at 3.3 ppm denotes residual methanol signal.....	101

Figure A16. $^1\text{H}$ NMR spectrum of PGAm <sub>1au-5</sub> (400 MHz, D <sub>2</sub> O). Extra peak at 3.3 ppm denotes residual methanol signal. ....	101
Figure A17. $^1\text{H}$ NMR spectrum of PGAm <sub>1au-10</sub> (400 MHz, D <sub>2</sub> O).....	102
Figure A18. $^1\text{H}$ NMR spectrum of PEtG <sub>AMT</sub> (400 MHz, CDCl <sub>3</sub> ). Extra peaks at 3.5 and 5.3 ppm denote residual methanol and dichloromethane signals. ....	102

## List of Abbreviations

ATR	Attenuated total reflectance
Bn	Benzyl
(TMS) <sub>2</sub> NLi	Bis(trimethylsilyl)amide
T <sub>c</sub>	Ceiling temperature
δ	Chemical shift (ppm)
J	Coupling constant
CMC	Critical micelle concentration
°C	Degrees Celsius
DP <sub>n</sub>	Degree of polymerization
<i>D</i>	Dispersity
DI	Deionized water
DMF	Dimethylformamide
DMSO	Dimethyl sulfoxide
DNA	Deoxyribonucleic acid
DLS	Dynamic light scattering
Et	Ethyl
EtG	Ethyl Glyoxylate
FT-IR	Fourier transform infrared spectroscopy
T <sub>g</sub>	Glass transition temperature
g	Grams
g/mol	Grams per mole
Hz	Hertz
h	Hours
HLB	Hydrophilic-lipophilic balance

kg/mol	Kilograms per mole
kCPS	Kilo counts per second
min	Minutes
$M_i$	Molar mass of polymer chain
mmol	Millimole
mol	Mole
MTT	4-monomethoxytrityl
MWCO	Molecular weight cut-off
$N_i$	Number of polymer chains with mass $M_i$
$M_n$	Number average molar mass
NMR	Nuclear magnetic resonance
O/W	Oil-in-water emulsion
PIT	Phase inversion temperature
PAA	Poly(acrylic acid)
PCL	Polycaprolactone
PEG	Poly(ethylene glycol)
PE	Polyethylene
PEG-PEtG	Poly(ethylene glycol)-poly(ethyl glyoxylate) block copolymer
PMMA	Poly(methyl methacrylate)
PDI	Polydispersity index
PEA	Poly(ester amide)
PEtG	Poly(ethyl glyoxylate)
PG	Polyglyoxylate
PGAm	Polyglyoxylamide

PLA	Poly(lactic acid)
PP	Polypropylene
PS	Polystyrene
PVA	Poly(vinyl alcohol)
PVC	Poly(vinyl chloride)
PVAc	Poly(vinyl acetate)
ppm	Parts per million
{ <sup>1</sup> H}	Proton decoupled
rpm	Rotations per minute
SIP	Self-immolative polymer
s	Singlet
SEC	Size exclusion chromatography
THF	Tetrahydrofuran
TEM	Transmission electron microscopy
UV	Ultraviolet
M <sub>w</sub>	Weight average molar mass
W/O	Water-in-oil emulsion
cm <sup>-1</sup>	Wavenumber



## Chapter 1

### 1 Introduction

#### 1.1 Introduction to Polymers

Polymers are macromolecules composed of large numbers of repeating units and prepared through the process of polymerization. Historically, the term polymer comes from the Greek words ‘poly’ meaning several and ‘meros’ meaning parts.<sup>1</sup> Polymers have been used for more than a thousand years and Ancient Mesoamerican peoples were processing rubber 3500 years ago.<sup>2</sup> They can be categorized into two groups: natural polymers and synthetic polymers. Natural polymers are found in nature. Cellulose, proteins, and carbohydrates are among natural polymers.<sup>3</sup> In 1962, Watson, Crick, and Wilkins were awarded the Nobel Prize in Medicine for their discoveries of the structure of deoxyribonucleic acid (DNA), a remarkable natural polymer which contains the instructions needed for an organism to develop, survive, and reproduce.<sup>4</sup> On the other hand, synthetic polymers are synthesized by scientists using various types of polymerization reactions. Both natural and synthetic polymers are widely used. They are employed in many areas such as medicine, communication, clothing, nutrition, and transportation.<sup>5</sup> Polystyrene, polyethylene, and Teflon are examples of widely used synthetic polymers with various applications in everyday life.<sup>6-8</sup> Plastics or “pliable and easily shaped” polymers are a group of common synthetic polymers. They have been used in various aspects of life which makes it unimaginable to live a life without them.<sup>9</sup> The rapid market growth of plastics increased solid waste plastics from less than 1% by mass in 1960 to more than 10% by 2005 in developed countries.<sup>10</sup> Plastics and other synthetic polymers are being extensively produced and used all over the world (**Figure 1.1**).<sup>9</sup> An increase in plastic usage in the future has also been predicted by scientists, and the accumulation of plastic waste in the environment has turned into a significant global concern.<sup>11</sup>

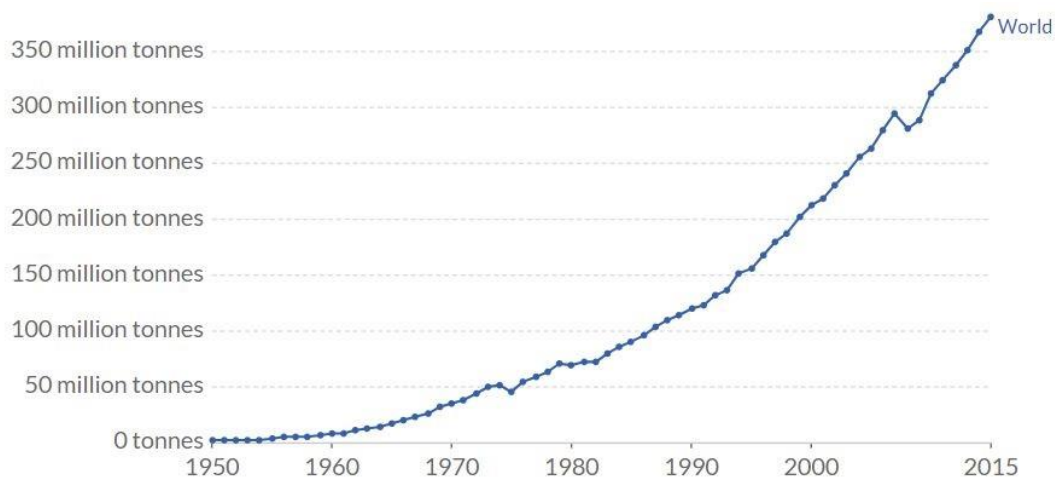


**Figure 1.1** Global plastic consumption, from 1950 through 2015, measured in metric tonnes per year, showing the increase in plastic usage during the past few decades.<sup>9</sup>

### 1.1.1 Polymerization Mechanisms

Polymerization reactions can be classified into two groups: step-growth or condensation polymerization, and chain-growth or addition polymerization. The main difference between the two polymerization approaches is the reaction between the repeating units that produce the polymer. In chain-growth polymerization, an initiator, usually a free radical or an ion, initiates the polymerization reaction by reacting with a repeating unit and turning it into an initiating species (**Figure 1.2a**). The active species later reacts with another repeating unit, and this process continues rapidly until the polymerization is terminated. In step-growth polymerization, the reaction proceeds by individual reactions of the functional groups between the monomers. During the reaction, dimers, trimers, tetramers and so on will be produced. This process continues until polymers with long chains are produced (**Figure 1.2b**).<sup>12</sup>

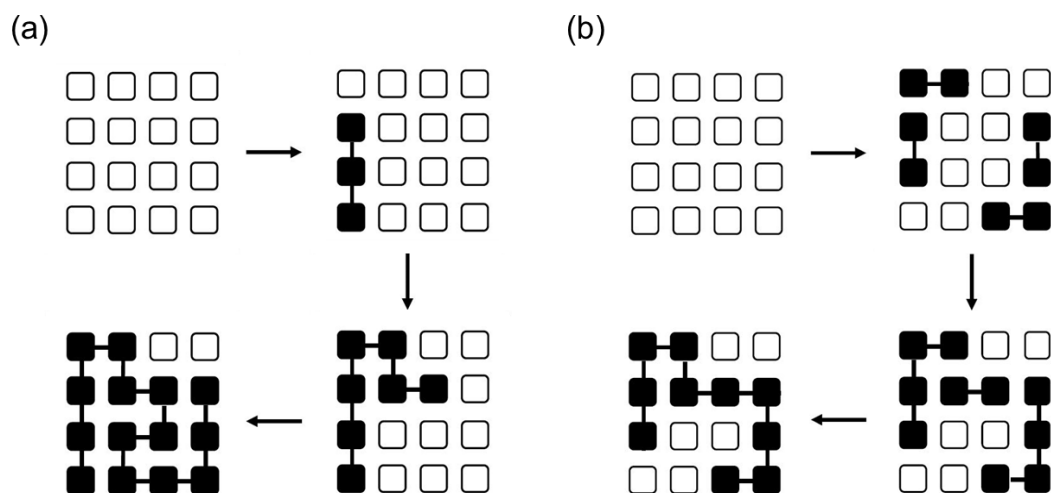


**Figure 1.2** Representation of (a) chain-growth and (b) step-growth polymerization.

### 1.1.2 Copolymers

Polymers may also be classified based on the number and the arrangement of different monomers in their structures. A copolymer is defined as a polymer that incorporates two or more types of monomers into the polymer chain through a process called copolymerization.<sup>13</sup> Its homopolymer counterpart is made up of one type of monomer. The properties of a copolymer rely on the nature of the monomers and their positioning in the polymer chain, allowing for multiple polymerization pathways.<sup>14</sup> The monomers can polymerize randomly, alternate, give blocks or one polymer may be grafted onto another one (**Figure 1.3**). By introducing another suitably chosen repeating unit, or by combining two or more desired types of monomers, a copolymer with desirable properties in a single structure may be formed. The copolymerization process offers the ability to produce an appropriate structure for an intended application.<sup>15</sup>

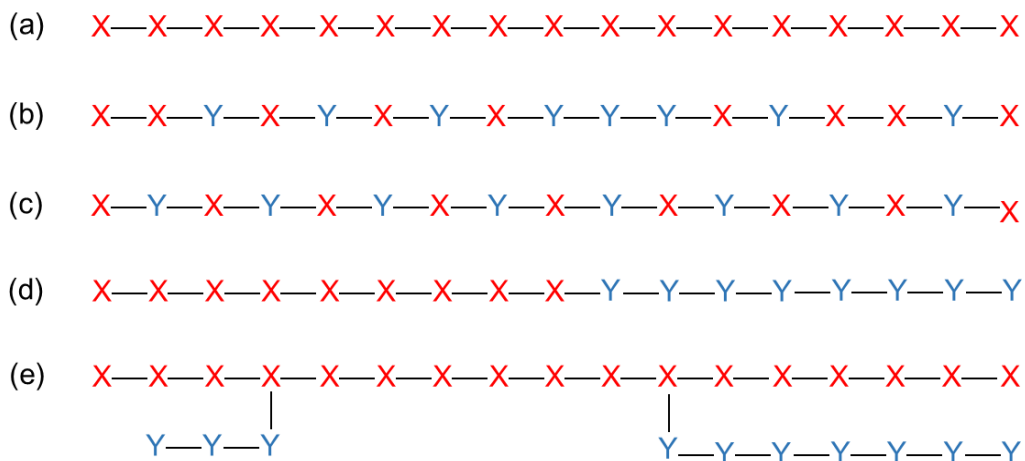


**Figure 1.3** Representation of a (a) homopolymer, (b) random copolymer, (c) alternating copolymer, (d) block copolymer, and (e) graft copolymer. X and Y represent the repeating units.

### 1.1.3 Physical Properties of Polymers

There are considerable differences between the physical properties of polymers and those of small molecules. Polymers generally have higher viscosities and may show enhanced mechanical properties over small molecules.<sup>16</sup>

Degree of polymerization ( $DP_n$ ) is defined as the number of repeating units in the polymer chain. Thus, the molecular weight of a polymer depends on both  $DP_n$  and the molecular weight of the repeating units. The molar mass of a polymer plays a significant role in determining the physical properties of the polymer. There are different ways to represent the molar mass of a polymer. Number-average molar mass is given by:

$$M_n = \frac{\sum N_i M_i}{\sum N_i} \quad \text{Equation 1-1}$$

Where  $N_i$  is the number of polymers having the molecular weight of  $M_i$ . The weight-average molar mass is described as:

$$M_w = \frac{\sum N_i M_i^2}{\sum N_i M_i} \quad \text{Equation 1-2}$$

The ratio of the weight-average molar mass to the number-average molar mass is called dispersity ( $\mathcal{D}$ ) which is an indication of the variation within a polymer sample in terms of molecular weights. The value of  $\mathcal{D}$  is equal to or greater than 1, and as the value becomes closer to 1, the polymer chains approach the same length.

$$\mathcal{D} = \frac{M_w}{M_n} \quad \text{Equation 1-3}$$

### 1.1.4 Non-degradable Polymers

There is not an exact definition for non-degradable polymers as all polymers will be degraded eventually with the passage of time. However, non-degradable polymers may be generally defined as polymers that will not entirely breakdown long after the time they are meant to be used. For instance, poly(vinyl chloride) (PVC) is a polymer that has been considered as non-degradable and has been used in many areas such as construction.<sup>17</sup> PVC does not entirely degrade for decades. Polyethylene (PE), polypropylene (PP), and polystyrene (PS) are other examples of non-degradable polymers that are widely used. Non-degradable polymers mostly have carbon-carbon bonds along their backbones, which resist many severe conditions.

Aside from disadvantages and environmental issues associated with non-degradable polymers, they could be of interest in areas that require the polymer to be stable to carry out its role during a long period of time. In one study, a non-degradable methacrylate-based polymer was used in dental resins.<sup>18</sup>

## 1.2 Degradable Polymers

Unlike non-degradable polymers, degradable polymers exhibit instability which can also be of interest in many areas. The degradation can be achieved by physical, chemical, mechanical or biological agents.<sup>19</sup> Their degradation manner relies on their structure and the presence of functional groups along their backbones or end-caps. During the degradation process, the polymer breaks down, which results in the production of the starting monomers or other small molecules (**Figure 1.4**).

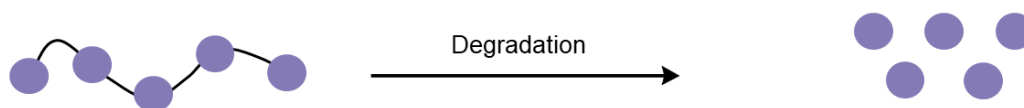


**Figure 1.4** Degradation of a polymer produces its starting monomer or other small molecules.

Recently, there has been increasing interest in degradable polymers. Degradable polymers are of substantial interest for many biological applications such as drug delivery<sup>20-22</sup>, sensors<sup>23-24</sup>, and tissue engineering.<sup>25</sup> Furthermore, degradable polymers provide more environmentally-friendly alternatives than non-degradable polymers.<sup>26-28</sup> Regardless of being a synthetic or natural, all degradable polymers possess functional groups such as esters or amides that can be cleaved during the degradation process. However, synthetic degradable polymers can in some cases be advantageous compared to natural degradable polymers as their structures and properties can be readily tuned. Ideally, a degradable polymer would stay stable during application and soon after its intended purpose would degrade.

### 1.2.1 Natural Degradable Polymers

A portion of natural polymers undergo gradual degradation. In most cases, these polymers produce natural byproducts such as water and carbon dioxide upon degradation. Polysaccharides are among the useful natural polymers for applications such as drug delivery.<sup>29</sup> They are polymers formed from monosaccharide repeating units covalently bound together by glycosidic linkages.<sup>30</sup> They are considered as vital polymers for living organisms. In one study, natural polysaccharides were used as drug carriers to deliver 5-amino salicylic acid for localized treatment of inflammatory bowel disease. The polysaccharides remained intact in the stomach, however, they degraded in the environment of the colon. Therefore, the drug was released when the polysaccharides entered the colon.<sup>31</sup> Additionally, polysaccharides have inherently low immunogenicity which ranks them among the most appropriate degradable polymers for biological applications.<sup>29</sup> Some examples of common polysaccharides are cellulose, starch, alginic acid, chitosan, hyaluronic acid, and chondroitin sulphate.<sup>32</sup>

## 1.2.2 Synthetic Degradable Polymers

Synthetic degradable polymers allow for human intervention to fit specific applications. For example, the degradation rate and triggering can be manipulated. Synthetic degradable polymers have extensively been used in various fields such as drug delivery,<sup>33</sup> tissue engineering,<sup>34</sup> and gene delivery.<sup>35</sup> Poly(lactic acid) (PLA) and polycaprolactone (PCL) are among the widely used conventional degradable polymers. PLA is a biodegradable polymer and is mostly used as packaging material and disposable tableware.<sup>36</sup> PCL is a biodegradable polyester exhibiting chemical and solvent resistance features with potential biomedical applications<sup>37</sup> and is also widely used in the food industry.<sup>38</sup>

## 1.2.3 Stimuli-responsive Degradable Polymers

As the usage and applications of degradable polymers progressively increase, interest in controlling polymer degradation increases. Stimuli-responsive polymers are a class of polymers that are able to react, sense, and respond to an external environment with changes in their properties. They are called stimuli-sensitive and smart or intelligent polymers.<sup>39-41</sup> Stimuli-responsive polymers can be sensitive to several factors and their degradation can be triggered by changes in physical or chemical conditions.<sup>42</sup> There are various types of stimuli that can trigger the degradation of stimuli-responsive polymers (**Figure 1.5**).<sup>43</sup>

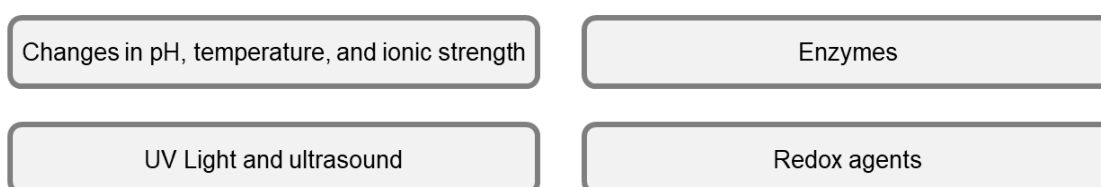


**Figure 1.5** Various types of stimuli that can trigger the degradation of stimuli-responsive polymers.

pH-responsive polymers are able to change their structure or cleave off their pH-sensitive bonds or groups as a result of changes in pH. These changes can be useful in drug delivery systems wherein the changes in the structure of the polymer can result in the release of loaded drugs for example. Based on the pH of the targeted organ, a suitable pH-responsive

polymer can be designed to release the drug at its intended target pathological conditions.<sup>44-</sup>  
<sup>45</sup> For instance, the pH of tumor extracellular sites and inflammatory tissues is slightly acidic as opposed to the slightly basic pH in blood circulation and normal tissues.<sup>46</sup> Two examples of common pH-responsive polymers are poly(glutamic acid) (**Figure 1.6a**) which has pendent carboxylic acid groups, and poly(histidine) (**Figure 1.6b**) which has imidazole pendent groups.<sup>47</sup> The acidic and basic groups in poly(glutamic acid) and poly(histidine) are prone to deprotonation and protonation upon exposure to basic or acidic conditions. Each of these two polymers has shown promising results for pH-triggered drug release.<sup>48-49</sup>

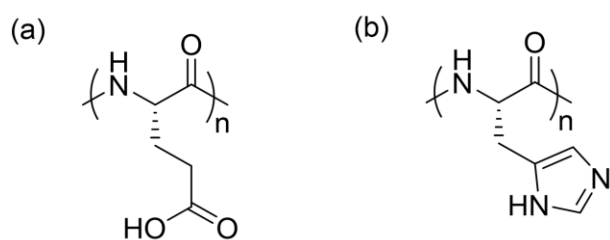


**Figure 1.6** Chemical structures of pH-responsive polymers (a) poly(glutamic acid) and (b) poly(histidine).<sup>47</sup>

Stimuli-responsive polymers undergo degradation upon exposure to specific external stimuli. The major drawback is that they require many stimuli-mediated cleavage events to achieve full degradation. This requirement is not cost-effective and most importantly, may not be feasible in natural or *in vivo* environments.

### 1.3 Self-immolative Polymers (SIPs)

Self-immolative polymers (SIPs) are a relatively recent class of stimuli-responsive polymers that undergo controlled end-to-end depolymerization upon exposure to a stimulus that cleaves the end-cap from the polymer (**Figure 1.7**).<sup>24, 50-52</sup> SIPs combine the characteristics of both stimuli-responsive and degradable polymers. Different end-caps that are sensitive to heat,<sup>53</sup> light,<sup>20</sup> and reducing or oxidizing agents<sup>54-55</sup> have been explored and incorporated onto SIPs to enable depolymerization in response to different stimuli. Furthermore, their unique degradation mechanism allows scientists to select the desired stimulus easily by changing the end-cap.



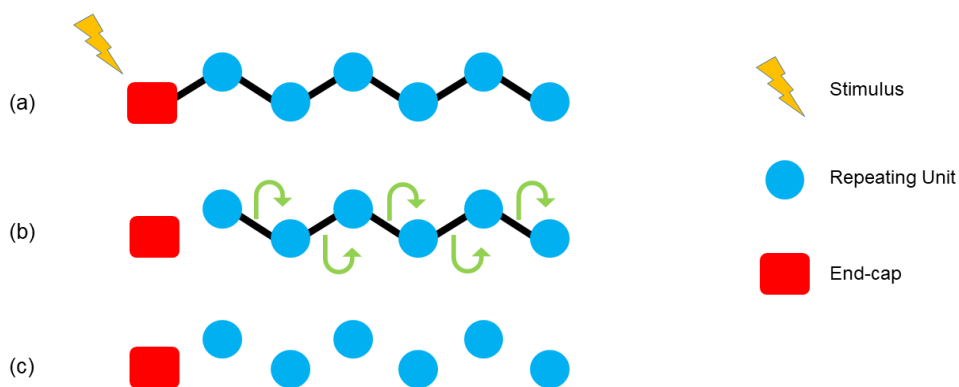


**Figure 1.7** Depolymerization of SIPs. (a) The end-cap can be cleaved off of the polymer in the presence of a stimulus. (b) Removal of the end-cap results in end-to-end depolymerization. (c) The degradation products include the end-cap and small molecules.

SIPs have the capability to undergo a complete end-to-end depolymerization as a consequence of a single bond cleavage by a stimulus (**Figure 1.7**). Since the introduction of SIPs, various backbones have been investigated. The most widely used backbones are polycarbamates,<sup>56-57</sup> polyethers,<sup>58</sup> polyphthalaldehydes,<sup>59-60</sup> polycarbonates,<sup>61</sup> and polyglyoxylates.<sup>62-63</sup> Generally, depolymerizable SIP backbones can be classified as reversible or irreversible backbones. After the depolymerization of reversible SIPs, the starting monomers are produced which makes the repolymerization reaction possible, at least theoretically (**Figure 1.8a**). On the contrary, the depolymerization of the irreversible SIPs produces products that differ from the starting monomers which prevents potential repolymerization (**Figure 1.8b**).<sup>64</sup>

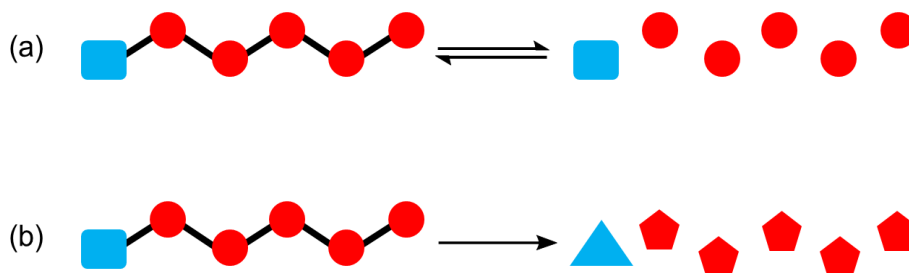


**Figure 1.8** (a) A reversible SIP depolymerizes to its starting monomers. (b) The depolymerization of the irreversible SIP results in products that differ from the starting monomers.

### 1.3.1 Reversible SIPs

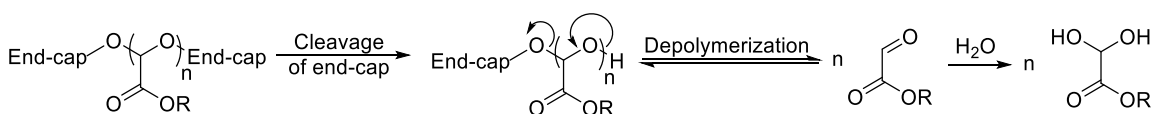
Reversible SIPs are a class of SIPs with low ceiling temperatures ( $T_c$ ),  $T_c$  is the temperature at which the rates of depolymerization and polymerization are equal. Above the ceiling temperature, the depolymerization reaction is thermodynamically favourable and polymers of high molar mass are not produced.<sup>65</sup> At the ceiling temperature, the free energy change ( $\Delta G$ ) = 0 for the polymerization reaction, and  $T_c = \Delta H/\Delta S$ , where H is enthalpy and S is entropy. To prevent the depolymerization at temperatures above the  $T_c$ , polymers that are synthesized below the  $T_c$  need to be capped. This feature enables reversible SIPs to be recyclable as depolymerization can occur by cleavage of the end-cap. The most widely used classes of reversible SIPs are poly(benzyl ether)s,<sup>58, 66</sup> polyglyoxylates,<sup>62,63</sup> polyphthalaldehydes,<sup>59,60, 67</sup> and polyglyoxylamides.<sup>68</sup>

### 1.3.2 Polyglyoxylates (PGs)

PGs are a potentially versatile group of polyaldehydes with low  $T_c$ . To access and benefit from PGs with different properties, various types of glyoxylate monomers such as methyl glyoxylate, ethyl glyoxylate, n-butyl glyoxylate, and benzyl glyoxylate can be used during the polymerization process.<sup>63</sup> Ethyl glyoxylate is commercially available as a solution in toluene and other glyoxylate monomers can be synthesized.<sup>63, 69</sup>

In 2014, by introducing stimuli-responsive end-caps to PGs, their controlled end-to-end depolymerization was achieved by the Gillies group.<sup>63</sup> It was shown that the molar masses

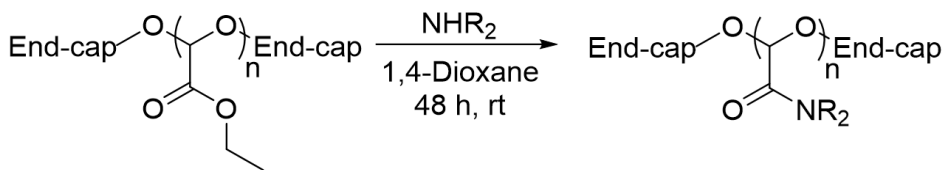
of PGs is highly dependent on the purity of the monomer as the polymerization could be initiated by ethyl glyoxylate hydrate. A new purification process was developed by the Gillies group to prepare highly pure ethyl glyoxylate to control the  $DP_n$  of the synthesized poly(ethyl glyoxylate)s (PEtGs).<sup>70</sup> In this method, glyoxylate monomers were purified by thermal distillation over  $P_2O_5$ . With the optimized purification process, higher  $DP_n$ s of PGs are achievable. PGs degrade gradually, ultimately resulting in corresponding alcohols and glyoxylic acid hydrate (**Scheme 1.1**).<sup>71</sup> They are of interest for applications such as agriculture,<sup>72</sup> drug delivery,<sup>69, 73-74</sup> and smart coatings.<sup>62, 75</sup> PEtGs are of particular interest as their degradation produces glyoxylic acid hydrate and ethanol.<sup>71, 76</sup> These degradation products can be metabolized in the environment and were confirmed nontoxic in a *Caenorhabditis elegans* model.<sup>77</sup>



**Scheme 1.1** Depolymerization of PGs upon cleavage of the end-cap.

### 1.3.3 Polyglyoxylamides (PGAMs)

Due to the presence of ester groups at each of the repeating units of PGs, which increases the hydrophobicity of the polymer, all of the synthesized PGs have been insoluble in water.<sup>63, 69, 78</sup> This lack of water-solubility can limit the applications of PGs where water-soluble polymers are required. By replacing the ester pendent groups of PGs with more hydrophilic groups, such as amides, a water-soluble SIP can be formed. In comparison to the starting PGs, PGAMs should also exhibit decreased rates of side chain hydrolysis and therefore be more stable in the absence of the degradation stimulus. PGAMs also differ from the original PGs in physical and thermal properties, such as glass transition temperature ( $T_g$ ).<sup>63, 68</sup> Therefore, PGAMs can be classified as a new class of reversible SIPs that are synthesized via postpolymerization modification of PGs (**Scheme 1.2**). However, the synthesis is limited to PGs with end-caps that are stable to the amidation reaction.



**Scheme 1.2** Postpolymerization modification of PGs to synthesize PGAMs.

## 1.4 Surfactants

SURFace ACTive AgeNTs (SURFACTANTS) are amphipathic molecules containing both hydrophilic and hydrophobic moieties with the ability to stabilize interfaces.<sup>79</sup> For instance, regular soaps have carboxylate groups as their hydrophilic component with affinity for water and hydrocarbon chains as their hydrophobic part that have an affinity for lipophilic molecules. Surfactants can serve as effective emulsifiers, dispersing, and foaming agents.<sup>80</sup> They lower the surface tension between two immiscible liquids or a liquid and a gas. They may solubilize a polar molecule in an organic (non-polar) solvent or solubilize a non-polar molecule in an aqueous (polar) solution. Surfactants have been widely used in a variety of areas such as agricultural,<sup>81</sup> cosmetics,<sup>82</sup> pharmaceutical,<sup>83-84</sup> and food-processing industries.<sup>85-86</sup> The efficiency of a surfactant can be determined by its ability to lower surface tension and stabilize emulsions.<sup>79</sup>

In an emulsion, surfactants are at a higher concentration at the surface than in the bulk of a liquid. This characteristic of surfactants is known as adsorption.<sup>87</sup> Critical micelle concentration (CMC) is the concentration of a surfactant above which micelles form as a result of the aggregation of surfactant molecules. At the CMC, monolayer adsorption is complete and surface-active properties are at optimum.<sup>88-89</sup> Under the CMC, modifications in concentration of the surfactant greatly change the surface tension while at concentrations above the CMC, such changes are not significant.

### 1.4.1 Classification and Applications of Surfactants

Surfactants can be classified in various ways. They can be categorized into natural and synthetic surfactants which is a classification based on their origin. Natural surfactants are obtained directly from natural sources. The very first time that natural surfactants were

used by humanity can be dated back to Egyptian times, when vegetable and animal oil were combined with alkaline salts producing a soap that was used for cleaning and treating skin diseases.<sup>90</sup> Mostly, natural surfactants are biological compounds obtained from different animal and vegetable sources. Sugars and amino acids are common examples of surfactant hydrophilic moieties of natural origin.<sup>91</sup> In contrast, synthetic molecules such as sodium laurel sulfate, alcohol ether sulphates, and poly(vinyl alcohol) are of synthetic origin.<sup>79</sup> Synthetic surfactants are advantageous compared to natural surfactants as they allow for human design and manipulation.

Generally, the hydrophobic parts of surfactants consist of long chain of hydrocarbons while hydrophilic parts consist of ionic or non-ionic polar groups. Based on the presence or absence of charges in surfactants, they can be categorized into non-ionic and ionic surfactants. Non-ionic surfactants do not dissociate into ions upon dissolution in organic or aqueous solutions. Triton X-100, Cocodiethanolamide, and Tween 80 are among the widely used non-ionic surfactants (**Figure 1.9**).<sup>92-94</sup>

The sizes of surfactant micelles mostly depend on the structure and concentration of the surfactant, as well as the temperature of the solution. Additionally, non-ionic surfactants usually have lower CMC values compared to ionic surfactants due to the strong electrostatic repulsion of the hydrophilic groups in ionic surfactants which makes the micellization process more difficult.<sup>92</sup>

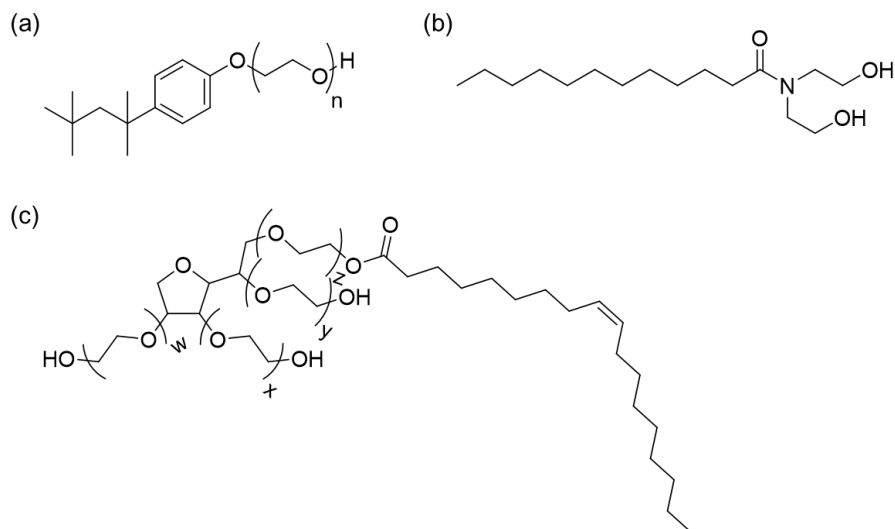


**Figure 1.9** Chemical structures of non-ionic surfactants (a) Triton X-100 ( $n= 9-10$ ) (b) Cocodiethanolamide and (c) Tween 80 ( $w+x+y+z= 20$ ).

Ionic surfactants have negatively or positively charged hydrophilic groups and can be further classified into cationic and anionic surfactants. Cationic surfactants have positively charged hydrophilic groups such as quaternary ammonium ion ( $-R_4N^+$ ) and other ammonium ions. Hydroxyethyl laurdimonium chloride and benzalkonium chloride (**Figure 1.10a** and **b**) are examples of widely used cationic surfactants.<sup>95</sup> Anionic surfactants have negatively charged hydrophilic groups such as carboxylate ( $-COO^-$ ), sulfonate ( $SO_3^-$ ), sulfate ( $-OSO_3^-$ ), and phosphate ( $-OPO_3^{2-}$ ). Ammonium lauryl sulfate solution and sodium lauryl sulfate (**Figure 1.10c** and **d**) are examples of widely used anionic surfactants. Ionic surfactants are quite popular for their applications in detergents, personal care products, and soaps.<sup>96</sup>

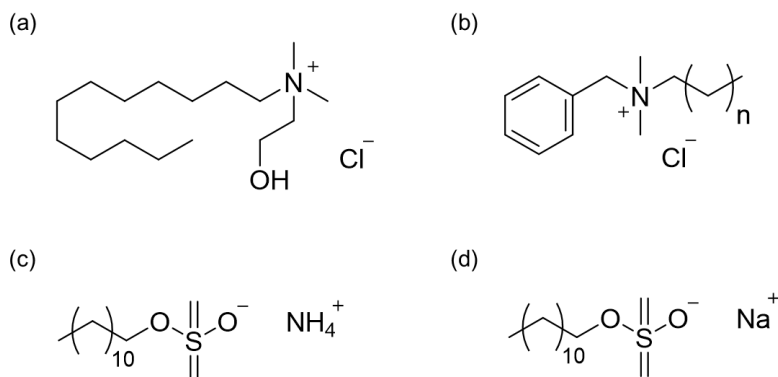


**Figure 1.10** Chemical structures of widely used cationic surfactants (a) hydroxyethyl laurdimonium chloride and (b) benzalkonium chloride, and anionic surfactants (c) ammonium lauryl sulfate solution and (d) sodium lauryl sulfate.

Gemini surfactants are another group of surfactants that emerged in the late 1980s. Most conventional surfactants have a single hydrophilic head and a single hydrophobic tail while Gemini surfactants have at least two hydrophilic groups and two hydrophobic tails that are linked by a spacer group (**Figure 1.11**). Characteristics and features of Gemini surfactants depend on not only the hydrophilic and hydrophobic parts but also on the spacer linker. These linker structures allow for the synthesis of different surfactants, each with particular features, while hydrophobic and hydrophilic groups remain the same.<sup>97</sup> Gemini surfactants have a number of advantages over conventional surfactants, namely low CMC values and increased surface activity.

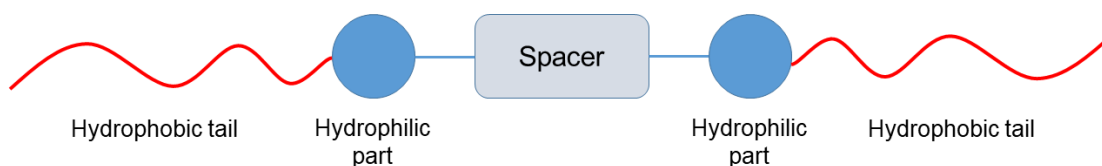


**Figure 1.11** Schematic representation of a Gemini surfactant.

In the food industry, natural surfactants such as lecithin are used to prepare a large number of food products such as mayonnaise and salad creams.<sup>98</sup> Additionally, synthetic surfactants such as sorbitan esters, their ethoxylates, and sucrose esters are extensively used in many food products such as butter, margarine, mayonnaise, coffee creamers, cream liqueurs, some juices, and in whippable toppings.<sup>99-101</sup>

Emulsions consist of two phases, wherein the dispersed phase exists as droplets dispersed within the continuous phase. The diameters of droplets usually vary from 10 nm to 100  $\mu\text{m}$ . There are two main classes of emulsions, oil-in-water (O/W) and water-in-oil (W/O) emulsions. In oil-in-water emulsions, oil droplets are emulsified and suspended in the aqueous phase. Mayonnaise, cream liqueur, whippable toppings, and ice creams are examples of oil-in-water emulsions. The second type is water-in-oil emulsions in which oil and water reverse roles with water taking on the dispersive phase. Butter, margarine, and fat-based products are examples of water-in-oil emulsions in the food industry.<sup>102-103</sup>

In cosmetics, surfactants are used for cleansing, foaming, thickening, emulsifying, solubilizing, penetration enhancement, and antimicrobial effects. Sophorolipids, rhamnolipids, and mannosylerythritol lipids are among the widely used glycolipid surfactants in cosmetics.<sup>104-105</sup>

Over the past several decades, surfactants have also been of interest to the pharmaceutical industry. They have been used mostly as drug carriers and targeting systems. In the application of surfactants as drug carriers, they have no role in the biodistribution of the drug itself, but are used primarily for drug solubilization. For instance, many non-ionic and ionic surfactants have been examined for preparing stable suspensions of insoluble or poorly water-soluble drugs for oral or intravenous administration.<sup>83, 106</sup> On the other hand, surfactants as targeting systems can transport the drug to its intended site either by natural biodistribution of the carrier or by incorporating specific ligands onto the carrier to deliver the drug to its target.<sup>107-109</sup> Targeted drug delivery has the advantage of reducing the side effects of the drug while delivering the drug at the target site.

#### 1.4.2 Hydrophilic-lipophilic Balance (HLB)

HLB is a dimensionless scale representing the ratio of weight percent of the hydrophilic moiety to the hydrophobic moiety.<sup>110</sup> HLB values typically range from 0 to 20 for non-ionic surfactants on an increasing scale from least hydrophilic (0) to most hydrophilic (20). Surfactants with low values of HLB (<9), lipophilic surfactants, are suitable for the formation of water-in-oil emulsions while those with high values (>11), hydrophilic surfactants, are suitable for oil-in-water emulsions.<sup>111</sup> Ionic surfactants usually have HLB



values higher than 20. If the HLB value for a surfactant is unknown, it could be measured experimentally using other surfactants with known HLB values.<sup>112</sup> Nevertheless, these methods are time consuming and require a large quantity of the surfactant.<sup>113</sup> It is also possible to theoretically calculate the HLB value through the Griffin method giving an approximate number for HLB.  $M_H$  and  $M_T$  correspond to the molar mass of hydrophilic part and the molar mass of the whole molecule, respectively.<sup>110, 114</sup> However, the HLB values of ionic surfactants or surfactants with complicated structures cannot be determined using the Griffin method, which limits the applicability of this equation.

$$\text{HLB}_{\text{Griffin}} = \frac{M_H}{M_T} * 20 \quad \text{Equation 1-4}$$

Davies and coworkers also introduced an equation that takes into consideration the effect of commonly used chemical functional groups.  $H_{h,i}$  and  $H_{l,i}$  correspond to the hydrophilic and lipophilic parts respectively. The values of common chemical functional groups in the equation 1-5 are reported in Shinoda and Friberg reports.<sup>115</sup>

$$\text{HLB}_{\text{Davies}} = 7 + \sum H_{h,i} - \sum H_{l,i} \quad \text{Equation 1-5}$$

The HLB value indicates the emulsifying characteristics of the surfactant and not necessarily its effectiveness. This means that there could be a difference in the efficiency of different emulsifiers with the same HLB value for any given system. The HLB values also alter with temperature as the solubility of the surfactant changes with temperature. The phase inversion temperature (PIT) is defined as the temperature at which surfactant changes from stabilizing oil-in-water to water-in-oil and vice versa.<sup>116</sup>

### 1.4.3 Polymeric Surfactants

Polymeric surfactants provide more complex structures in comparison to the low molecular weight surfactants and offer a wider range of functionalities. They can possess a number

of different hydrophilic and hydrophobic moieties along their backbones or pendent groups at the same time.<sup>117</sup> Polymeric surfactants can be classified into homopolymers and copolymers. Generally, homopolymers are the simplest group of polymeric surfactants as they are composed of the same repeating units along the chain. Hydrophilic-hydrophobic diblock and multi-block copolymers are a major group of polymeric surfactants in which both hydrophilic and hydrophobic blocks can be tuned.<sup>118-119</sup> Many groups have reported the synthesis and use of polymeric surfactants. In one study, the synthesis of copolymers having octadecyl side chains and carboxylic acid groups along the backbone were reported as latex stabilizers.<sup>120</sup>

Poly(ethylene oxide) (PEO), poly(acrylic acid) (PAA), poly(styrene sulfonate) (PSS), and poly(dimethyl acrylamide) (PDMAAm) are among the typical hydrophilic blocks used for designing polymeric surfactants, and poly(lactic acid) (PLA), poly(isobutylene) (PIB), poly(propylene oxide) (PPO), and poly(butadiene) (PB) are among common hydrophobic blocks used in polymeric surfactants.<sup>121</sup> Polystyrene-*b*-poly(acrylic acid) (PS-*b*-PAA) (**Figure 1.12a**), poly(caprolactone)-*b*-poly(acrylic acid) (PCL-*b*-PAA) (**Figure 1.12b**), and poly(ethylene oxide)-*b*-poly(ethyl acrylate) (PEO-*b*-PEtA) (**Figure 1.12c**) are examples of amphiphilic diblock copolymers that were used in preparation of polymer micelles, and their self-assembling properties were studied.<sup>117, 122-123</sup>

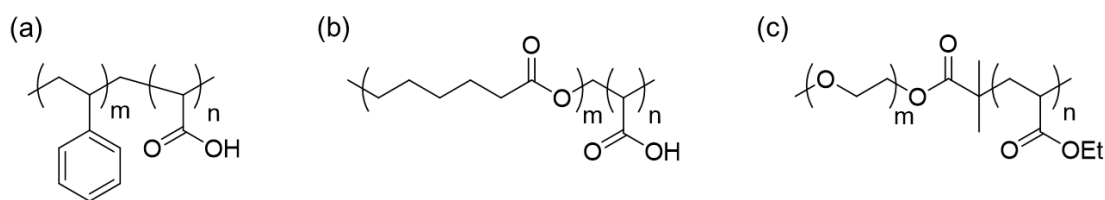


**Figure 1.12** Chemical structures of common amphiphilic diblock copolymers (a) PS-*b*-PAA (b) PCL-*b*-PAA and (c) PEO-*b*-PEtA.

Polymeric surfactants have applications in areas such as coatings, biotechnology, pharmaceuticals, cosmetics, water purification, and oil recovery.<sup>124-128</sup> Their applications are quite widespread, and they have also been extensively employed as emulsion stabilizers for preparation of oil-in-water and water-in-oil emulsions where the hydrophobic groups of the surfactant interacts with the oil phase while the hydrophilic portion interacts with

water molecules.<sup>117, 129</sup> In one study, oil-in-water emulsion were stabilized by inulins, a group of polysaccharides.<sup>130</sup>

Poly(vinyl alcohol) (PVA) is a synthetic polymer with various applications and also has been used as a polymeric surfactant.<sup>131-133</sup> Studies by the Gillies group showed its promising properties as a polymeric surfactant for drug delivery systems to prepare stable particle emulsions as the drug carrier to deliver celecoxib and GSK 3787.<sup>134-135</sup> In another study, PVA was combined with tocopheryl polyethylene glycol 1000 succinate (TPGS) as a drug carrier to increase the encapsulation efficiency and sustained release of the drug.<sup>136</sup>

Stabilized emulsions are used in cosmetics and pharmaceutical industries as carriers for ingredients. PVA has also been used as an emulsifier for oil-in-water systems.<sup>137</sup> PVA used as a surfactant typically has 5 – 15% of its pendent alcohol groups acetylated (**Figure 1.13**). It is synthesized by partial hydrolysis of poly(vinyl acetate) (PVAc), leaving a portion of acetate groups unhydrolyzed.<sup>138</sup> The acetate and alcohol groups along the PVA chain are considered as the hydrophobic and hydrophilic moieties of PVA as a polymeric surfactant.

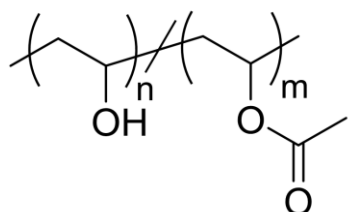


**Figure 1.13** Chemical structure of PVA containing both acetate and alcohol groups.

After the usage of surfactants in many applications, they are mainly released into the environment by wastewater pathways, hence many environments are directly or indirectly affected by surfactants. Despite the fact that most surfactants are eventually biodegradable, their toxicities are critical to consider, based on their degradation times. For instance, it may take decades for a polymeric surfactant to be fully degraded.<sup>139-140</sup> Since surfactants are soluble in a wide range of polar and non-polar solvents, their separation after usage can be quite costly and difficult.

To overcome the problem of surfactant accumulation in the environment, degradable polymers with desired degradation behaviours, such as stimuli-responsive polymers, can potentially be used as surfactants instead of their non-degradable counterparts. For example, an amphiphilic SIP-based block copolymer was synthesized by reacting PEG with PEG to produce PEG-PEtG-PEG triblock copolymers, which were then self-assembled to create micellar nanoparticles with SIP cores. The application of specific stimuli led to the disintegration of particles as a result of the degradation of the polymer. Doxorubicin, a chemotherapy medication used in cancer treatment, and curcumin, a medicine with anti-inflammatory properties, were encapsulated into the particles and then the release of the loaded drugs was induced in a selective manner by the application of specific stimuli.<sup>156</sup>

Despite all the research that has been carried out in surfactant chemistry, there is still room for the development of degradable polymeric surfactants. In particular, the use of degradable surfactants outside of the drug delivery area is quite rare. There has been increasing interest in degradable surfactants as they could address human and environmental toxicity concerns associated with non-degradable surfactants and provide more environmentally-friendly alternatives than their non-degradable counterparts in numerous potential applications.

## 1.5 Thesis Scope and Objectives

SIPs are a recently-developed class of stimuli-responsive polymers that undergo a controlled end-to-end depolymerization when a specific stimulus removes their end-caps and triggers the depolymerization. To the best of our knowledge, aside from their use to form the cores of degradable nanoparticle cores for drug delivery, the properties and applications of SIPs as potential degradable surfactants have not yet been investigated. Therefore, evaluating their potential for stabilizing particle suspensions and emulsions was the focus of this thesis. They offer the potential to serve as surfactants that can be degraded on demand under specific conditions after their use, thereby avoiding environmental contamination, and potentially reducing the toxicity of surfactants in biomedical applications. The goal of this thesis was therefore to investigate the properties of SIPs as potential degradable surfactants. Specifically, it was hypothesized that PGAMs with

pendent hydroxyls and acylated hydroxyls could serve as depolymerizable analogues of PVA, and that PEtG-based block copolymers could serve as depolymerizable analogues of surfactants such as PEO-*b*-PEA (**Figure 1.14**).

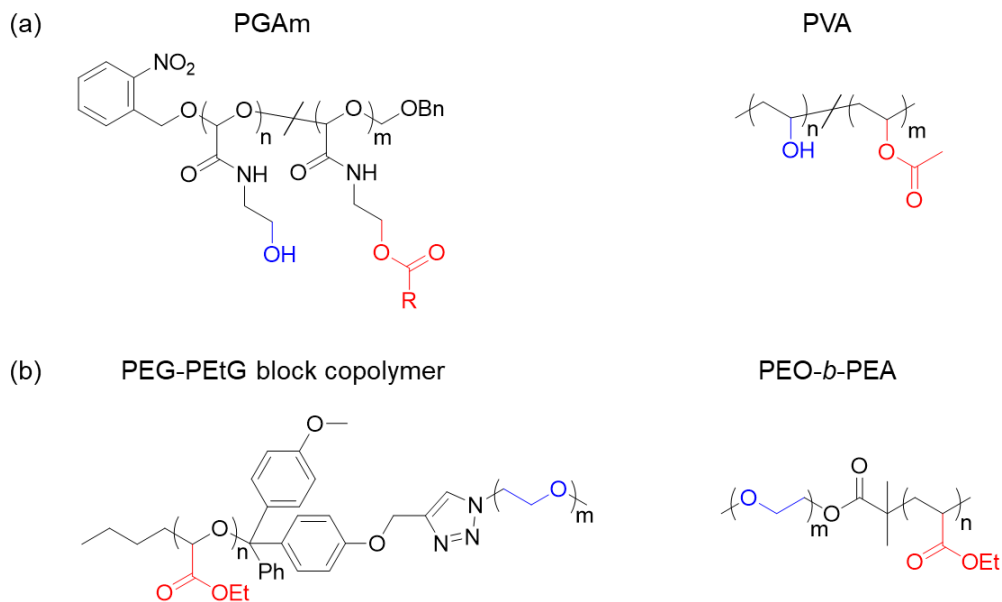


**Figure 1.14** Chemical structures of (a) synthesized PGAm as depolymerizable analogues of PVA and (b) synthesized PEtG-based block copolymers as depolymerizable analogues of surfactants such as PEO-*b*-PEA.

This thesis describes the synthesis of different hydroxyl-functionalized PGAm derivatives and their exploration as emulsifying agents to stabilize suspensions of PEA and PLA particles. The synthesis of PGAm with different end-caps and side chains is described, followed by their use in emulsion preparations. The effects of stimuli on the depolymerization of PGAm and its consequent effects on the stabilities of the particle suspensions are explored. Afterwards, the synthesis and characterization of a PEG-PEtG block copolymers and their potential for stabilizing oil-in-water and water-in-oil emulsions are described.

## Chapter 2

# 2 Investigation of Polyglyoxylamides (PGAMs) and PEtG-based Block Copolymers as Degradable Surfactants

## 2.1 Experimental

### 2.1.1 General Materials and Procedures

PEG-azide<sup>63, 141</sup> and alkyne-methoxy-trityl end-cap<sup>62</sup> were synthesized as previously reported. Phosphorus pentoxide, 1,4-dioxane, ethanolamine, acetyl chloride, butyryl chloride, hexanoyl chloride, lauroyl chloride, stearoyl chloride, *n*-butyl lithium solution (2.5 M in hexanes), benzyl chloromethyl ether (technical, ~60%), CaH<sub>2</sub>, benzyl chloroformate, (+)-sodium L-ascorbate, Nile red, deuterated methanol, deuterated acetonitrile, deuterium oxide, and lithium bis(trimethylsilyl)amide [(TMS)<sub>2</sub>NLi] were purchased from Sigma Aldrich and used as received. Mineral oil was purchased from Fisher Scientific and used as received. 2-Nitrobenzyl alcohol was purchased from AK Scientific and used as received. Copper(II) sulfate, ethyl glyoxylate (EtG) solution (ca. 50% in toluene), and silver trifluoromethanesulfonate (AgOTf) were purchased from Alfa Aesar. Poly(methyl methacrylate) (PMMA) standards purchased from Viscotek. Chromatography-grade tetrahydrofuran (THF), acetone, deuterated chloroform, magnesium sulfate, and hydrochloric acid were purchased from Caledon Laboratories. Toluene was obtained from Caledon Laboratories and distilled over sodium and benzophenone under nitrogen at atmospheric pressure to remove water before use. NEt<sub>3</sub>, CH<sub>2</sub>Cl<sub>2</sub>, and pyridine were distilled over CaH<sub>2</sub> under nitrogen at atmospheric pressure to remove water before use. Anhydrous *N,N*-dimethyl formamide (DMF) was obtained from a PureSolv MD 5 solvent purification system equipped with aluminum oxide columns. All other chemicals were of reagent grade and were used without further purification unless otherwise stated. Dialysis was performed using Spectra/Por regenerated cellulose membrane tubing with 6-8, 10, 25, and 50 kg/mol molecular weight cut-offs (MWCOs). For UV irradiation, a mercury light source (450 W bulb, 2.8 mW/cm<sup>2</sup> of UVA radiation) was used. For sonication, a Branson Digital Sonifier 450D with a standard 13mm tapped horn was used, and the sonication amplitude was set to 10% intensity.

## 2.1.2 General Methods

$^1\text{H}$  NMR spectra were obtained on a Bruker AvIII HD spectrometer at 400 MHz, a Varian INOVA spectrometer at 400 MHz, or a Varian INOVA spectrometer at 600 MHz.  $^{13}\text{C}$  NMR spectra were obtained on a Varian INOVA spectrometer at 150 MHz or a Bruker AvIII HD Spectrometer at 100 MHz. Chemical shifts ( $\delta$ ) are in parts per million (ppm) and were calibrated against the residual solvent signals of  $\text{CHCl}_3$  ( $\delta$  7.27 ppm [ $^1\text{H}$ ], 77.16 ppm [ $^{13}\text{C}$ ]), HOD ( $\delta$  4.79 ppm [ $^1\text{H}$ ]), or  $\text{CHD}_2\text{OD}$  ( $\delta$  3.31 ppm [ $^1\text{H}$ ]) in the spectra. Fourier-transform infrared (FT-IR) spectroscopy was conducted using a PerkinElmer Spectrum two FT-IR Spectrometer using the attenuated total reflectance (ATR) sampling. Fluorescence spectra were obtained using a QM-4 SE spectrofluorometer equipped with both excitation and emission monochromators from Photon Technology International. An excitation wavelength of 552 nm was used for Nile red and the emission spectra were recorded from 570 to 700 nm. Size exclusion chromatography (SEC) experiments were conducted using THF or aqueous chromatography systems. The THF system was equipped with a Viscotek GPCmax VE 2001 SEC instrument, an Agilent PolyPore guard column (PL1113-1500) and two sequential Agilent PolyPore SEC columns packed with porous poly(styrene-co-divinylbenzene) particles (molar mass range 200–2,000,000 g/mol; PL1113-6500) regulated at a temperature of 30 °C. Signal responses were measured using a Viscotek VE 3580 RI detector, and molar masses were determined by calibrations using poly(methyl methacrylate) (PMMA) standards. The aqueous system was equipped with a Waters Separations Module 2695, a refractive index detector (Waters 2414) and two PLaquagel-OH Mixed-M 8  $\mu\text{m}$  (300  $\times$  7.5mm) columns (Polymer Laboratories) connected in series with a PLaquagel-OH 8  $\mu\text{m}$  guard column. The mobile phase was composed of a pH 7.0 buffer solution containing 0.2 M  $\text{NaNO}_3$  and 10 mM  $\text{NaH}_2\text{PO}_4$ , which was eluted at 1 mL/min at room temperature for 40 min/run. Molar masses were determined by calibrations using poly(ethylene glycol) (PEG) standards. SEC samples were prepared at a concentration of  $\sim$ 5 mg/mL. Syntheses of PEGs were performed under a nitrogen atmosphere using Schlenk techniques.

## 2.1.3 Synthetic Procedures

### Synthesis of PEtG<sub>UV</sub>

EtG monomer was purified as previously reported.<sup>70</sup> 2-Nitrobenzyl alcohol (150 mg, 1.0 mmol, 1.0 equiv.) and (TMS)<sub>2</sub>NLi (170 mg, 1.0 mmol, 1.0 equiv.) were dissolved in dry toluene (100 mL) and stirred for 1 h. Afterwards, freshly distilled EtG (24 mL, 200 mmol, 200 equiv.) was rapidly added to the solution followed by cooling the flask to -20 °C. After 20 min of stirring, NEt<sub>3</sub> (2.0 mL, 16 mmol, 16 equiv.) was added and the solution was stirred for another 30 min prior to the rapid addition of benzyl chloromethyl ether (5.0 mL, 20 mmol, 20 equiv.). The resulting solution was stirred for 2 h at -20 °C before the flask was sealed under N<sub>2</sub> gas and transferred into a -20 °C freezer where it was kept for 1 day. The mixture was then precipitated into a mixture of 400 mL of methanol and 40 mL of water. The solvent was then decanted and the resulting residue was dried under vacuum. Yield = 13 g, 65%. <sup>1</sup>H NMR (400 MHz, CDCl<sub>3</sub>, δ): 5.80–5.48 (m, 1H), 4.31–4.10 (s, 2H), 1.37–1.19 (s, 3H). <sup>13</sup>C{<sup>1</sup>H} NMR (CDCl<sub>3</sub>, 100 MHz): δ 167.0–168.5, 92.2–95.3, 62.8, 14.1. FT-IR: 2990, 1750 cm<sup>-1</sup>. SEC: M<sub>n</sub> = 12.1 kg/mol, M<sub>w</sub> = 17.6 kg/mol, Đ = 1.4.

### Synthesis of PEtG<sub>control</sub>

Dry toluene (40 mL) and *n*-BuLi solution (160 μL, 0.40 mmol, 1.0 equiv.) were combined in a Schlenk flask, and the solution was stirred for 10 min at 20 °C prior to the rapid addition of freshly distilled EtG (10 mL, 100 mmol, 250 equiv.) The solution was then stirred for 10 min before it was cooled to -20 °C and stirred for 30 min. NEt<sub>3</sub> (2.2 mL, 16 mmol, 40 equiv.) was then added to the solution and it was stirred for another 30 min at -20 °C. Benzyl chloromethyl ether (1.9 mL, 8.1 mmol, 20 equiv.) was instantly added to the solution and the solution was stirred for 2 h at -20 °C before it was transferred into a -20 °C freezer where it was kept for 3 days. Afterwards, toluene was removed under vacuum and the resulting mixture was dissolved in a mixture of 10 mL of methanol and 10 mL of CH<sub>2</sub>Cl<sub>2</sub> before being precipitated into -20 °C methanol (390 mL) followed by the addition of water (40 mL). The resulting mixture was kept in a -20 °C freezer for 20 h, then the solvent was decanted and the resulting residue was dried under vacuum. Yield = 8.5 g, 85%. <sup>1</sup>H NMR (400 MHz, CDCl<sub>3</sub>, δ): 5.75–5.48 (m, 1H), 4.27–4.03 (s, 2H), 1.32–1.28 (s,



3H).  $^{13}\text{C}\{^1\text{H}\}$  NMR ( $\text{CDCl}_3$ , 100 MHz):  $\delta$  165.7–166.8, 91.6–94.7, 62.3, 14.0. FT-IR: 2990, 1750  $\text{cm}^{-1}$ . SEC:  $M_n = 18.1$  kg/mol,  $M_w = 26.9$  kg/mol,  $D = 1.5$ .

### Synthesis of PEtG<sub>T</sub>

Dry toluene (40 mL) and *n*-BuLi solution (200  $\mu\text{L}$ , 0.50 mmol, 1.0 equiv.) were combined in a Schlenk flask, and the solution was stirred for 10 min at 20 °C prior to the rapid addition of freshly distilled EtG (10 mL, 100 mmol, 200 equiv.). The solution was then stirred for 15 min before it was cooled to –20 °C and stirred for 30 min. Dry  $\text{NEt}_3$  (2.7 mL, 20 mmol, 40 equiv.) was then added to the solution and it was stirred for another 30 min at –20 °C. In another Schlenk flask,  $\text{AgNO}_3$  (5.5 g, 32 mmol, 130 equiv.) and trityl chloride (5.0 g, 20 mmol, 80 equiv.) were dissolved in dry toluene (10 mL). The mixture was then heated at 70 °C for 90 min before it was cooled to –20 °C for 30 min before being added to the first Schlenk flask. The reaction flask was stirred at –20 °C for 1 h and then allowed to gradually warm up to room temperature over 15 h. The solvent was then removed under vacuum, the crude product was dissolved in 30 mL of  $\text{CH}_2\text{Cl}_2$ , and precipitated into a mixture of 800 mL of methanol and 100 mL of  $\text{H}_2\text{O}$ . The resulting mixture was kept in a –20 °C freezer for 20 h, the liquid was decanted, and the resulting residue was dried under vacuum. Yield = 7.0 g, 68%.  $^1\text{H}$  NMR ( $\text{CDCl}_3$ , 400 MHz): 5.47–5.72 (m, 1H), 4.20 (s, 2H), 1.28 (s, 3H).  $^{13}\text{C}\{^1\text{H}\}$  NMR ( $\text{CDCl}_3$ , 100 MHz):  $\delta$  165.5–167.1, 92.5–94.9, 62.7, 14.2. FT-IR: 2990, 1750  $\text{cm}^{-1}$ . SEC:  $M_n = 10.1$  kg/mol,  $M_w = 14.3$  kg/mol,  $D = 1.4$ .

### Synthesis of PEtG<sub>MMT</sub>

Dry toluene (40 mL) and *n*-BuLi solution (200  $\mu\text{L}$ , 0.50 mmol, 1.0 equiv.) were combined in a Schlenk flask, and the solution was stirred for 10 min at 20 °C prior to the rapid addition of freshly distilled EtG (10 mL, 100 mmol, 200 equiv.). The solution was then allowed to mix for 15 min before it was cooled to –20 °C and stirred for 30 min. Dry  $\text{NEt}_3$  (2.5 mL, 18 mmol, 36 equiv.) was then added to the polymerization flask and it was stirred for another 30 min at –20 °C. In another Schlenk flask,  $\text{AgNO}_3$  (0.85 g, 5.0 mmol, 10 equiv.) and 4-monomethoxytrityl chloride (1.5 g, 4.8 mmol, 9.7 equiv.) were dissolved in dry toluene (5 mL). The mixture was then heated at 50 °C for 40 min before it was cooled to –20 °C for 30 min, and then added to the first Schlenk flask. The reaction was stirred at –20

°C for 1 h and then allowed to gradually warm up to room temperature over 16 h. The solvent was then removed under vacuum, the crude product was dissolved in 600 mL of CH<sub>2</sub>Cl<sub>2</sub>, mixed with activated charcoal, and filtered. The filtrate was then washed with brine (2 × 200 mL) and water (100 mL). Afterwards, it was dried over MgSO<sub>4</sub>, filtered, and concentrated under vacuum. The resulting residue was precipitated into 700 mL of methanol. The liquid was then decanted, and the resulting residue was dried under vacuum. Yield = 5.5 g, 54%. <sup>1</sup>H NMR (CDCl<sub>3</sub>, 400 MHz): δ 5.48–5.75 (m, 1H), 4.23 (s, 2H), 1.30 (s, 3H). <sup>13</sup>C{<sup>1</sup>H} NMR (CDCl<sub>3</sub>, 100 MHz): δ 165.1–165.9, 90.7–94.2, 61.9, 14.0. FT-IR: 2990, 1750 cm<sup>-1</sup>. SEC: M<sub>n</sub> = 13.5 kg/mol, M<sub>w</sub> = 19.2 kg/mol, *D* = 1.4.

### Synthesis of PEtG<sub>AMT</sub>

Dry toluene (120 mL) and EtG (20 mL, 200 mmol, 200 equiv.) were combined in a 250 mL Schlenk flask, and the solution was stirred for 10 min at 20 °C prior to the rapid addition of *n*-BuLi solution (400 μL, 1.0 mmol, 1.0 equiv.). The solution was then stirred for 10 min before it was cooled to -20 °C and stirred for 30 min. NEt<sub>3</sub> (1.5 mL, 12 mmol, 12 equiv.) was then added to the solution and the solution was stirred for another 30 min at -20 °C. In another Schlenk flask, alkyne-methoxy-trityl end-cap<sup>62</sup> (1.5 g, 4.1 mmol, 4.1 equiv.) was combined with NEt<sub>3</sub> (2.0 mL, 15 mmol, 15 equiv.) in 14 mL of dry CH<sub>2</sub>Cl<sub>2</sub>. The mixture was then added to the first Schlenk flask. The resulted solution was stirred for 2 h at -20 °C before it was allowed to gradually warm up to room temperature over 16 h. The mixture was then concentrated under vacuum and precipitated into 750 mL of methanol. The liquid was then decanted, and the resulting residue was dried under vacuum. Yield = 13.5 g, 41%. <sup>1</sup>H NMR (CDCl<sub>3</sub>, 400 MHz): δ 5.42–5.76 (m, 1H), 4.21 (s, 2H), 1.27 (s, 3H). <sup>13</sup>C{<sup>1</sup>H} NMR (CDCl<sub>3</sub>, 100 MHz): δ 165.4–166.4, 90.8–94.7, 62.3, 14.1. FT-IR: 2990, 1750 cm<sup>-1</sup>. FT-IR: 2990, 1750 cm<sup>-1</sup>. SEC: M<sub>n</sub> = 10.4 kg/mol, M<sub>w</sub> = 14.1 kg/mol, *D* = 1.4.

### Synthesis of PGAm<sub>UV</sub>

PEtG<sub>UV</sub> (2.0 g, 19 mmol of ethyl ester units, 1.0 equiv.) was dissolved in dry 1,4-dioxane (20 mL) followed by the addition of ethanolamine (4.1 g, 68 mmol, 3.6 equiv. per ester) to the reaction flask. The reaction mixture was then stirred for 24 h at room temperature.

Afterwards, the solvent was decanted and the resulting residue was subsequently purified by dissolution in methanol (10 mL) and precipitation into CH<sub>2</sub>Cl<sub>2</sub> (120 mL). After decanting the solvent, the precipitate was dried under vacuum to afford an off-white powder. Yield = 1.6 g, 68%. <sup>1</sup>H NMR (400 MHz, D<sub>2</sub>O): δ 5.47–5.79 (m, 1H), 3.71 (s, 2H), 3.42 (s, 2H). <sup>13</sup>C {<sup>1</sup>H} NMR (150 MHz, D<sub>2</sub>O): δ 167.4, 91.1–93.8, 62.4, 14.1. FT-IR (ATR): 3290, 2950, 2890, 1660, 1540 cm<sup>-1</sup>. SEC: M<sub>n</sub> = 9.7 kg/mol, M<sub>w</sub> = 14.7 kg/mol, *D* = 1.5.

### Synthesis of **PGAm<sub>control</sub>**

**PGAm<sub>control</sub>** was synthesized by the same procedure as for **PGAm<sub>UV</sub>** except that **PEtG<sub>control</sub>** (2.0 g, 20 mmol of ethyl ester units, 1.0 equiv.) was used as the starting material. Yield = 1.4 g, 59%. <sup>1</sup>H NMR (400 MHz, D<sub>2</sub>O): δ 5.48–5.81 (m, 1H), 3.73 (s, 2H), 3.46 (s, 2H). <sup>13</sup>C {<sup>1</sup>H} NMR (150 MHz, D<sub>2</sub>O): δ 169.1, 91.7–95.1, 63.8, 14.5. FT-IR (ATR): 3300, 2950, 2880, 1650, 1550 cm<sup>-1</sup>. SEC: M<sub>n</sub> = 11.8 kg/mol, M<sub>w</sub> = 17.5 kg/mol, *D* = 1.5.

### Synthesis of **PGAm<sub>MMT</sub>**

**PGAm<sub>MMT</sub>** was synthesized by the same procedure as for **PGAm<sub>UV</sub>** except that **PEtG<sub>MMT</sub>** (2.9 g, 29 mmol of ethyl ester units, 1.0 equiv.) was used as the starting material. Yield = 1.8 g, 54%. <sup>1</sup>H NMR (400 MHz, D<sub>2</sub>O): δ 5.30–5.75 (m, 1H), 3.45 (s, 2H), 3.20 (s, 2H). <sup>13</sup>C {<sup>1</sup>H} NMR (150 MHz, D<sub>2</sub>O): δ 168.2, 91.2–94.4, 63.3, 14.0. FT-IR (ATR): 3290, 2940, 2890, 1660, 1540, cm<sup>-1</sup>. SEC: M<sub>n</sub> = 7.4 kg/mol, M<sub>w</sub> = 10.4 kg/mol, *D* = 1.4.

### Synthesis of **PGAm<sub>T</sub>**

**PGAm<sub>T</sub>** was synthesized by the same procedure as for **PGAm<sub>UV</sub>** except that **PEtG<sub>T</sub>** (2.3 g, 23 mmol of ethyl ester units, 1.0 equiv.) was used as the starting material. Yield = 1.7 g, 61%. <sup>1</sup>H NMR (400 MHz, D<sub>2</sub>O): δ 5.50–5.75 (m, 1H), 3.70 (s, 2H), 3.40 (s, 2H). <sup>13</sup>C {<sup>1</sup>H} NMR (150 MHz, D<sub>2</sub>O): δ 170.1, 91.9–95.5, 64.2, 14.7. FT-IR (ATR): 3280, 2940, 2880, 1650, 1530 cm<sup>-1</sup>. SEC: M<sub>n</sub> = 8.4 kg/mol, M<sub>w</sub> = 12.1 kg/mol, *D* = 1.4.

### Synthesis of **PGAm<sub>ac-100</sub>**

**PGAmuv** (0.20 g, 1.3 mmol of hydroxyl, 1.0 equiv.) was placed into a flask and it was evacuated and charged with nitrogen at atmospheric pressure several times followed by the addition of dry pyridine (5 mL) to the reaction flask. Subsequently, acetyl chloride (0.20 mL, 2.2 mmol, 1.7 equiv. per pendent hydroxyl) was added to the reaction flask and it was stirred for 24 hours. The resulting mixture was dialyzed (6-8 kg/mol MWCO) against acetone for 24 h and against methanol for the next 24 h. The resulting residue was then dried under vacuum to afford 80 mg of a powder. Yield = 53%.  $^1\text{H NMR}$  (400 MHz,  $\text{D}_2\text{O}$ ):  $\delta$  5.50–5.85 (m, 1H), 4.30 (s, 2H), 3.45 (s, 2H), 2.00 (s, 3H).

#### **Synthesis of PGAm<sub>buty-100</sub>**

The same procedure as described above for the synthesis of **PGAm<sub>ac-100</sub>** was used except that butyryl chloride (0.30 mL, 2.6 mmol, 1.9 equiv. per pendent hydroxyl) was used instead of acetyl chloride to afford 120 mg of a powder. Yield = 42%.  $^1\text{H NMR}$  (400 MHz,  $\text{CDCl}_3$ ):  $\delta$  5.55–5.80 (m, 1H), 4.20 (s, 2H), 3.50 (d, 2H), 2.28 (s, 2H), 1.65 (s, 2H), 0.85 (t,  $J = 6.8$  Hz, 4H).

#### **Synthesis of PGAm<sub>hex-100</sub>**

The same procedure as described above for the synthesis of **PGAm<sub>ac-100</sub>** was used except that hexanoyl chloride (0.40 mL, 2.8 mmol, 1.9 equiv. per pendent hydroxyl) was used instead of acetyl chloride to afford 160 mg of a powder. Yield = 55%.  $^1\text{H NMR}$  (400 MHz,  $\text{CDCl}_3$ ):  $\delta$  5.60–5.81 (m, 1H), 4.20 (s, 1H), 3.50 (s, 1H), 2.31 (s, 2H), 1.61 (s, 2H), 1.30 (s, 7H), 0.81 (t,  $J = 7.8$  Hz, 5H).

#### **Synthesis of PGAm<sub>lau-100</sub>**

The same procedure as described above for the synthesis of **PGAm<sub>ac-100</sub>** was used except that lauroyl chloride (0.80 mL, 3.7 mmol, 2.0 equiv. per pendent hydroxyl) was used instead of acetyl chloride to afford 210 mg of a powder. Yield = 39%.  $^1\text{H NMR}$  (400 MHz,  $\text{CDCl}_3$ ):  $\delta$  5.57–5.80 (m, 1H), 4.19 (s, 2H), 3.51 (s, 2H), 2.30 (s, 2H), 1.61 (s, 4H), 1.25 (s, 36H), 0.81 (t,  $J = 9.4$  Hz, 7H).

#### **Synthesis of PGAm<sub>ste-100</sub>**

The same procedure as described above for the synthesis of **PGAm<sub>ac-100</sub>** was used except that stearoyl chloride (1.6 mL, 6.0 mmol, 2.5 equiv. per pendent hydroxyl) was used instead of acetyl chloride to afford 350 mg of a powder. Yield = 40%. <sup>1</sup>H NMR (400 MHz, CDCl<sub>3</sub>): δ 5.55–5.89 (m, 1H), 4.15 (s, 1H), 3.50 (s, 3H), 2.30 (s, 2H), 1.61 (s, 3H), 1.29 (s, 28H), 0.89 (t, *J* = 8.5 Hz, 3H).

#### Synthesis of **PGAm<sub>ac-5</sub>**

The same procedure as described above for the synthesis of **PGAm<sub>ac-100</sub>** was used except that **PGAm<sub>UV</sub>** (0.60 g, 5.5 mmol of hydroxyl, 1.0 equiv.) and acetyl chloride (20 μL, 0.30 mmol, 0.050 equiv. per pendent hydroxyl) were used to afford 480 mg of a powder. Yield = 68%. <sup>1</sup>H NMR (400 MHz, D<sub>2</sub>O): δ 5.50–5.85 (m, 1H), 3.79 (s, 2H), 3.42 (s, 2H), 2.21 (s, 0.1).

#### Synthesis of **PGAm<sub>ac-10</sub>**

The same procedure as described above for the synthesis of **PGAm<sub>ac-100</sub>** was used except that **PGAm<sub>UV</sub>** (0.70 g, 5.5 mmol of hydroxyl, 1.0 equiv.) and acetyl chloride (40 μL, 0.55 mmol, 0.10 equiv. per pendent hydroxyl) were used to afford 400 mg of a powder. Yield = 57%. <sup>1</sup>H NMR (400 MHz, D<sub>2</sub>O): δ 5.50–5.85 (m, 1H), 3.79 (s, 2H), 3.42 (s, 2H), 2.21 (s, 0.3).

#### Synthesis of **PGAm<sub>hex-5</sub>**

The same procedure as described above for the synthesis of **PGAm<sub>ac-100</sub>** was used except that **PGAm<sub>UV</sub>** (0.20 g, 1.8 mmol of hydroxyl, 1.0 equiv.) and hexanoyl chloride (12 μL, 0.10 mmol, 0.050 equiv. per pendent hydroxyl) were used to afford 130 mg of a powder. Yield = 54%. <sup>1</sup>H NMR (400 MHz, D<sub>2</sub>O): δ 5.45–5.75 (m, 1H), 3.67 (s, 2H), 3.29 (s, 2H), 2.26 (s, 0.1), 1.50 (s, 0.1), 1.22 (s, 0.2), 0.76 (s, 0.1).

#### Synthesis of **PGAm<sub>hex-10</sub>**

The same procedure as described above for the synthesis of **PGAm<sub>ac-100</sub>** was used except that **PGAm<sub>UV</sub>** (0.20 g, 1.8 mmol of hydroxyl, 1.0 equiv.) and hexanoyl chloride (25 μL, 0.20 mmol, 0.10 equiv. per pendent hydroxyl) were used to afford 130 mg of a powder.

Yield = 51%.  $^1\text{H}$  NMR (400 MHz,  $\text{D}_2\text{O}$ ):  $\delta$  5.45–5.80 (m, 1H), 3.71 (s, 2H), 3.43 (s, 2H), 2.29 (s, 0.1), 1.57 (s, 0.2), 1.26 (s, 0.3), 0.85 (s, 0.2).

### Synthesis of **PGAm<sub>lau-5</sub>**

The same procedure as described above for the synthesis of **PGAm<sub>ac-100</sub>** was used except that **PGAm<sub>UV</sub>** (0.30 g, 2.2 mmol of hydroxyl, 1.0 equiv.) and lauroyl chloride (30  $\mu\text{L}$ , 0.10 mmol, 0.060 equiv. per pendent hydroxyl) were used to afford 150 mg of a powder. Yield = 57%.  $^1\text{H}$  NMR (400 MHz,  $\text{D}_2\text{O}$ ):  $\delta$  5.50–5.80 (m, 1H), 3.73 (s, 2H), 3.43 (s, 2H), 2.29 (s, 0.1), 1.61 (s, 0.1), 1.27 (s, 0.2), 0.90 (s, 0.1).

### Synthesis of **PGAm<sub>lau-10</sub>**

The same procedure as described above for the synthesis of **PGAm<sub>ac-100</sub>** was used except that **PGAm<sub>UV</sub>** (0.30 g, 2.2 mmol of hydroxyl, 1.0 equiv.) and lauroyl chloride (75  $\mu\text{L}$ , 0.30 mmol, 0.15 equiv. per pendent hydroxyl) were used to afford 160 mg of a powder. Yield = 52%.  $^1\text{H}$  NMR (400 MHz,  $\text{D}_2\text{O}$ ):  $\delta$  5.50–5.80 (m, 1H), 3.74 (s, 2H), 3.41 (s, 2H), 2.30 (s, 0.1), 1.58 (s, 0.1), 1.26 (s, 0.3), 0.81 (s, 0.1).

### Synthesis of **PEG-PEtG block copolymers**

PEG<sub>5k</sub>-azide<sup>63, 141</sup> (1.4 g, 0.28 mmol, 2.8 equiv.), PEtG<sub>AMT</sub> (1.3 g, 0.10 mmol, 1.0 equiv.), copper(II) sulfate (0.019 g, 0.10 mmol, 1.0 equiv.), and sodium L-ascorbate (0.025 g, 0.10 mmol, 1.0 equiv.) were placed in a Schlenk flask, which was subsequently evacuated and purged with  $\text{N}_2$ . Afterwards, anhydrous DMF (5 mL) was added to the mixture and it was stirred for 1 h while being purged with  $\text{N}_2$ . The reaction mixture was then heated at 40 °C and stirred for 20 h before being dialyzed (6–8 kg/mol MWCO) against water for 1 day. The resulting product was dispersed in water (10 mL) and then centrifuged (6000 rpm, 5 min) followed by decanting the solvent. The previous dispersion procedure was repeated and then the resulting residue was lyophilized to afford 800 mg of product. Yield = 45%.  $^1\text{H}$  NMR (400 MHz,  $\text{CDCl}_3$ ):  $\delta$  7.22–6.75 (m, 14H), 5.80–5.48 (m, 140H), 4.27–4.03 (m, 290H), 3.74–3.38 (s, 3H), 4.99 (s, 2H), 4.20–4.13 (m, 458H), 1.37–1.19 (m, 460H). SEC:  $M_n$  = 14.5 kg/mol,  $M_w$  = 18.1 kg/mol,  $D$  = 1.2.

### 2.1.4 Degradation Studies of PGAMs

All samples were prepared at ~ 20 mg/mL concentration, transferred to NMR tubes, and promptly sealed. They were then kept at room temperature, and investigated via  $^1\text{H}$  NMR spectroscopy over time.

#### **Degradation studies of PGAM<sub>UV</sub>**

Two NMR samples were prepared by dissolving **PGAM<sub>UV</sub>** in D<sub>2</sub>O. The first sample was irradiated with UV light (450 W bulb, 2.8 mW/cm<sup>2</sup> of UVA radiation) for 10, 20, 30, 45, and 60 minutes and was checked by  $^1\text{H}$  NMR at each time point. The second sample was kept in dark and was monitored as a control sample to measure the background polymer degradation.

#### **Degradation studies of PGAM<sub>control</sub>**

Four different NMR samples of **PGAM<sub>control</sub>** were prepared. The first sample was prepared by dissolving **PGAM<sub>control</sub>** in D<sub>2</sub>O. The second sample was prepared by dissolving **PGAM<sub>control</sub>** in a 0.1 M deuterated citrate buffer which was prepared by dissolving 95 mg of citric acid in 5 mL of D<sub>2</sub>O and adjusting the pH to 3.0 using NaOH. The third NMR sample was prepared by dissolving **PGAM<sub>control</sub>** in D<sub>2</sub>O followed by adjusting the pH to 3.0 using a 0.5 M acetic acid solution. The fourth NMR sample was prepared in the same manner as the first sample but was irradiated with UV light (450 W bulb, 2.8 mW/cm<sup>2</sup> of UVA radiation) for 45 minutes.

#### **Degradation studies of PGAM<sub>T</sub> and PGAM<sub>MMT</sub>**

NMR samples of **PGAM<sub>T</sub>** and **PGAM<sub>MMT</sub>** were prepared by dissolving the polymer in D<sub>2</sub>O or in 0.1 M deuterated citrate buffer at pH 3.0.

## 2.1.5 Particle Suspension Preparation and Triggered Destabilization of the Suspensions

### Particle preparation

Particle suspensions were prepared using an emulsification-evaporation technique. The dispersed phase of the emulsion was prepared by dissolving 10 mg of the hydrophobic polymer, PEA or PLA, in 1 mL of CH<sub>2</sub>Cl<sub>2</sub>. For particles with Nile red, the hydrophobic polymer was dissolved in 1 mL CH<sub>2</sub>Cl<sub>2</sub> containing 0.01 mg/mL Nile red. The aqueous phase was prepared by dissolving 20 mg of emulsifying agent in 3 mL of deionized water. The ratios of water:organic solvent and mass of emulsifying agent were varied according to **Tables 2.3 to 2.7**. The organic phase was then added to the aqueous phase. The resulting solution was stirred for 10 minutes, and then subjected to sonication while stirring at 250-300 rpm for three 30 s intervals with 10 s breaks in between. The resulting emulsion was stirred for 4 hours to evaporate the organic solvent.

### Triggered destabilization of the PGAm-stabilized particle suspensions

To trigger the degradation of PGAm coating the **PGAm<sub>UV</sub>**-stabilized particle suspensions, they were irradiated with UV light (450 W bulb, 2.8 mW/cm<sup>2</sup> of UVA radiation) for 90 minutes while stirring (150 rpm). For **PGAm<sub>T</sub>**-stabilized and **PGAm<sub>MMT</sub>**-stabilized particle suspensions, the pH of particle suspensions was adjusted to 3.0 using 0.5 M acetic acid or addition of 0.75 mL of 0.1 M citrate buffer, which was prepared by dissolving 380 mg of citric acid in 20 mL of deionized water and adjusting the pH to 3.0 using NaOH. To adjust the pH of particle suspensions to 7 using buffer, 0.75 mL of 0.1 M phosphate buffer was added to the particle suspensions, which was prepared by dissolving 420 mg KH<sub>2</sub>PO<sub>4</sub> and 340 mg K<sub>2</sub>HPO<sub>4</sub> into 50 mL deionized water.

### Dynamic light scattering (DLS)

Particle diameters and count rates were determined by DLS using a Zetasizer Nano ZS instrument from Malvern Instruments. Analyses were conducted at 25 °C in 1.5 mL disposable plastic cuvettes that were purchased from Fisherbrand. To study the triggered particle suspensions over time, the stimuli were applied as described above (Triggered



destabilization of the PGAm-stabilized particle suspensions), then the suspensions were incubated at ambient temperature. DLS measurements of the diameter and count rate were obtained over time, while fixing the attenuator and position of the beam.

### **Fluorescence spectroscopy of triggered of PGAm-stabilized particle suspensions**

Fluorescence intensities were obtained using a QM-4 SE spectrofluorometer equipped with both excitation and emission monochromators from Photon Technology International. Analyses were conducted at 25 °C in a 3.0 mL 101-QS quartz cuvette that was purchased from Hellma Analytics. To study the triggered particles over time, the stimuli were applied as described above (Triggered destabilization of the PGAm-stabilized particle suspensions), then the suspensions were incubated at ambient temperature. Fluorescence measurements were obtained over time while the slit width was set to 2 nm. An excitation wavelength of 552 nm was used for Nile red and the emission spectra were recorded from 570 to 700 nm.

## **2.1.6 Oil-in-water and Water-in-oil Preparation and Triggered Destabilization of the Suspensions**

### **Oil-in-water and water-in-oil preparation**

For oil-in-water and water-in-oil emulsions, the emulsifier was dissolved in deionized water and added to the oil. The resulting mixture was subjected to sonication while stirring at 250-300 rpm for three 30 s intervals with 10 s breaks in between. The solvent ratios and concentrations of emulsifiers were varied according to tables **Tables 2.8, 2.9, 2.11, and 2.12**.

### **Triggered destabilization of the stabilized water-in-toluene emulsions**

To trigger the degradation of the emulsifier, PEG-PEtG block copolymers, in water-in-toluene emulsions, 18 µL of glacial acetic acid was added to the samples.

## 2.2 Results and Discussion

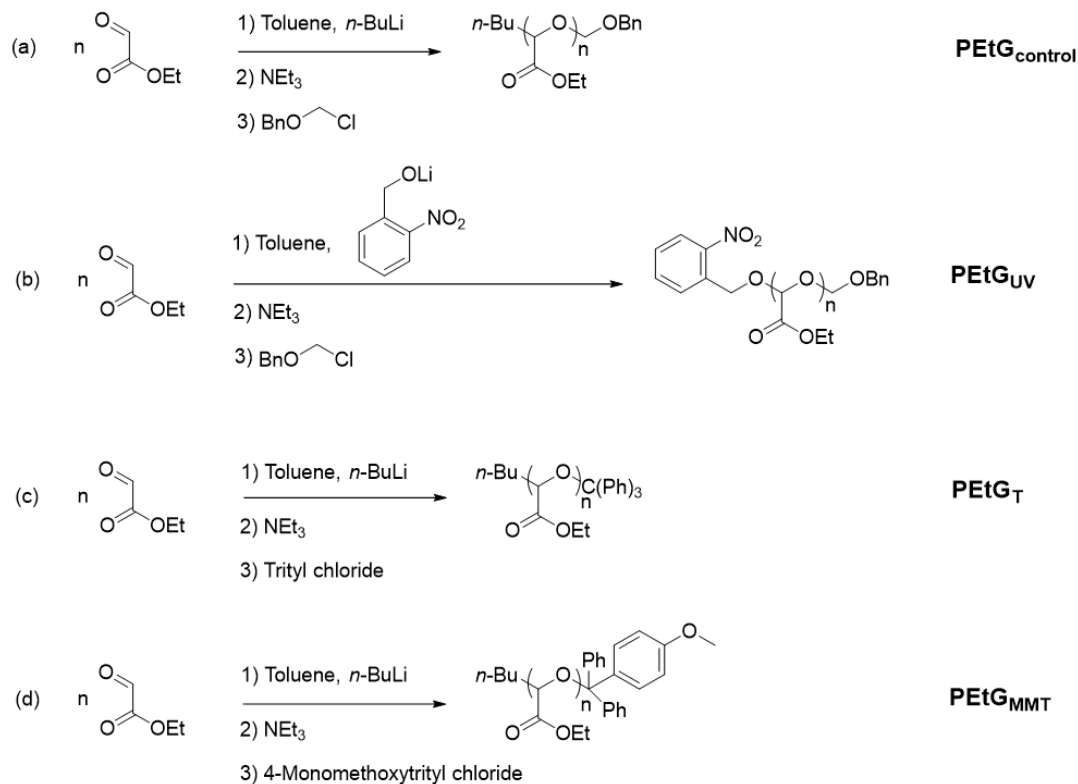
### 2.2.1 Syntheses and Characterization of Poly(ethyl glyoxylate)s (PEtGs)

Syntheses of PEtGs were performed using modified versions of the previously reported anionic polymerization method.<sup>70</sup> In this method, the purity of EtG monomer was highly improved which allowed for controlling the DP<sub>n</sub> of the synthesized polymer using alkylolithium reagents as initiators at optimized polymerization conditions. Due to the low ceiling temperature (T<sub>c</sub>) of PEtGs,<sup>142</sup> the polymerizations were conducted at -20 °C as this has been determined to be the optimal temperature for EtG polymerization.<sup>70</sup>

Four different PEtGs with different end-caps were synthesized (**Scheme 2.1**). **PEtG<sub>control</sub>** was synthesized using benzyl chloromethyl ether as the end-cap, as this end-cap is stable and its cleavage is not triggered by the conditions used for triggering the other end-caps. To synthesize **PEtG<sub>UV</sub>**, lithium bis(trimethylsilyl)amide [(TMS)<sub>2</sub>NLi], which is a strong non-nucleophilic base, was reacted with 2-nitrobenzyl alcohol. The resulting alkoxide was then used as an initiator for the polymerization of EtG, and benzyl chloromethyl ether was used to end-cap the other terminus of the polymer. The 2-nitrobenzyl end-cap can be cleaved by irradiation with UV light,<sup>64, 143</sup> so **PEtG<sub>UV</sub>** was expected to be UV-responsive. Even though UV-responsive polymers may not be suitable for biological applications, it was chosen as a model system and also could be applicable to non-biological applications. Syntheses of **PEtG<sub>MMT</sub>** and **PEtG<sub>T</sub>** were initiated by *n*-BuLi and employed trityl chloride and 4-monomethoxytrityl chloride as their end-caps, respectively. The two aforementioned trityl-based end-caps are cleavable in water. Their depolymerization proceeds faster in acidic conditions, and additionally **PEtG<sub>MMT</sub>** more rapidly compared to **PEtG<sub>T</sub>**.<sup>144</sup> As they undergo depolymerization in aqueous solution, they are of interest for biological applications. Based on the SEC results of the four synthesized PEtGs, all four polymers had similar molar masses and relatively low dispersities (**Table 2.1**).

To characterize the synthesized PEtGs, <sup>1</sup>H NMR of the resulting polymers confirmed the formation of the polymers as gave rise to broad peaks located at ca. 5.6, 4.2, and 1.3 ppm associated with CH in the backbone, CH<sub>2</sub>, and CH<sub>3</sub> in the pendent group, respectively

(Figures 2.1a, A1, A2, and A4). Further evidence of characterization of polymers can also be found by FT-IR spectrum of PEtG. The strong C=O stretch peak around  $1750\text{ cm}^{-1}$  is characteristic of esters and is present in the PEtG spectrum (Figure 2.2).



**Scheme 2.1** Synthetic approaches for obtaining (a) **PEtG<sub>control</sub>** (b) **PEtG<sub>UV</sub>** (c) **PEtG<sub>T</sub>** and (d) **PEtG<sub>MMT</sub>**.

**Table 2.1** SEC results of the synthesized PEtGs representing all four PEtGs had similar molar masses and relatively low dispersities.

Polymer name	$M_n$ (kg/mol)	$M_w$ (kg/mol)	$\mathcal{D}$
<b>PEtG<sub>control</sub></b>	18.1	26.9	1.5
<b>PEtG<sub>UV</sub></b>	12.1	17.6	1.4
<b>PEtG<sub>T</sub></b>	10.1	14.3	1.4
<b>PEtG<sub>MMT</sub></b>	13.5	19.2	1.4

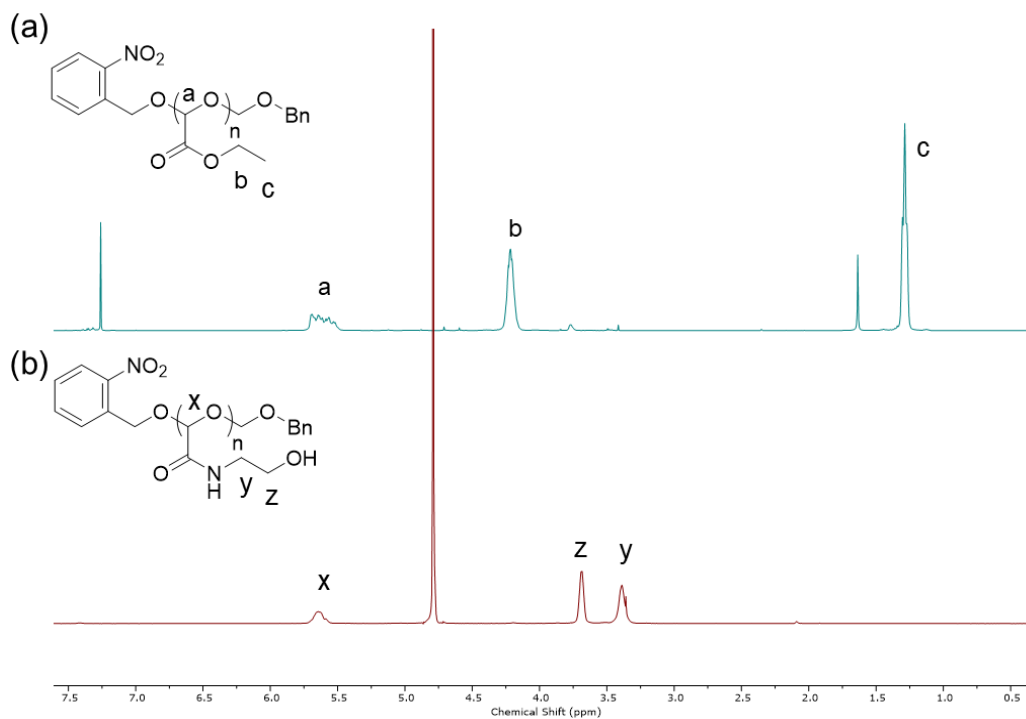


**Figure 2.1** Comparison of the  $^1\text{H}$  NMR spectra of (a) **PEtG<sub>UV</sub>** and (b) **PGAm<sub>UV</sub>** (400 MHz,  $\text{CDCl}_3$  and  $\text{D}_2\text{O}$ ).

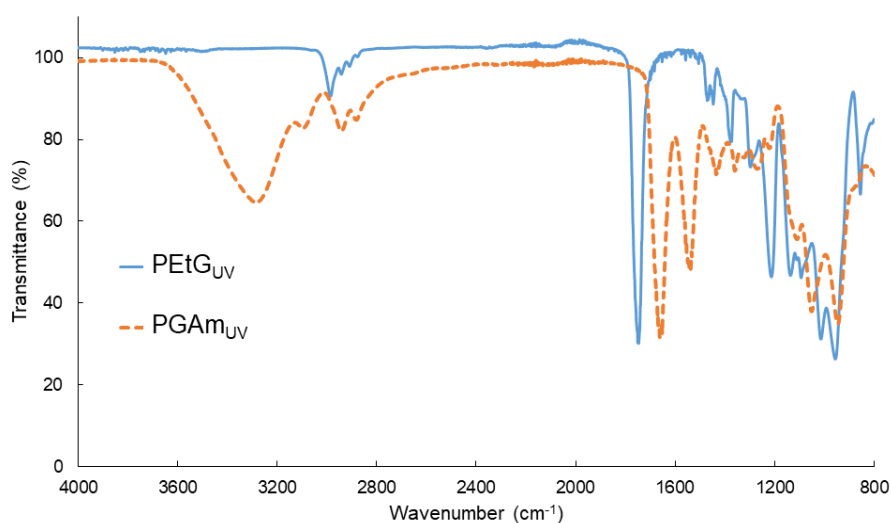
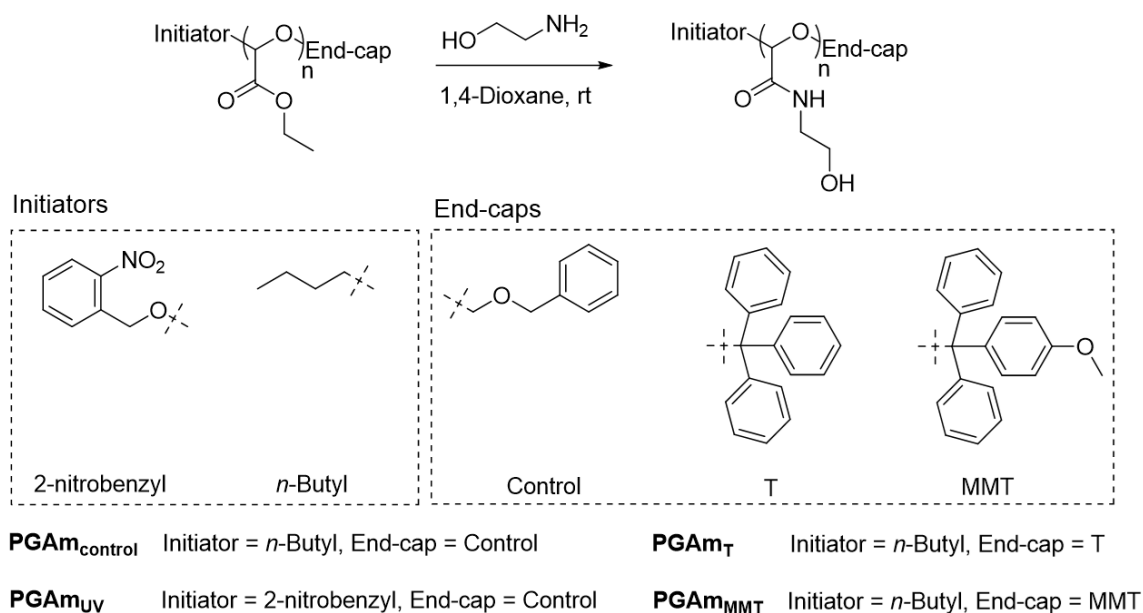


**Figure 2.2** Overlay of the FT-IR spectra of **PEtG<sub>UV</sub>** and **PGAm<sub>UV</sub>**. The peak around  $1750\text{ cm}^{-1}$  in **PEtG<sub>UV</sub>** spectrum disappears in the corresponding **PGAm<sub>UV</sub>** spectrum, and is instead replaced by the peaks around  $1650\text{ cm}^{-1}$  and  $3300\text{ cm}^{-1}$ .

## 2.2.2 Syntheses and Characterization of Polyglyoxylamides (PGAmS)

To first synthesize water-soluble PGAmS via post-polymerization modification (**Scheme 2.2**), the PEtGS were reacted with excess ethanolamine in 1,4-dioxane for 24 hours to reach full conversion and install hydroxyl groups on every repeating unit of the polymers. PGAmS with four different end-caps were synthesized using the four PEtG precursors (**Scheme 2.1**).



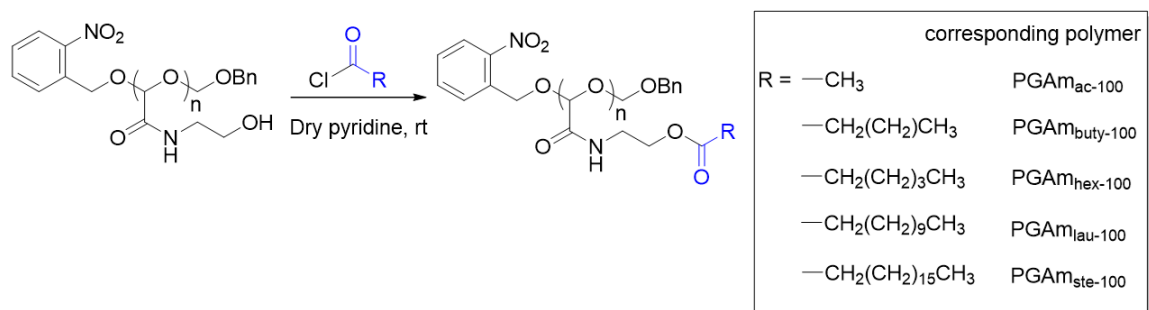
**Scheme 2.2** Synthetic approaches for obtaining PGAmS via post-polymerization modifications of PEtGS.

<sup>1</sup>H NMR spectroscopy of the PGAmS confirmed that full conversion was achieved (**Figure 2.1b, A5, A6, and A8**). Specifically, the two peaks located at 1.4 and 4.3 ppm in the PEtG spectra that correspond to the pendent ethyl groups disappeared in the PGAm spectra, and instead were replaced by two peaks located at 3.4 and 3.7 ppm which were assigned to two methylene groups in the pendent group of the PGAm. Further evidence of the conversion from ester to amide pendent groups can also be found by comparing the FT-IR spectra of the PEtG precursors to that of the PGAmS (**Figure 2.2**). The strong C=O stretch peak around 1750 cm<sup>-1</sup> is characteristic of esters and is present in PEtG spectrum while it disappears in the corresponding PGAm spectrum, and is instead replaced by a strong C=O

stretch peak around  $1650\text{ cm}^{-1}$ , which is characteristic of an amide. There is also a broad peak in the spectrum of PGAm around  $3300\text{ cm}^{-1}$  which represents the N-H stretch of the pendent amides.

### 2.2.3 Reaction of **PGAm<sub>UV</sub>** with Acid Chlorides

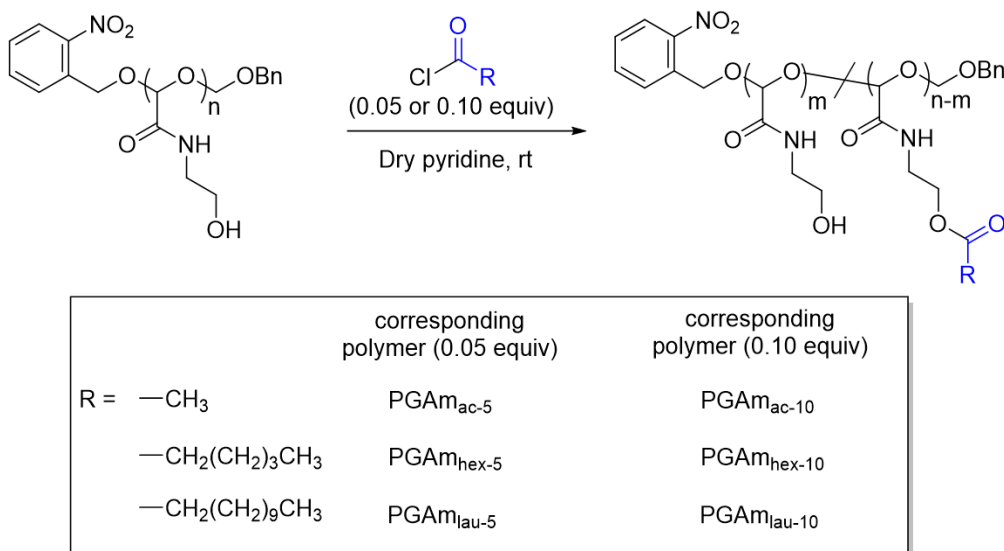
While the introduction of the ethanolamine moieties made the polymers water-soluble, the next step was to mimic the amphiphilic properties of polyvinyl alcohol (PVA) by acylating a portion of the pendent hydroxyl groups to introduce hydrophilicity. PVA used as a surfactant typically has 5 – 15% of its pendent alcohol groups acetylated. Thus, the reactivity of PGAm with different acid chlorides was investigated to subsequently synthesize polymers with different hydrophilic-lipophilic balances (HLBs). **PGAm<sub>UV</sub>** is stable and does not undergo degradation as long as it is kept in the dark and hence, it was chosen for this purpose. First, **PGAm<sub>UV</sub>** was reacted with an excess amount of different acid chlorides to fully convert the hydroxyl pendent groups into ester groups (**Scheme 2.3**). Various acid chlorides were used (acetyl chloride, butyryl chloride, hexanoyl chloride, lauroyl chloride, and stearoyl chloride) to synthesize PGAm with different HLB values. Based on  $^1\text{H NMR}$  spectroscopy results showing the appearance of peaks corresponding to the pendent groups, the reactions occurred successfully, regardless of the acid chloride used (**Figures A9 to A13**). The resulting polymers were not purified thoroughly as the aim of these experiments was to determine whether PGAm reacted effectively with acid chlorides. As expected, none of the synthesized polymers were soluble in water, indicating that lower conversions with more hydrophilicity were required to have a water-soluble emulsifying agent.



**Scheme 2.3** Acylation of **PGAm<sub>UV</sub>** with different acid chlorides.

## 2.2.4 Partially Acylated PGAMs

With the aim of obtaining water-soluble amphiphilic acylated PGAMs as potential emulsifiers, **PGAM<sub>UV</sub>** was reacted with 5 or 10 mol% of acid chlorides (**Scheme 2.4**). Three acid chlorides – acetyl chloride, hexanoyl chloride, and lauroyl chloride – with different alkyl chain lengths were used to partially acylate **PGAM<sub>UV</sub>**.



**Scheme 2.4** Syntheses of partially acylated PGAMs with different alkyl chain lengths.

The actual conversions of synthesized polymers were determined via <sup>1</sup>H NMR spectroscopy (**Table 2.2**). The conversions of **PGAM<sub>ac-5</sub>** and **PGAM<sub>ac-10</sub>** were calculated based on integration of the methyl hydrogens located at 2.1 ppm (**Figure 2.3**). The conversions of **PGAM<sub>hex-5</sub>** and **PGAM<sub>hex-10</sub>** were calculated based on integration of peaks located at 0.7, 1.3, 1.6, and 2.4 ppm that are assigned to the hydrogens in the pendent groups (**Figures A14** and **A15**). Likewise, the conversions of **PGAM<sub>lau-5</sub>** and **PGAM<sub>lau-10</sub>** were calculated based on integration of peaks located at 0.8, 1.3, and 2.4 ppm (**Figures A16** and **A17**).

**Table 2.2** Targeted and actual conversions of partially acylated PGAMs.

Polymer name	Targeted conversion (%)	Actual conversion (%)	Polymer name	Targeted conversion (%)	Actual conversion (%)
<b>PGAm<sub>ac-5</sub></b>	5	4	<b>PGAm<sub>ac-10</sub></b>	10	9
<b>PGAm<sub>hex-5</sub></b>	5	4	<b>PGAm<sub>hex-10</sub></b>	10	7
<b>PGAm<sub>lau-5</sub></b>	5	3	<b>PGAm<sub>lau-10</sub></b>	10	7

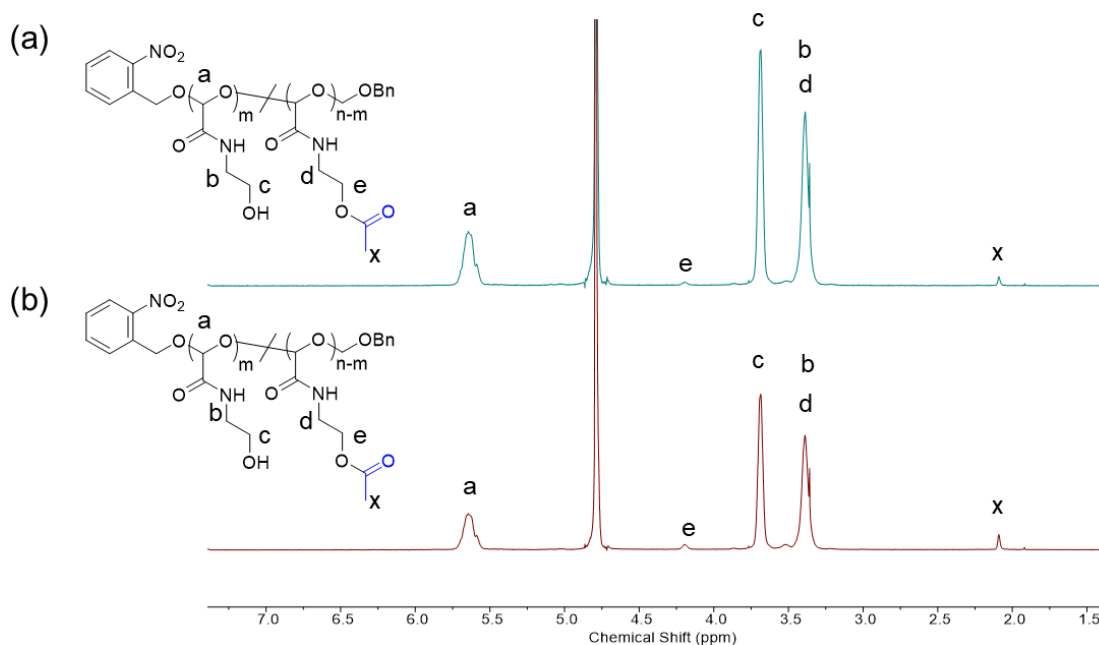


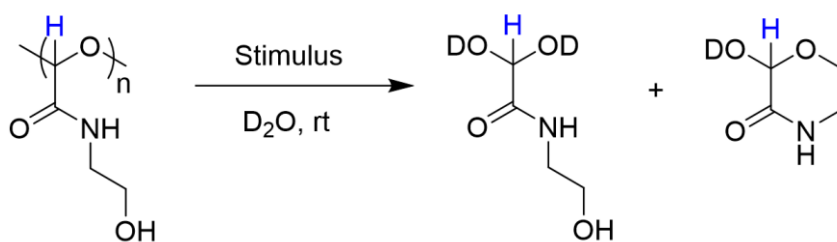
**Figure 2.3**  $^1\text{H}$  NMR spectra (400 MHz,  $\text{D}_2\text{O}$ ) of (a) **PGAm<sub>ac-5</sub>** and (b) **PGAm<sub>ac-10</sub>**. The conversions were calculated based on the peaks located at 2.1 ppm corresponding to the methyl protons on the acetyl group.

### 2.2.5 Degradation Studies of PGAMs

As discussed earlier, SIPs are a class of stimuli-responsive polymers that undergo an end-to-end depolymerization when a stimulus triggers their depolymerization by removing their



end-caps. To determine whether the synthesized PGAMs retained the depolymerization properties of SIPs, degradation experiments were performed, and their degradation was studied by  $^1\text{H}$  NMR spectroscopy. The percent degradation was calculated based on the relative integrations of the peaks at  $\sim 5.6\text{--}5.7$  ppm corresponding to the polymer backbone methine protons and the peaks at  $\sim 5.2\text{--}5.4$  ppm corresponding to the methine proton of the degradation products (**Scheme 2.5**). As the degradation proceeded, the hydrogen peak of the polymer's backbone started to disappear followed by the appearance of the same hydrogen of the degradation products (**Figure 2.4**).



**Scheme 2.5** General degradation scheme for PGAMs in  $\text{D}_2\text{O}$ . The methine protons that were used to calculate the percent degradation by  $^1\text{H}$  NMR spectroscopy are shown in blue.

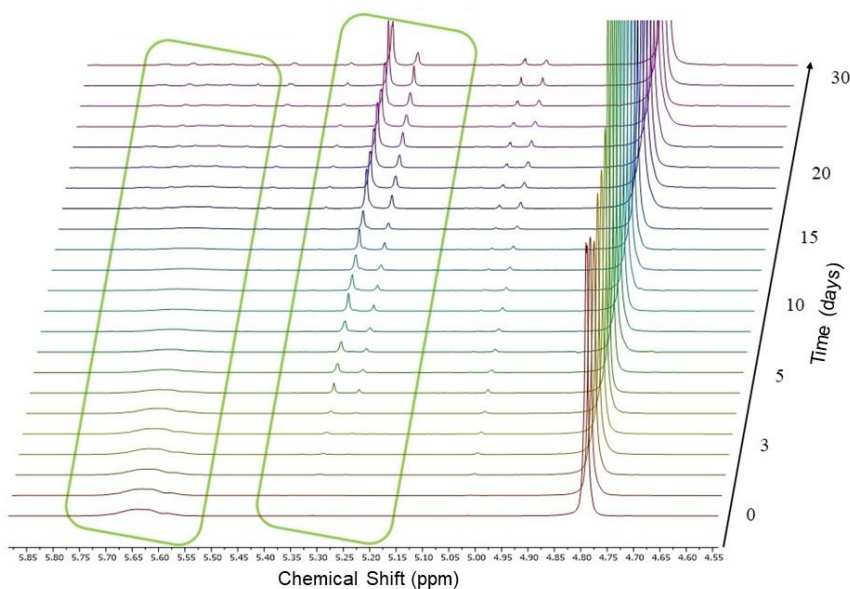


**Figure 2.4** An NMR spectral overlay (400 MHz,  $\text{D}_2\text{O}$ ) of the degradation of PGAM<sub>T</sub> at pH 7 as a representative sample of how degradation was monitored by  $^1\text{H}$  NMR spectroscopy.

To study the degradation of **PGAm<sub>UV</sub>**, two NMR samples were prepared. The first sample was irradiated with UV light while the second NMR sample was kept in the dark to ensure the depolymerization of **PGAm<sub>UV</sub>** is due to the cleavage of the end-cap upon exposure to the UV light. The first sample was irradiated with UV light for 10, 20, 30, 45, and 60 minutes and was checked by NMR at each time point to probe the sufficient irradiation time for maximum degradation. Twenty minutes of UV irradiation was sufficient to obtain the maximum degradation of **PGAm<sub>UV</sub>**, however, it was only degraded to 60% at most (**Figure 2.5a**). Furthermore, no degradation was observed for the **PGAm<sub>UV</sub>** sample that was kept in the dark. Degradation of **PGAm<sub>control</sub>** was monitored under different conditions to ensure that this polymer was stable and that its cleavage was not triggered by the conditions used for triggering the other PGAMs. Its degradation at pH 7, pH 3 (citrate buffer), pH 3 (adjusted using acetic acid), and after 45 minutes of UV irradiation was monitored (**Figure 2.5b**). **PGAm<sub>control</sub>** did not show degradation under any of the investigated conditions, as expected. Degradation of **PGAm<sub>T</sub>** and **PGAm<sub>MMT</sub>** were determined at pH 7 and 3, using citrate buffer to adjust the pH to 3 (**Figure 2.5c** and **Figure 2.5d**). **PGAm<sub>T</sub>** and **PGAm<sub>MMT</sub>** both degraded faster at pH 3. **PGAm<sub>MMT</sub>** degraded within hours while it took weeks for **PGAm<sub>T</sub>** to be fully degraded.

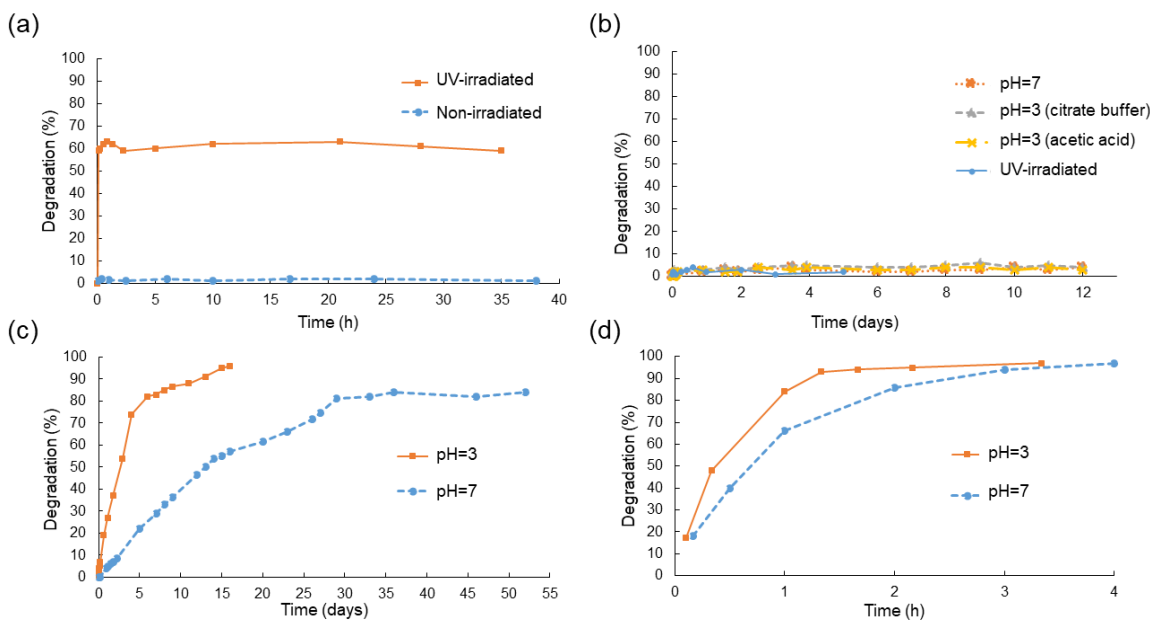


**Figure 2.5** Degradation over time for (a) **PGAM<sub>UV</sub>** after 10, 20, 30, 45, and 60 minutes of irradiation with UV light (b) **PGAM<sub>control</sub>** at pH 7, pH 3 (citrate buffer), pH 3 (adjusted using acetic acid), and after 45 minutes of irradiation with UV light (c) **PGAM<sub>r</sub>** at pH 3 (citrate buffer) and 7 and (d) **PGAM<sub>MMT</sub>** at pH 3 (citrate buffer) and 7.

## 2.2.6 PGAMs as Emulsifiers

The abilities of the PGAMs to stabilize emulsions of hydrophobic polymer particles were investigated. The goal was to use PGAMs as emulsifying agents instead of conventional non-degradable emulsifiers such as PVA.

### Preparation of poly(ester amide) (PEA) particle suspensions

PVA has been previously used by the Gillies group as a surfactant for preparation of PEA (**Figure 2.6**) particle suspensions.<sup>135</sup> PEA was synthesized as previously reported.<sup>3</sup> To study the properties of PGAMs as emulsifiers, they were used as emulsifying agents for preparation of PEA particle suspensions. The particle suspensions were prepared by an emulsification-evaporation method (**Figure 2.7**) in which PGAMs were dissolved in water followed by the addition of  $\text{CH}_2\text{Cl}_2$  containing PEA to the water. The resulting solution was stirred for 10 minutes, and then subjected to sonication while stirring (250-300 rpm) for 90 seconds. The resulting solution was stirred for 4 hours to evaporate off the organic

solvent. After the evaporation of  $\text{CH}_2\text{Cl}_2$ , the particle suspensions were ready for further experiments.  $\text{CH}_2\text{Cl}_2$  was chosen as the organic phase as it is a water immiscible solvent and PEA is soluble in it.

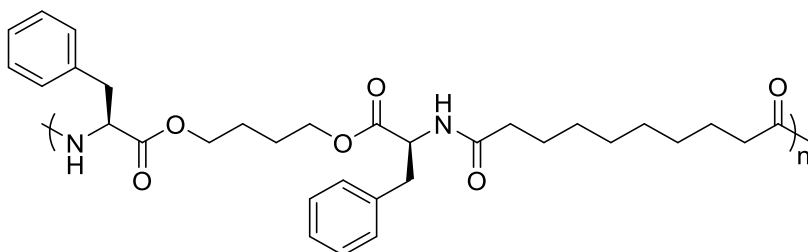


**Figure 2.6** Structure of PEA that was used as the hydrophobic core for the preparation of particle suspensions.

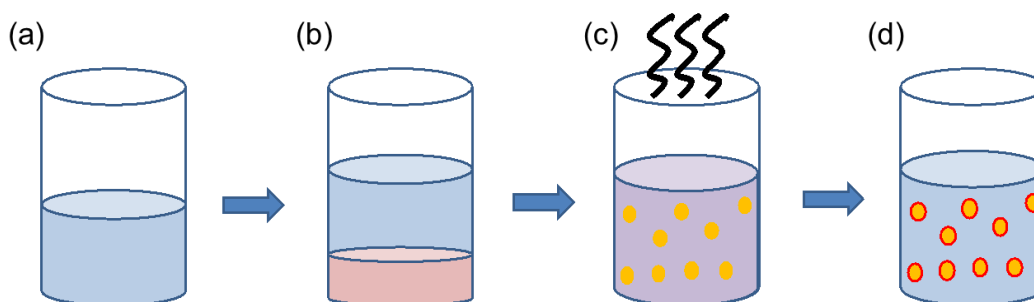


**Figure 2.7** Preparing PEA particle suspensions by the emulsification-evaporation method. (a) PGAm dissolved in water (b) organic phase containing PEA added to the first solution (c) solution subjected to sonication and then stirred for 4 hours to evaporate off  $\text{CH}_2\text{Cl}_2$  and (d) prepared particle suspensions by the emulsification-evaporation method.

### Preparation of PEA particle suspensions using partially acylated PGAMs as emulsifying agents

PVA used as an emulsifier typically has 5 – 15% of its pendent alcohol groups acetylated. To mimic the amphiphilic properties of PVA, the synthesized partially acylated PGAMs (**Scheme 2.4**) were used as emulsifying agents for preparation of PEA particle suspensions. First, **PGAM<sub>ac-5</sub>** and **PGAM<sub>ac-10</sub>** were used for preparation of particle suspensions. PEA

particle suspensions were prepared at different concentrations of emulsifying agents and solvent ratios (**Table 2.3** and **2.4**) and monitored by DLS after preparation. The concentration of emulsifying agents and solvent ratios were selected based on the previous studies by the Gillies group on PEA particle suspension preparation.<sup>135, 145</sup> For all experiments, the resulting particle suspensions were assessed both quantitatively and qualitatively. For the qualitative assessment, photos of the resulting suspensions were taken. As the particles were formed and remained stable, the solution became opaque and milky while unstable particles resulted in aggregation and eventually, sedimentation of PEAs which was observable with naked eyes (**Figure 2.8**).

**Table 2.3** DLS results for PEA particle suspensions prepared using **PGAm<sub>ac-5</sub>** and **PGAm<sub>ac-10</sub>** as the emulsifying agents. Ratio of water:CH<sub>2</sub>Cl<sub>2</sub> was 3:1 (% V/V). The mass of PEA was fixed at 10 mg.

<b>Emulsifying agent</b>	<b>Mass of emulsifying agent (mg)</b>	<b>Volume of water (mL)</b>	<b>Volume of CH<sub>2</sub>Cl<sub>2</sub> (mL)</b>	<b>Z-average diameter (nm)</b>	<b>Polydispersity index (PDI)</b>
<b>PGAm<sub>ac-5</sub></b>	10	3.0	1.0	300 ± 30	0.40 ± 0.10
<b>PGAm<sub>ac-5</sub></b>	20	3.0	1.0	3000 ± 1000	0.80 ± 0.25
<b>PGAm<sub>ac-10</sub></b>	10	3.0	1.0	300 ± 200	0.30 ± 0.10
<b>PGAm<sub>ac-10</sub></b>	20	3.0	1.0	10 ± 10	0.30 ± 0.10

**Table 2.4** DLS results for PEA particles prepared using **PGAm<sub>ac-5</sub>** and **PGAm<sub>ac-10</sub>** as the emulsifying agents. Ratio of water:CH<sub>2</sub>Cl<sub>2</sub> was 2:1 (% V/V). The mass of PEA was fixed at 10 mg.

Emulsifying agent	Mass of emulsifying agent (mg)	Volume of water (mL)	Volume of CH <sub>2</sub> Cl <sub>2</sub> (mL)	Z-average diameter (nm)	Polydispersity index (PDI)
<b>PGAm<sub>ac-5</sub></b>	10	2.0	1.0	100	0.30
<b>PGAm<sub>ac-5</sub></b>	20	2.0	1.0	10	0.30
<b>PGAm<sub>ac-10</sub></b>	10	2.0	1.0	20	0.10
<b>PGAm<sub>ac-10</sub></b>	20	2.0	1.0	$1 \times 10^5$	0.90

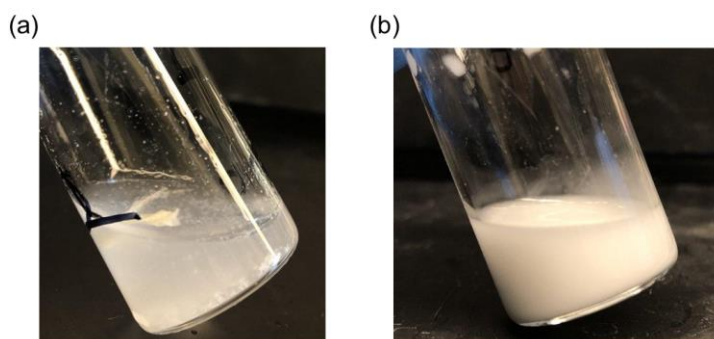


**Figure 2.8** Representative samples of how PEA particle suspensions were monitored qualitatively (a) unstable PEA particle suspensions (b) stable PEA particle suspensions. Stable particle suspensions were opaque and milky while unstable particles resulted in aggregation and eventually, sedimentation of PEAs.

Even though a small degree of hydrophobicity was imparted by installing 5% or 10% acetyl groups on the pendent hydroxyls, the final solutions were all transparent with large PEA aggregates observed, rather than milky and opaque, indicating that particles did not form or were destabilized during the preparation process.

The failure of **PGAm<sub>ac-5</sub>** and **PGAm<sub>ac-10</sub>** to stabilize PEA particles might be due to their poor solubility in water. **PGAm<sub>ac-5</sub>** and **PGAm<sub>ac-10</sub>** are more hydrophilic compared to **PGAm<sub>hex-5</sub>**, **PGAm<sub>hex-10</sub>**, **PGAm<sub>lau-5</sub>**, and **PGAm<sub>lau-10</sub>**. Hence, it was predictable that the remaining of partially acylated PGAMs would also not likely be suitable to prepare and stabilize PEA particle suspensions. To further confirm the ineffectiveness of these more hydrophobic derivatives, they were investigated in PEA particle preparation, but no stable particle suspensions were obtained.

As partially acylated PGAMs were not effective as emulsifying agents for PEA particle preparation, the focus was then placed on the non-acylated PGAMs, which are more hydrophilic, yet could still exhibit amphiphilic properties due to their hydrophobic backbones and hydrophilic pendent groups.

#### **Preparation of PEA particle suspensions using PGAM<sub>UV</sub>**

The initial ethanolamine functionalized **PGAM<sub>UV</sub>** with no ester groups was then investigated as the emulsifying agent to prepare PEA particle suspensions. **PGAM<sub>UV</sub>** was chosen for the initial work, as it is stable and does not undergo degradation as long as it is kept in the dark while **PGAM<sub>T</sub>** and **PGAM<sub>MMT</sub>** undergo degradation in water. In preliminary experiments, compared to acylated PGAMs, **PGAM<sub>UV</sub>** was more effective in emulsifying PEA particles, as shown by quantitative and qualitative assessments (**Figure 2.9**). Therefore, the effect of parameters such as concentration of emulsifying agent and solvent ratio were investigated.

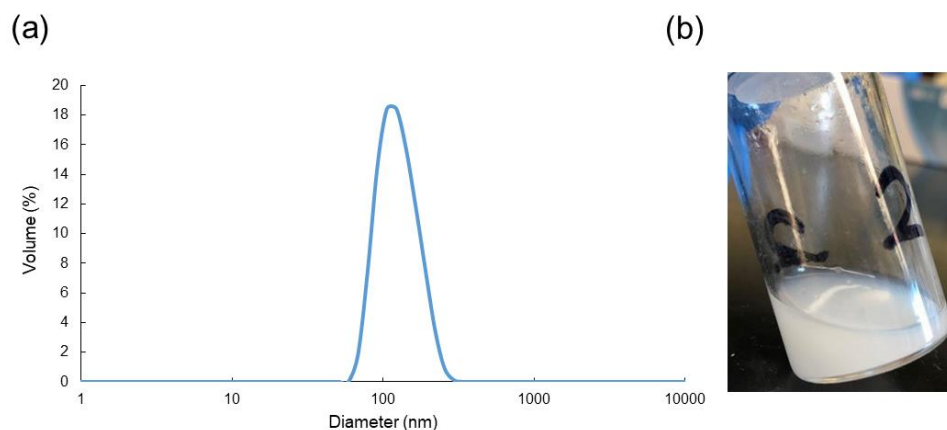


**Figure 2.9** Preliminary results of PEA particle suspensions using **PGAm<sub>UV</sub>** as the emulsifying agent. (a) DLS results and (b) the photo of the resulting suspension indicating the formation of PEA particles.

First, the ratio of water:CH<sub>2</sub>Cl<sub>2</sub> was studied at two different emulsifying agent:PEA ratios. The amount of PEA was fixed at 10 mg, which was dissolved in 1 mL of CH<sub>2</sub>Cl<sub>2</sub> and added to 6 different samples of water containing **PGAm<sub>UV</sub>**. The prepared particle suspensions were evaluated by DLS (**Table 2.5**). From an environmental or biological application perspective, using lower fractions of organic solvent is preferable. However, the PDIs of the particles in experiments 1 and 2 were higher than those in experiments 3 and 4. With regards to the water:CH<sub>2</sub>Cl<sub>2</sub> ratios of 3:1 and 2:1, both ratios resulted in particles with similar sizes and low PDIs. Therefore, a ratio of 3:1 was selected for the solvent ratio as it uses a lower percentage of the organic solvent.



**Table 2.5** DLS results for PEA particle suspensions prepared at various ratios of water:CH<sub>2</sub>Cl<sub>2</sub>. The mass of PEA was fixed at 10 mg.

Experiment number	Mass of PGAm <sub>UV</sub> (mg)	Volume of water (mL)	Volume of CH <sub>2</sub> Cl <sub>2</sub> (mL)	Z-average diameter (nm)	Polydispersity index (PDI)
1	10	5.0	1.0	2200 ± 800	0.70 ± 0.18
2	20	5.0	1.0	150 ± 50	0.20 ± 0.09
3	10	3.0	1.0	180 ± 40	0.10 ± 0.02
4	20	3.0	1.0	140 ± 30	0.10 ± 0.04
5	10	2.0	1.0	180 ± 40	0.30 ± 0.04
6	20	2.0	1.0	150 ± 30	0.30 ± 0.05

Next, the ratio of PGAm<sub>UV</sub>:PEA was varied (**Table 2.6**). PEA was dissolved in 1 mL of CH<sub>2</sub>Cl<sub>2</sub> and added to 3 mL of water containing the PGAm<sub>UV</sub>. Ideally, a low ratio of PGAm<sub>UV</sub>:PEA would be used to minimize any toxicity arising from the surfactant. Although particles were detected by DLS (**Table 2.6**), qualitative evaluations showed clearly that it was not possible to effectively emulsify the PEA into particles using the 1:1 ratio (**Figure 2.10a**). However, the 2:1 ratio was more effective and no further benefits in terms of particle diameter or reproducibility were obtained using the 3:1 or 4:1 ratio so the 2:1 ratio was selected for further work. TEM image of the particle suspension prepared at the 2:1 ratio of PGAm<sub>UV</sub>:PEA, confirmed the formation of spherical PEA particles (**Figure 2.11a**). In addition to the TEM image, photo (**Figure 2.11b**) and DLS result (**Figure 2.11c**) of the particle suspension confirmed the formation of PEA particles as further qualitative and quantitative assessments.

**Table 2.6** DLS results for PEA particles prepared at two different ratios of emulsifying agent to PEA.

Experiment number	Mass of PGAm <sub>UV</sub> (mg)	Mass of PEA (mg)	Z-average diameter (nm)	Polydispersity index (PDI)
1	10	10	200 ± 20	0.10 ± 0.08
2	20	10	160 ± 30	0.20 ± 0.03
3	30	10	190 ± 50	0.10 ± 0.06
4	40	10	150 ± 40	0.20 ± 0.05

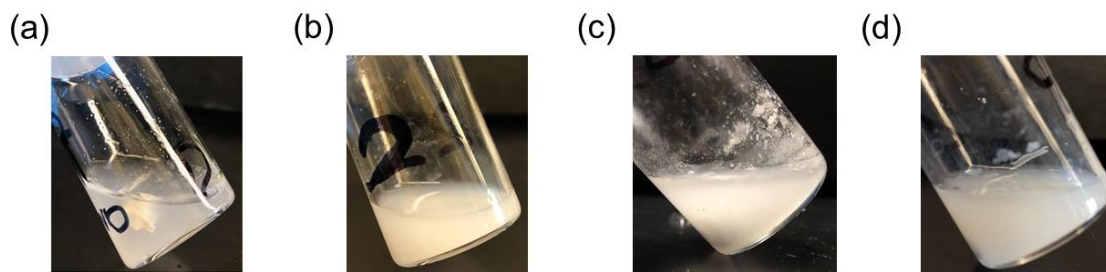


**Figure 2.10** Representative samples of PEA particle suspensions from (a) experiment 1 (b) experiment 2 (c) experiment 3 and (d) experiment 4 in **Table 2.6**, showing that emulsions were effectively obtained for the 2:1,3:1, and 4:1 ratios but not for the 1:1 ratio.

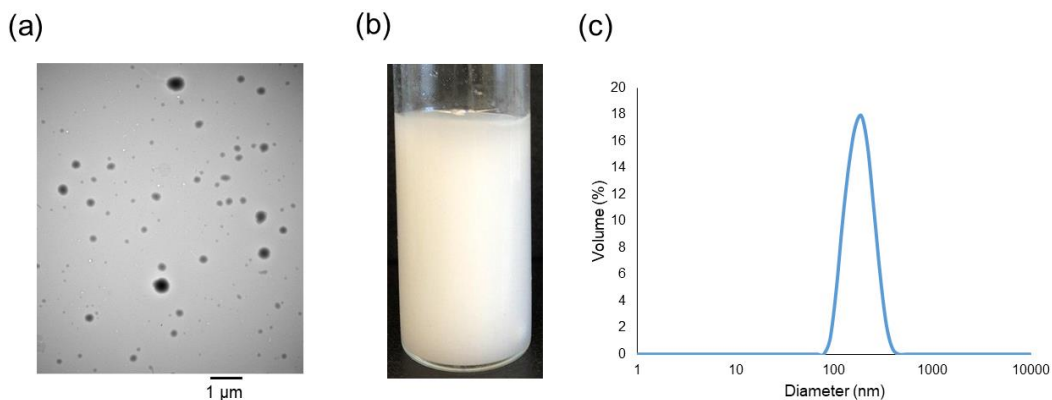


**Figure 2.11** (a) TEM image, (b) photo, and (c) DLS result of the PEA particle suspension that was prepared at the optimized conditions confirming the formation of PEA particles.

### Preparation of PEA particles using **PGAm<sub>T</sub>** and **PGAm<sub>MMT</sub>**

In spite of the fact that **PGAm<sub>UV</sub>** serves as an ideal model system,<sup>63</sup> it may not be suitable for potential biological applications as it only undergoes degradation upon exposure to UV light. Therefore, **PGAm<sub>T</sub>** and **PGAm<sub>MMT</sub>** were also investigated as emulsifying agents in this regard. In addition, PEA particle suspensions were also prepared using the synthesized non-responsive **PGAm<sub>control</sub>** as a control for further experiments. **PGAm<sub>T</sub>** and **PGAm<sub>MMT</sub>** possess trityl and 4-monomethoxytrityl end-caps, respectively, which are acid sensitive. PEA particle suspensions were prepared using **PGAm<sub>control</sub>**, **PGAm<sub>T</sub>**, and **PGAm<sub>MMT</sub>** as their emulsifying agents at two different concentrations of emulsifying agent and monitored by DLS after the preparation (**Table 2.7**). The ratio of 2:1 for **PGAm**:PEA, which was also successful for **PGAm<sub>UV</sub>**, resulted in particles with lower PDIs compared to the particles prepared at the ratio of 1:1. Therefore, the ratio of 2:1 was selected for further experiments. Based on the degradation studies, more than 70% of **PGAm<sub>MMT</sub>** (**Figure 2.5d**) degrades within two hours upon dissolution in water. However, **PGAm<sub>MMT</sub>** used in PEA particle preparation was present in the emulsion for 4 hours before being monitored by DLS. We hypothesize that **PGAm<sub>MMT</sub>** degraded more slowly in the suspension as it is surrounded not only by water but also by PEA particles and  $\text{CH}_2\text{Cl}_2$  during this time.

**Table 2.7** DLS results for the particle suspensions prepared using **PGAm<sub>T</sub>**, **PGAm<sub>MMT</sub>**, and **PGAm<sub>control</sub>** as emulsifying agents.

<b>Polymers used as the emulsifying agent</b>	<b>Mass of emulsifying agent (mg)</b>	<b>Mass of PEA (mg)</b>	<b>Z-average diameter (nm)</b>	<b>Polydispersity index (PDI)</b>
<b>PGAm<sub>T</sub></b>	10	10	260 ± 20	0.30 ± 0.06
<b>PGAm<sub>T</sub></b>	20	10	280 ± 10	0.20 ± 0.06
<b>PGAm<sub>MMT</sub></b>	10	10	230 ± 100	0.30 ± 0.05
<b>PGAm<sub>MMT</sub></b>	20	10	250 ± 60	0.20 ± 0.03
<b>PGAm<sub>control</sub></b>	10	10	250 ± 20	0.30 ± 0.05
<b>PGAm<sub>control</sub></b>	20	10	240 ± 10	0.20 ± 0.04

### **Triggered degradation of PGAm-stabilized PEA particle suspensions**

The main advantage of PGAm<sub>s</sub> over conventional emulsifying agents is their self-immolative characteristic, which allows them to be degraded in a triggered manner. Hence, their degradation was investigated. PEA particle suspensions were prepared using the conditions selected as described above, and the particle suspensions were monitored qualitatively and quantitatively after exposure to the appropriate stimulus.

First, PEA particle suspensions having **PGAm<sub>UV</sub>** as emulsifying agent were investigated. Samples were prepared using **PGAm<sub>UV</sub>** and **PGAm<sub>control</sub>**, as the control experiment. Based on the degradation studies (**Figure 2.5a**), 20 minutes of UV exposure is sufficient to reach the highest possible degradation for **PGAm<sub>UV</sub>** sample in NMR tube. However, particles were irradiated with UV light for 90 minutes to ensure the highest possible degradation

was achieved. Four sets of samples were prepared. First, particles were prepared using **PGAm<sub>UV</sub>** and irradiated with the UV light (**PGAm<sub>UV-irrad</sub>**). A second set of samples were prepared using the same polymer but without the UV irradiation and were kept in dark throughout the experiment (**PGAm<sub>UV-non-irrad</sub>**). A third set of samples were prepared using **PGAm<sub>control</sub>** as their emulsifying agent which were irradiated with UV light for 90 minutes (**PGAm<sub>control-irrad</sub>**). Last, a set of samples were prepared using **PGAm<sub>control</sub>** and were kept in dark throughout the experiment (**PGAm<sub>control-non-irrad</sub>**). The samples were then monitored by DLS over time.

It was expected that we would observe selectively a change in diameter of the **PGAm<sub>UV-irrad</sub>** (**Figure 2.12a**) particles by DLS. As UV light triggered the depolymerization of emulsifying agent, the PEA particles were expected to aggregate, leading to an increase in diameter. However, no substantial changes in diameter were observed for any of the different particle samples. This result may be due to the fact that the ratio of **PGAm<sub>UV</sub>**:PEA was 2:1 while **PGAm<sub>UV</sub>** only degrades up to 60%, leaving sufficient polymer to coat the particles. Another possibility is that size measurement by DLS is not an effective method to assess changes as it may not represent the entire system. For instance, a portion of particles might aggregate and sediment, while the remaining suspended particles have the same diameter.

Therefore, the count rate was also measured for the different particle samples over time. Count rate in DLS represents the number photons detected and is reported as kilo counts per second (kCPS). Count rate is mainly dependent on mass and concentration of particles.<sup>146</sup> For instance, an increase or decrease in count rate would be a sign of aggregation or sedimentation of particles, respectively.<sup>147</sup> For these measurements, instrument parameters such as the attenuator were fixed, to allow comparisons between different count rate measurements over time. If the particles aggregated and then sedimented, we expected to observe first an increase, then a decrease in the count rate. However, increases in count rates were observed for all four sets of samples (**Figure 2.12b**), indicating that they were all likely aggregating to a certain extent, suggesting a lack of stability of the particle suspensions.

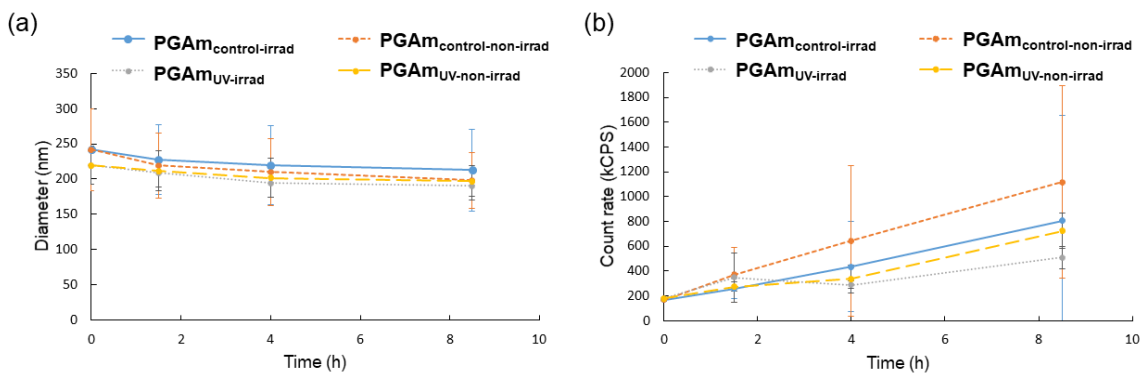


**Figure 2.12** (a) size and (b) count rate results. DLS was conducted after particle preparation, 90 minutes of irradiation with UV light, and later on after 2.5 and 7 hours of the UV irradiation. No noticeable changes in the diameters were observed while increases in count rates were observed for all samples indicating that they were all likely aggregating.

Next, PEA particle suspensions having **PGAm<sub>T</sub>** and **PGAm<sub>MMT</sub>** as their emulsifying agents were investigated. **PGAm<sub>T</sub>** and **PGAm<sub>MMT</sub>** are acid-sensitive and undergo degradation under acidic conditions. Citric acid/sodium hydroxide buffer (0.1 M) and phosphoric acid/potassium hydroxide buffer (0.1 M) with pH 3 and 7, respectively, were prepared and added to the particles after their preparation to adjust the pH values of the suspensions. However, the particle suspensions were immediately destabilized after the addition of both buffers with pH 3 and 7 (**Figure 2.13**). We believe that increasing the ionic strength of the solutions due to the addition of salt may destabilize the particle suspensions.<sup>148</sup>

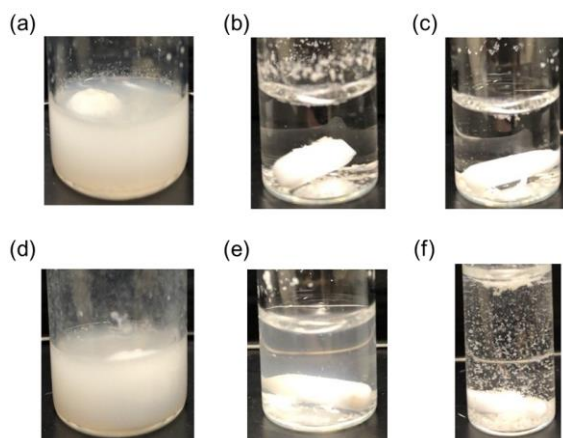


**Figure 2.13** Photos of PEA particle suspensions prepared using **PGAm<sub>T</sub>** as the emulsifying agent (a) after preparation (b) after the addition of buffer with pH 7 and (c) after the addition of buffer with pH 3. PEA particle suspensions prepared using **PGAm<sub>MMT</sub>** as the emulsifying agent (d) after preparation (e) after the addition of buffer with pH 7 and (f) after the addition of buffer with pH 3. Both sets of particles aggregated upon the addition of buffer.

Instead, acetic acid (0.1 M) was added to adjust the pH values to 3 for samples of PEA particle suspensions prepared using **PGAm<sub>T</sub>**, **PGAm<sub>MMT</sub>**, and **PGAm<sub>control</sub>** as emulsifying agents. Additionally, samples of the same sets of particles without the addition of acetic acid were studied to monitor the effect of acetic acid on the PEA particle suspensions. However, as for **PGAm<sub>UV</sub>** after irradiation, no significant trends were observed for the diameter or count rate for **PGAm<sub>control</sub>** and **PGAm<sub>T</sub>** (**Figure 2.14**). However, the diameter of particles prepared using **PGAm<sub>MMT</sub>** at pH 3 showed the expected size increase as a result of aggregation followed by a decrease in diameter resulting from sedimentation of aggregated PEA particles (**Figure 2.14c**). Overall, the DLS results were not completely in agreement with our initial assumption regarding the behaviour of particle suspensions upon the application of stimulus. This discrepancy could be either due to the ineffectiveness of DLS as a method to assess changes in the system or instability of the proposed system.

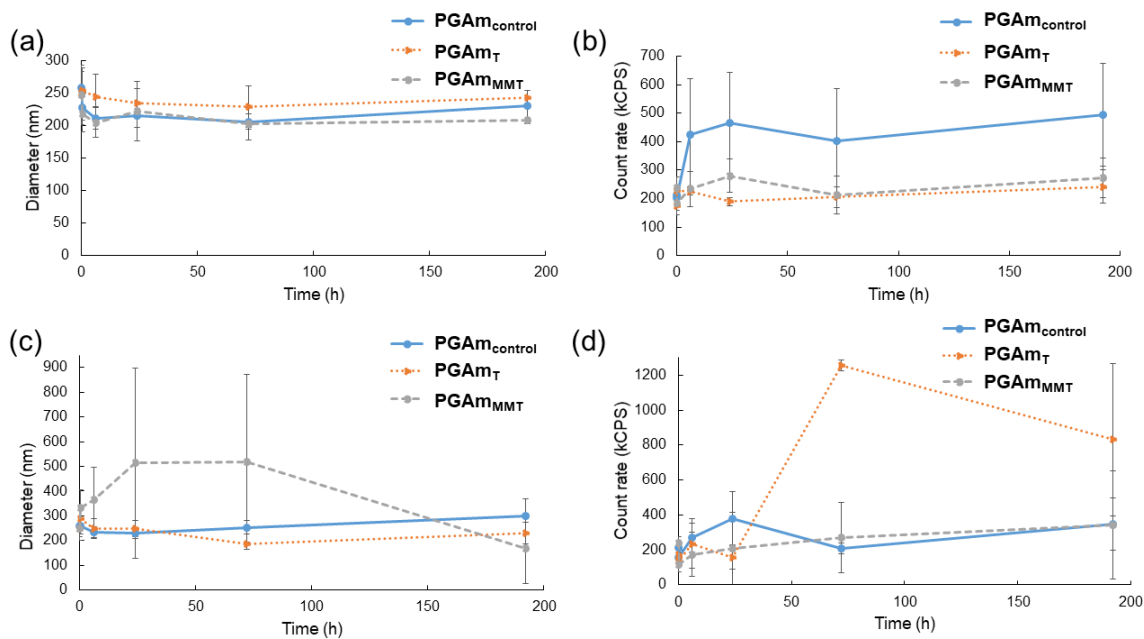


**Figure 2.14** DLS results for PEA particle suspensions prepared using **PGAm<sub>control</sub>**, **PGAm<sub>T</sub>**, and **PGAm<sub>MMT</sub>** as emulsifying agents. (a) Diameter and (b) count rate at pH 7; (c) diameter and (d) count rate at pH 3. Acetic acid (0.1 M) was added to adjust the pH values to 3. The **PGAm<sub>MMT</sub>** sample at pH 3 seemed to show the expected size increase followed by a decrease.

### 2.2.7 Nile Red as a Probe for PEA Particle Aggregation

Nile red was used as an additional probe to study the behaviour of the particle suspensions in response to stimuli. Nile red is a hydrophobic dye which is highly fluorescent in hydrophobic environments but undergoes aggregation and fluorescence quenching in water. It has been widely used as a stain for imaging and in biological applications.<sup>149-151</sup>

In this work, Nile red was dissolved in  $\text{CH}_2\text{Cl}_2$  during the particle preparation process. As it is not soluble in water, it remained inside the hydrophobic particles rather than in the aqueous phase. As long as it remained inside the particles (which was expected, as they should not degrade over the time scale of the experiment), and the particles remain fully suspended in the solution, its fluorescence was expected to remain constant. On the other hand, it was expected that a decrease in fluorescence intensity would be observed after the



application of the stimulus as degradation of emulsifying agent should lead to the destabilization of the particle suspension, followed by aggregation and sedimentation.

First, Nile red was used to study **PGAm<sub>control</sub>**, **PGAm<sub>T</sub>**, and **PGAm<sub>MMT</sub>** coated PEA particles. After their preparation, the particle suspensions were adjusted to pH 3 or 7. The resulting particle suspensions were monitored qualitatively (**Figure 2.15**) and quantitatively (**Figures 2.16** and **2.17**). Particle suspensions prepared using **PGAm<sub>MMT</sub>** at pH 3 (**Figure 2.15i**) showed the most destabilization, as expected, with the observation of large aggregates on the side of the vial. However, **PGAm<sub>control</sub>** particle suspension at pH 3 (**Figure 2.15c**) were also partly destabilized, which could be due to the disruption of the system caused by the addition of acetic acid. The addition of acetic acid also induced the instability of particles prepared by trityl-based end-caps (**Figures 2.15f**) that are acid-sensitive, but given the similar instability of the control, we cannot confirm that the aggregation arose from depolymerization of **PGAm<sub>T</sub>**. Changes in the fluorescence intensities over time for the particle suspensions were in agreement with the qualitative observations. In particular, **PGAm<sub>MMT</sub>** coated particle suspensions at pH 3 (**Figures 2.15i** and **2.16b**) exhibited an 80% drop in fluorescence over the first 3 hours, while less than a 50% drop in fluorescence was observed for all of the other systems over 50 hours. This drop in fluorescence confirms the gradual destabilization of the PGAm-coated PEA particles over time, which is also in agreement with the qualitative observations of the Nile red-loaded particles and the non-loaded particles that were measured by DLS.

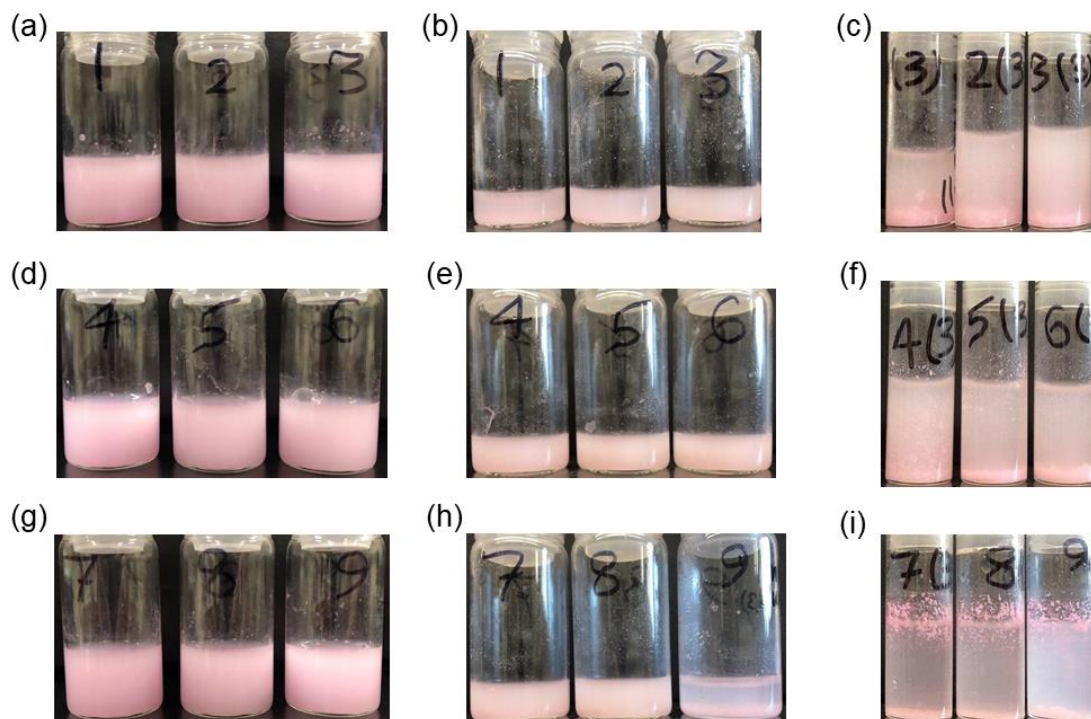


**Figure 2.15** Photos of PGAM-coated PEA particle suspensions using **PGAm<sub>control</sub>**, **PGAm<sub>T</sub>**, and **PGAm<sub>MMT</sub>** as their emulsifying agents. (a) **PGAm<sub>control</sub>** after preparation, (b) **PGAm<sub>control</sub>** after 2 days at pH 7, (c) **PGAm<sub>control</sub>** after 2 days at pH 3, (d) **PGAm<sub>T</sub>** after preparation, (e) **PGAm<sub>T</sub>** after 2 days at pH 7, (f) **PGAm<sub>T</sub>** after 2 days at pH 3, (g) **PGAm<sub>MMT</sub>** after preparation, (h) **PGAm<sub>MMT</sub>** after 2 days at pH 7, (i) **PGAm<sub>MMT</sub>** after 2 days at pH 3. Showing the destabilization of **PGAm<sub>MMT</sub>** coated PEA particle suspensions as a result of the degradation of **PGAm<sub>MMT</sub>**.

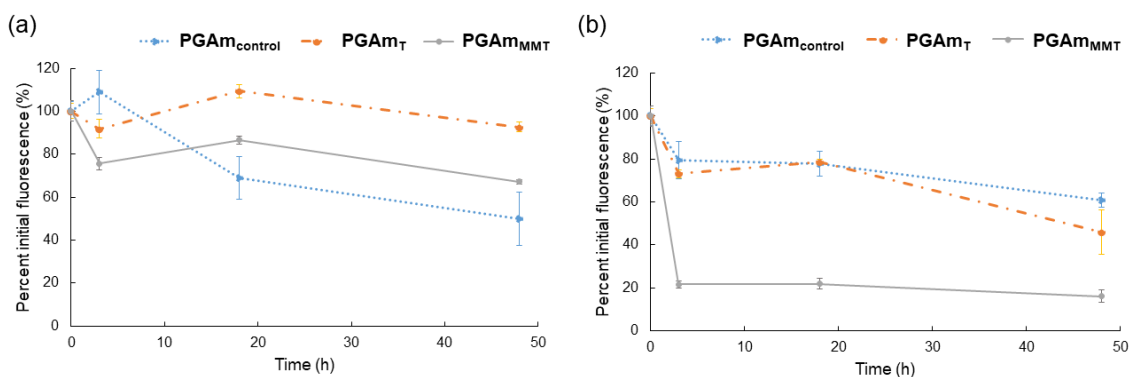


**Figure 2.16** Fluorescence intensity versus time for PGAm-coated PEA particles over time at (a) pH 7 and (b) pH 3 suggesting rapid destabilization and aggregation of the **PGAm<sub>MMT</sub>**-coated particle suspensions at pH 3.

DLS was also used to probe the behaviour of the Nile red-loaded particles (**Figure 2.17**). The results were very similar to those for the particles without Nile red (**Figures 2.14** and **2.12**) in that it was not possible to capture the obvious sedimentation observed for the **PGAm<sub>MMT</sub>** system at pH 3 by DLS, perhaps because the fraction remaining suspended and thus detected in the DLS measurement was not representative of the whole sample.

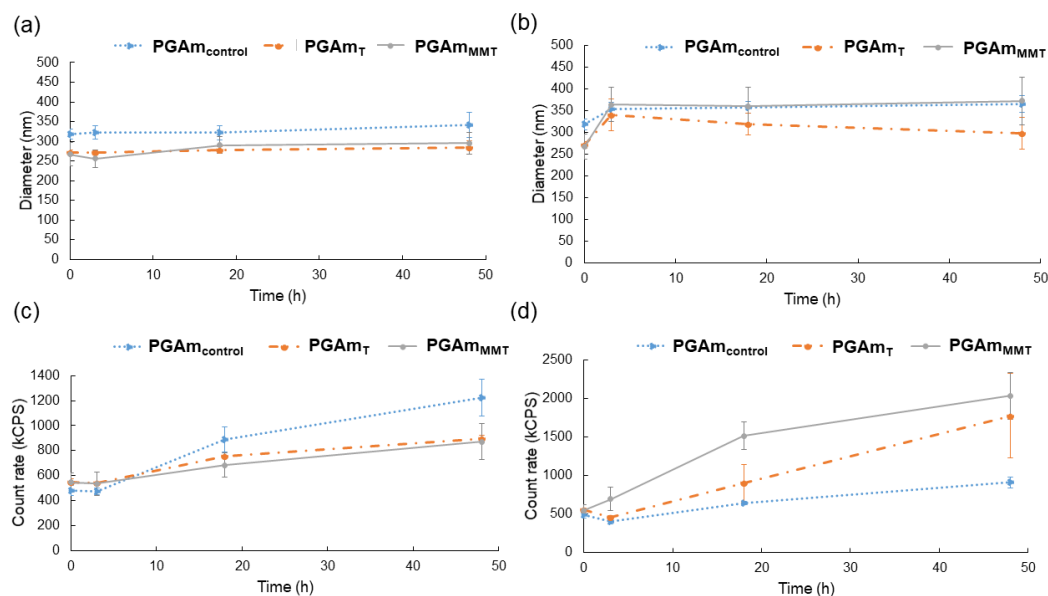


**Figure 2.17** DLS results for PEA particles after their preparation and over time. (a) Diameters of the particles at pH 7 (b) diameter of the particles at pH 3 (c) count rates of the particle suspensions at pH 7 and (d) count rates of the particle suspensions at pH 3.

Nile red was also used in preparing PEA particles using **PGAm<sub>control</sub>** and **PGAm<sub>UV</sub>** as their emulsifying agents. First, the particle suspensions were prepared using **PGAm<sub>UV</sub>** and irradiated with the UV light (**PGAm<sub>UV-irrad</sub>**). A second set of samples was prepared using the same polymer without the irradiation of the UV light, and was kept in dark throughout the experiment (**PGAm<sub>UV-non-irrad</sub>**). A third set of samples was prepared using **PGAm<sub>control</sub>** as their emulsifying agent and irradiated with the UV light for 90 minutes (**PGAm<sub>control-irrad</sub>**). Finally, a set of samples was prepared using **PGAm<sub>control</sub>** and kept in dark throughout the experiment (**PGAm<sub>control-non-irrad</sub>**). The resulting particle suspensions were monitored qualitatively (**Figure 2.18**) and quantitatively (**Figures 2.19** and **2.20**). There was a decrease in fluorescence intensity (**Figure 2.19**) of both **PGAm<sub>control-irrad</sub>** and **PGAm<sub>UV-irrad</sub>** which might be due to the photobleaching of Nile red during the 90 min of UV irradiation.<sup>152</sup> The fluorescence results (**Figure 2.19**) were compatible with the qualitative observations, as the colours of particle suspensions were dark pink to purple after preparation and faded to pale pink (**Figures 2.18f** and **2.18h**) after the application of the UV light.

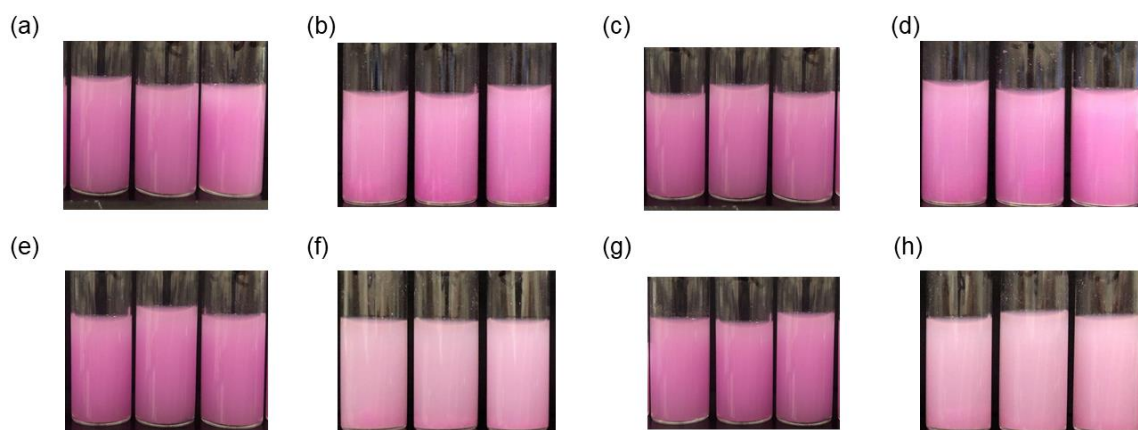


**Figure 2.18** Photos of PGAM-coated PEA particle suspensions (a) **PGAm<sub>control-non-irrad</sub>** after preparation, (b) **PGAm<sub>control-non-irrad</sub>** after 2 days, (c) **PGAm<sub>UV-non-irrad</sub>** after preparation, (d) **PGAm<sub>UV-non-irrad</sub>** after 2 days, (e) **PGAm<sub>control-irrad</sub>** after preparation, (f) **PGAm<sub>control-irrad</sub>** after 2 days, (g) **PGAm<sub>UV-irrad</sub>** after preparation, (h) **PGAm<sub>UV-irrad</sub>** after 2 days. No noticeable changes were observed except changes in the colours of particle suspensions after UV irradiation which was due to the photobleaching of Nile red during UV irradiation.

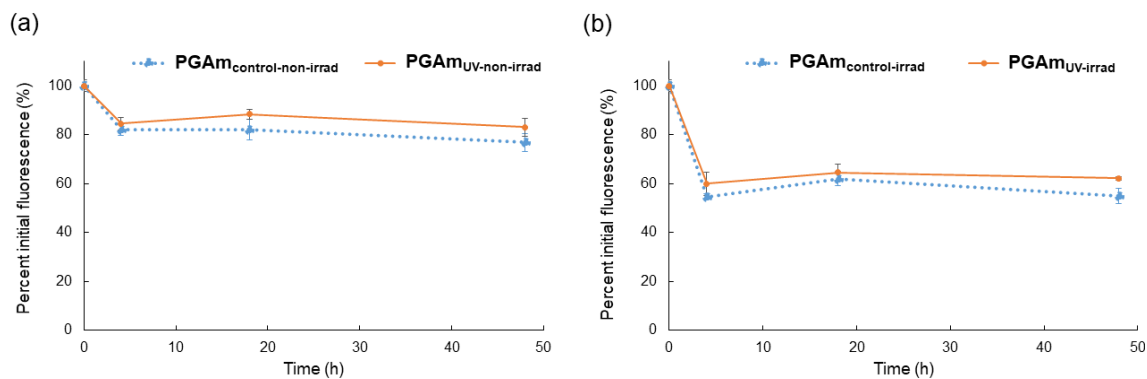


**Figure 2.19** Fluorescence intensity versus time for PGAM-coated PEA particle suspensions. (a) Samples were kept in the dark and (b) samples irradiated with UV light for 90 minutes after their preparation, suggesting the photobleaching of Nile red during the 90 min of UV irradiation.

There were decreases in count rates of all the prepared particles which we attribute to the general destabilization and sedimentation of a portion of particles over time (**Figure 2.20**). Unfortunately, as noted above, it was not possible to induce detectable selective aggregation of the particles prepared by **PGAm<sub>uv</sub>** by the application of UV light, likely because **PGAm<sub>uv</sub>** can only degrade to 60% at most (**Figure 2.5a**), leaving a substantial percentage of the polymer remaining on the particles. In addition, the solutions are turbid, which may make it difficult for the UV light to reach all of the UV-responsive end-caps.

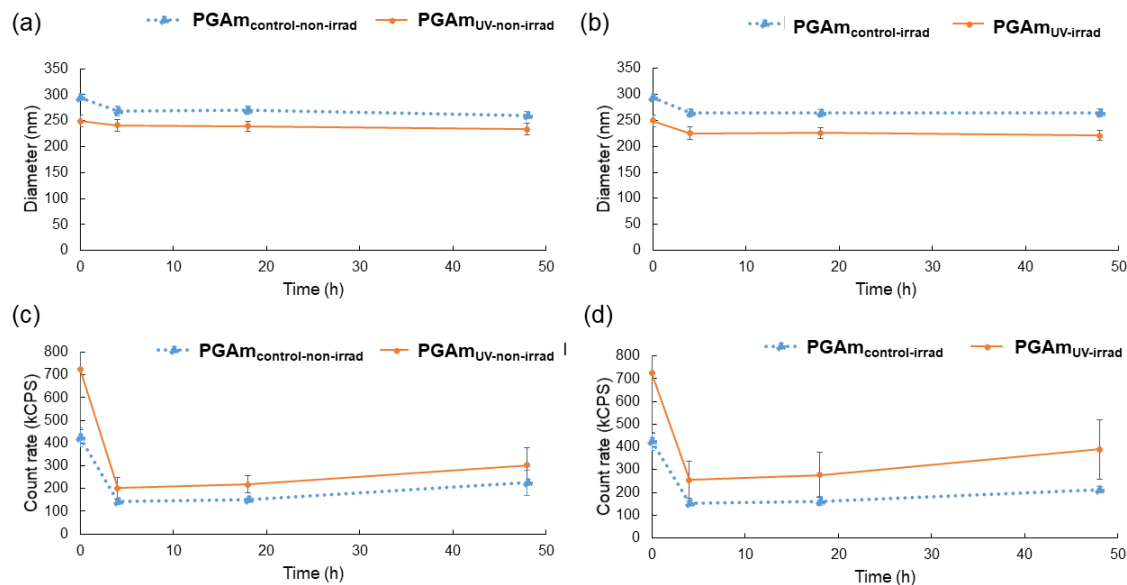


**Figure 2.20** DLS results for PGAm-coated PEA particle suspensions after their preparation and over 48 hours. (a) Diameter and (c) count rates for **PGAm<sub>control-non-irrad</sub>** and **PGAm<sub>UV-non-irrad</sub>**; (b) Diameter and (d) count rates for **PGAm<sub>control-irrad</sub>** and **PGAm<sub>UV-irrad</sub>**. Decreases in count rates were attributed to the general destabilization and sedimentation of the PEA particle suspensions.

Overall, for the PGAm coated PEA particles, it was apparent that the addition of acid to the **PGAm<sub>MMT</sub>** coated particles led to their aggregation and sedimentation more rapidly than for **PGAm<sub>T</sub>** or **PGAm<sub>control</sub>** coated particles. On the other hand, UV light was not effective as a stimulus for triggering the aggregation and sedimentation of the **PGAm<sub>UV</sub>** coated PEA particle suspensions compared to controls. In addition, all of the suspensions were unstable over time, making it difficult to demonstrate their stimuli-responsive properties quantitatively. Lack of long-term stability of the suspensions would also be problematic in applications.

### PGAm-coated poly(lactic acid) (PLA) particle suspensions

While PEA particles have been investigated in the Gillies lab,<sup>135</sup> the limited stability of the PGAm-coated PEA particle suspensions motivated us to examine other polymer particles. Poly-L-lactide (PLLA) has been commonly used for the preparation of micro- and nano-sized particles for drug delivery applications.<sup>153</sup>

Therefore, we examined the use of PLA in the particle preparation instead of the PEA following the same procedure used for PEA particle preparation, with encapsulated Nile red. First, PLA was used to prepare particle suspensions using **PGAm<sub>control</sub>**, **PGAm<sub>T</sub>**, and **PGAm<sub>MMT</sub>** as the emulsifying agents. The resulting particle suspensions were then adjusted to pH 3 or 7, and were monitored qualitatively (**Figure 2.21**) and quantitatively (**Figures 2.22** and **2.23**). Particle suspensions prepared using **PGAm<sub>MMT</sub>** at pH 3 (**Figure 2.21i**) showed the most destabilization, as expected. However, particles prepared by **PGAm<sub>control</sub>** at pH 3 (**Figure 2.21c**) were also partly destabilized, which as for the PEAs could be due to the disruption of the system caused by the addition of acetic acid or the instability of the control system. The addition of acetic acid to the **PGAm<sub>T</sub>**-coated particles also led to aggregation (**Figure 2.21f**), but as for the analogous PEA particles, we cannot confirm that this destabilization arose from the pH-sensitivity of **PGAm<sub>T</sub>**.

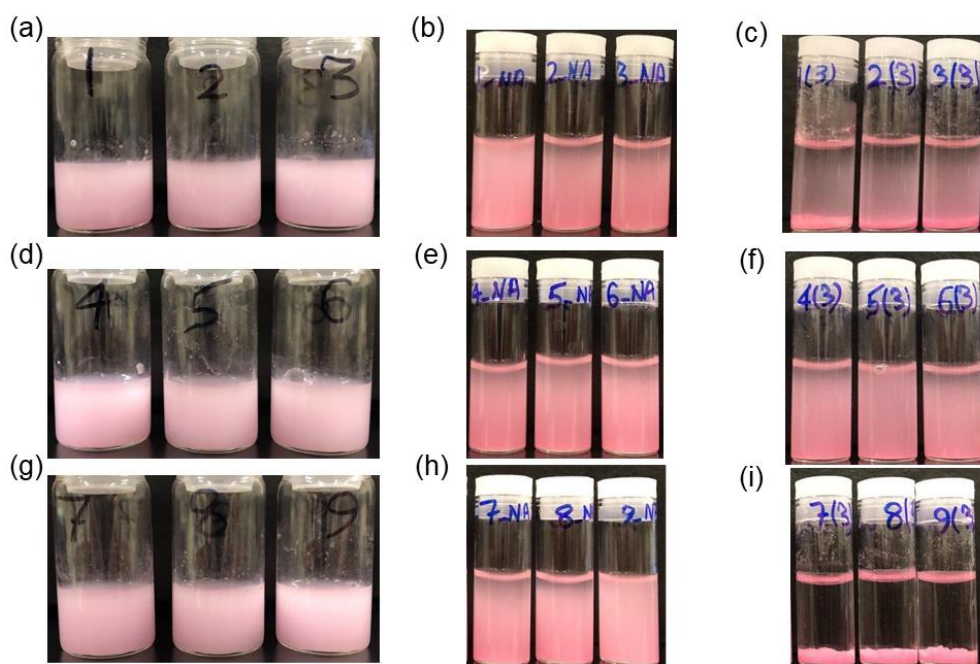


**Figure 2.21** Photos of PGAm-coated PLA particles: (a) **PGAm<sub>control</sub>** after preparation (b) **PGAm<sub>control</sub>** after 2 days at pH 7 (c) **PGAm<sub>control</sub>** after 2 days at pH 3 (d) **PGAm<sub>T</sub>** after preparation (e) **PGAm<sub>T</sub>** after 2 days at pH 7 (f) **PGAm<sub>T</sub>** after 2 days at pH 3 (g) **PGAm<sub>MMT</sub>** after preparation (h) **PGAm<sub>MMT</sub>** after 5 days at pH 7 (i) **PGAm<sub>MMT</sub>** after 2 days at pH 3. **PGAm<sub>MMT</sub>**-coated PLA particle suspensions showed the most destabilization at pH 3 as a result of the degradation of **PGAm<sub>MMT</sub>**.

The fluorescence results were in agreement with the qualitative observations, as the PLA particles prepared using **PGAm<sub>MMT</sub>** and incubated at pH 3 underwent more than an 80% decrease in fluorescence over the first 3 hours, with negligible fluorescence observed after 24 h (**Figure 2.22b**). In contrast, all of the other systems underwent a much slower decrease in fluorescence.

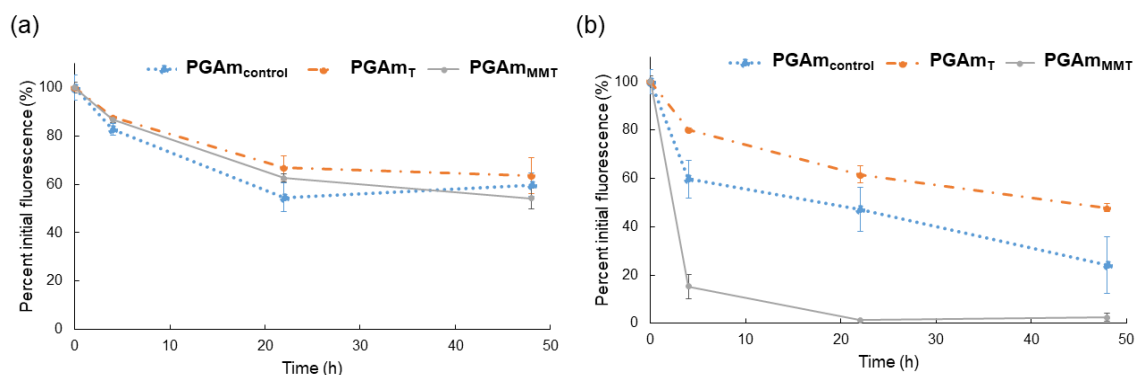


**Figure 2.22** Fluorescence intensities of suspensions of Nile red-loaded PLA particles coated with PGAMs at (a) pH 7 and (b) pH 3 over 48 hours. Particle suspensions prepared using **PGAm<sub>MMT</sub>** at pH 3 underwent the most rapid decrease in fluorescence.

DLS was also used to assess the **PGAm<sub>control</sub>**, **PGAm<sub>T</sub>**, and **PGAm<sub>MMT</sub>**-coated PLA particle suspensions. All of the samples at pH 7 showed similar trends in their particle diameters and count rates (**Figure 2.23**). The large increase in count rate observed for all systems at pH 7 over 48 h (**Figure 2.23c**) can likely be attributed to the gradual destabilization of the particles, which is in agreement with the gradual decrease in Nile red fluorescence that was observed. This count rate increase was also observed for **PGAm<sub>control</sub>** and **PGAm<sub>T</sub>** at pH 3 (**Figure 2.23d**). However, particles prepared using **PGAm<sub>MMT</sub>** at pH 3 underwent a rapid increase in particle diameter and a decrease in count rate as the particles aggregated and sedimented, likely due to the rapid acid-triggered depolymerization of **PGAm<sub>MMT</sub>**.



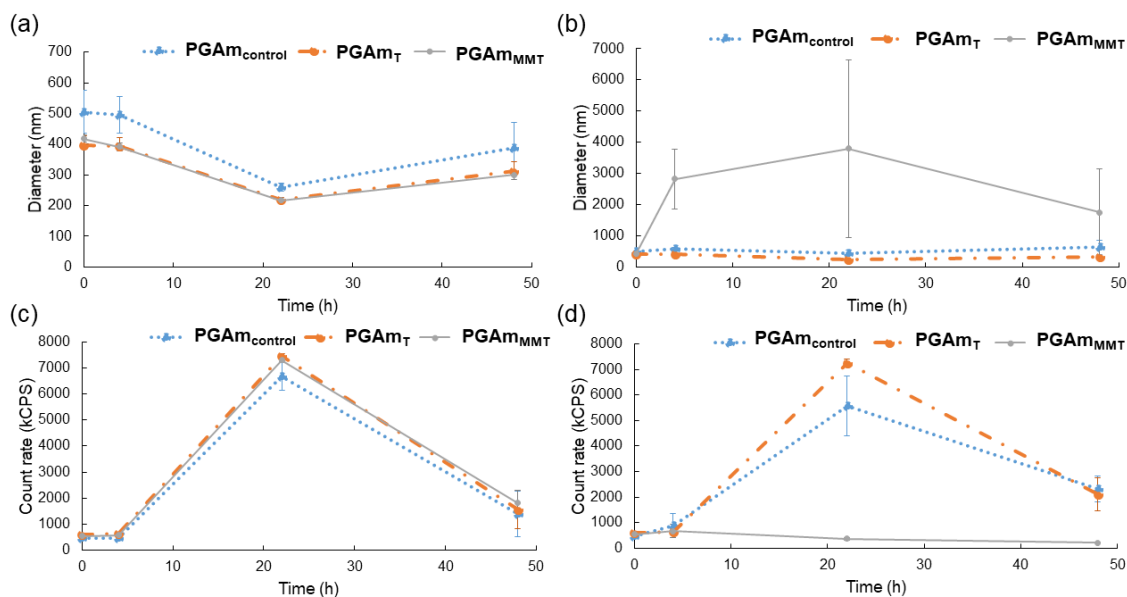


**Figure 2.23** DLS results for suspensions of Nile red-loaded PLA particles coated with PGAMs over 48 hours. (a) Diameters and (c) count rates at pH 7, and (b) diameters and (d) count rates at pH 3. The large increase in count rates can likely be attributed to the gradual destabilization of the particles. **PGAM<sub>MMT</sub>**-coated particle suspensions at pH 3 underwent a rapid increase in particle diameter and a decrease in count rate due to the rapid degradation of **PGAM<sub>MMT</sub>** at pH 3.

Finally, Nile red was used in preparation of PGAM-coated PLA particle suspensions using **PGAM<sub>control</sub>** and **PGAM<sub>UV</sub>** as the emulsifying agents. First, particles were prepared using **PGAM<sub>UV</sub>** and irradiated with the UV light (**PGAM<sub>UV-irrad</sub>**). A second set of samples was prepared using the same polymer without the irradiation of the UV light, and were kept in dark throughout the experiment (**PGAM<sub>UV-non-irrad</sub>**). A third set of samples was prepared using **PGAM<sub>control</sub>** as the emulsifying agent and irradiated with the UV light for 90 minutes (**PGAM<sub>control-irrad</sub>**). A last set of samples was prepared using **PGAM<sub>control</sub>** and kept in dark throughout the experiment (**PGAM<sub>control-non-irrad</sub>**). The resulting particle suspensions were monitored qualitatively (**Figure 2.24**) and quantitatively (**Figures 2.25** and **2.26**). There was a decrease in fluorescence intensity (**Figure 2.25**) of both **PGAM<sub>control-irrad</sub>** and **PGAM<sub>UV-irrad</sub>** which as for the PEA particle suspensions can likely be attributed to Nile red photobleaching. The fluorescence results (**Figure 2.25**) were in agreement with the qualitative assessments as the colours of the particle suspensions were dark pink to purple

after preparation and faded to pale pink faded (**Figures 2.24f** and **2.24h**) after the application of the UV light.

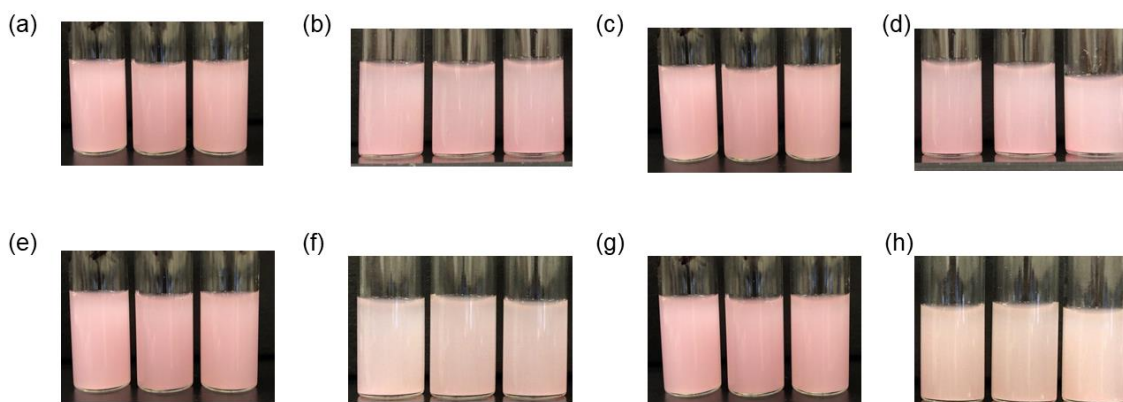


**Figure 2.24** Photos of PGAm-coated PLA particle suspensions: (a) **PGAm<sub>control-non-irrad</sub>** after preparation (b) **PGAm<sub>control-non-irrad</sub>** after 2 days (c) **PGAm<sub>UV-non-irrad</sub>** after preparation (d) **PGAm<sub>UV-non-irrad</sub>** after 2 days (e) **PGAm<sub>control-irrad</sub>** after preparation (f) **PGAm<sub>control-irrad</sub>** after 2 days (g) **PGAm<sub>UV-irrad</sub>** after preparation (h) **PGAm<sub>UV-irrad</sub>** after 2 days. No noticeable changes were observed except changes in the colours of particle suspensions after UV irradiation which was due to the photobleaching of Nile red during UV irradiation.

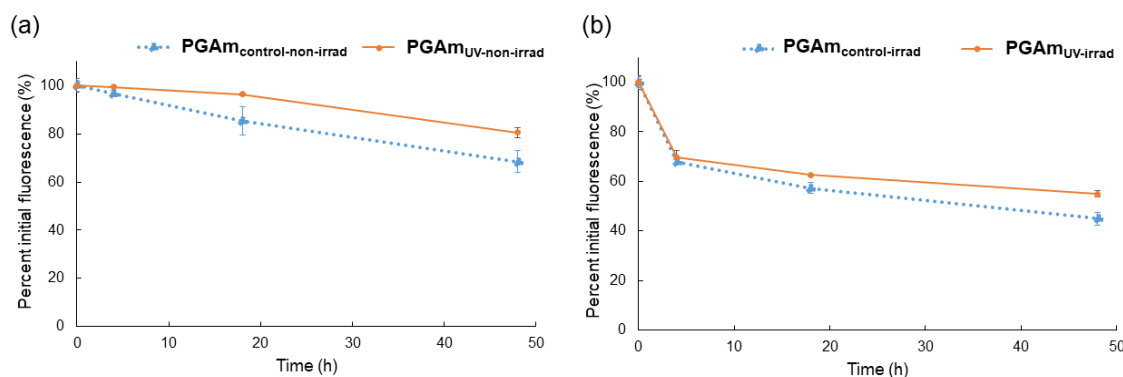


**Figure 2.25** Fluorescence intensity versus time for PGAm-coated PLA particle suspensions. (a) Samples were kept in the dark and (b) samples irradiated with UV light for 90 minutes after their preparation, suggesting the photobleaching of Nile red during the 90 min of UV irradiation.

DLS was also used to assess the prepared particle suspensions. There was an increase followed by a decrease in count rates of both irradiated and non-irradiated which we hypothesize are as a result of the aggregation followed by the sedimentation of a portion of particles. However, the diameters of the particles did not change substantially over time (**Figure 2.26**). These results can be explained in the same manner as for the PEA particle suspensions, and also considering that DLS may not represent the entire changes occurring in the system. As for the PEA particle suspensions, it was not possible to achieve full destabilization of particles due to incomplete depolymerization of **PGAm<sub>UV</sub>** and possibly the high turbidity of the suspensions.

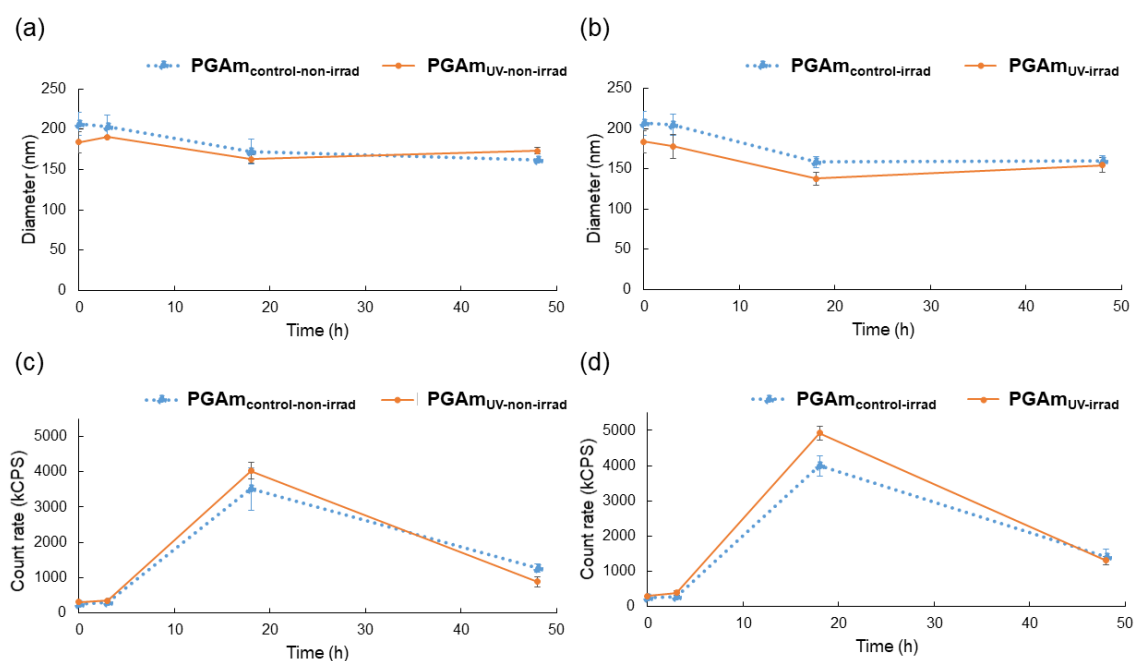


**Figure 2.26** DLS results for suspensions of Nile red-loaded PLA particles coated with PGAMs over 48 hours. (a) Diameter and (c) count rates for **PGAm<sub>control-non-irrad</sub>** and **PGAm<sub>UV-non-irrad</sub>**, and (b) diameter and (d) count rates for **PGAm<sub>control-irrad</sub>** and **PGAm<sub>UV-irrad</sub>**. Increases in count rates were attribute to the general destabilization and sedimentation of the particle suspensions.

Overall, for the results for the PGAM coated PLA particles were similar to those for the PEA particles. The addition of acid to the **PGAM<sub>MMT</sub>** coated particles led to their aggregation and sedimentation more rapidly than for **PGAM<sub>T</sub>** or **PGAm<sub>control</sub>** coated

particles and UV light was not effective as a stimulus for triggering the aggregation and sedimentation of the **PGAm<sub>UV</sub>** coated PLA particle suspensions compared to controls. All of the suspensions were relatively unstable over time, making it difficult to demonstrate their stimuli-responsive properties. It can be concluded based on the evaluated particle systems that PGAm<sub>s</sub> may be effective short-term stabilizers for emulsions and that they can exhibit pH-responsive properties, but they are not highly effective in stabilizing emulsions over the long term.

### 2.2.8 Oil-in-water and Water-in-oil Emulsions

To further evaluate the properties of SIPs as emulsifiers, they were investigated as potential emulsifying agents for the preparation of oil-in-water and water-in-oil emulsions. First, **PGAm<sub>UV</sub>** was used as the emulsifier since it is stable and does not undergo degradation as long as it is kept in the dark. Mineral oil was used as the initial oil phase since it is widely used in various industries such as cosmetics.<sup>154</sup> **PGAm<sub>UV</sub>** at varying concentrations (**Table 2.8**) was dissolved in 3.0 mL of deionized water followed by the addition of oil and then mixtures were stirred (10 minutes) before being subjected to sonication for three 30 s intervals with 10 s breaks in between. The process was also performed without using an emulsifier (**Table 2.8** experiment 7) as a control sample. Based on qualitative evaluations 15 hours after their preparation (**Figure 2.27**), the resulting emulsions, except experiment number 5 that had the highest oil:emulsifier ratio, showed stability as the samples were turbid. In addition, experiment number 7 (**Table 2.8**) used as the control showed the least turbidity and stability as expected. Even though the emulsions showed stability after 15 hours, further experiments on triggering the degradation of emulsifiers were not carried out since the emulsions started to show destabilization after 1 day (**Figure 2.27.o to u**). The polymers were not effective in stabilizing mineral oil-in-water emulsions as all the emulsions started to show destabilization after 1 day.

**Table 2.8** Preparation of oil-in-water emulsions at different concentrations of oil and PGAM<sub>UV</sub>. The volume of water was held constant at 3.0 mL.

Experiment number	Mass of PGAM <sub>UV</sub> (mg)	Mass of mineral oil (mg)
1	15	30
2	30	30
3	15	70
4	30	70
5	15	150
6	20	150
7	0	70

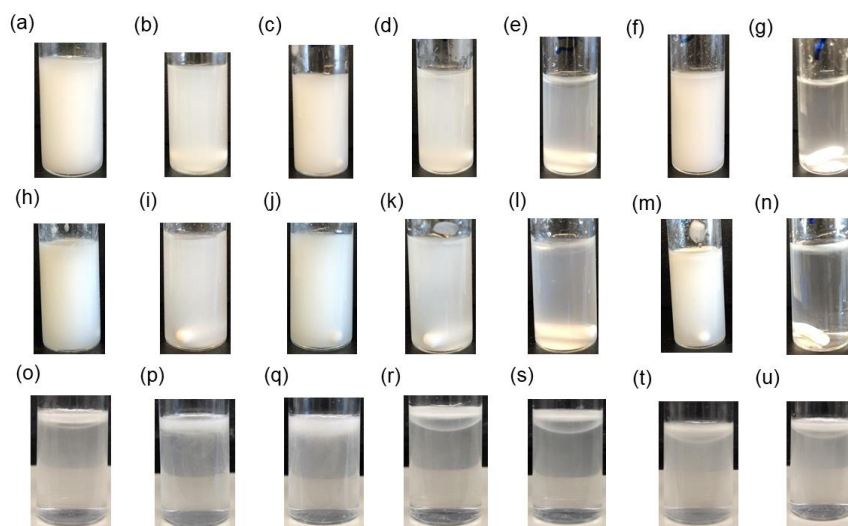


**Figure 2.27** Photos of emulsions described in **Table 2.8** experiment (a) 1 (b) 2 (c) 3 (d) 4 (e) 5 (f) 6 and (g) 7 after preparation, experiment (h) 1 (i) 2 (j) 3 (k) 4 (l) 5 (m) 6 and (n) 7 after 15 hours, and experiment (o) 1 (p) 2 (q) 3 (r) 4 (s) 5 (t) 6 and (u) 7 after 2 days. All the emulsions started to show destabilization after 1 day.

Additionally, all of the partially acylated PGAMs (**Scheme 2.4**) were also explored as emulsifiers for water-in-oil and oil-in-water emulsions. However, stable emulsions were not formed, likely due to the poor solubility of partially acylated polymers in water and oil.

To further evaluate the properties of PGAMs as emulsifiers, toluene-in-water emulsions were prepared using **PGAM<sub>control</sub>**, **PGAM<sub>UV</sub>**, **PGAM<sub>T</sub>**, and **PGAM<sub>MMT</sub>** (**Table 2.9**) as the emulsifiers. Toluene was selected as it is a water-immiscible solvent with a relative high boiling point, which prevents the solvent from rapid evaporation during the experiment. Photos of the emulsions were taken immediately after their preparation and after 6 hours (**Figure 2.28**). As expected, the sample without an emulsifier showed the most phase separation after 6 hours (**Figure 2.28e** and **j**). The sample using **PGAM<sub>MMT</sub>** as an emulsifier showed the second most destabilization and phase separation. This is mainly due to the rapid degradation of **PGAM<sub>MMT</sub>** in water. The PGAMs employed exhibited capability as emulsifiers to a certain extent, with **PGAM<sub>MMT</sub>** showing the least effectiveness due to its rapid depolymerization in aqueous solutions. However, no further experiment on triggering the degradation of the emulsifiers in the emulsions were carried out since the emulsions were destabilized and phase separated after 5-10 hours indicating the ineffectiveness of the polymers for stabilizing toluene-in-water emulsions.

**Table 2.9** Preparation of toluene-in-water emulsions using different PGAMs.

Experiment number	Emulsifier	Mass of emulsifier (mg)	Water (mL)	Toluene ( $\mu$ L)
1	<b>PGAM<sub>control</sub></b>	25	2.0	200
2	<b>PGAM<sub>UV</sub></b>	25	2.0	200
3	<b>PGAM<sub>T</sub></b>	25	2.0	200
4	<b>PGAM<sub>MMT</sub></b>	25	2.0	200
5	–	–	2.0	200

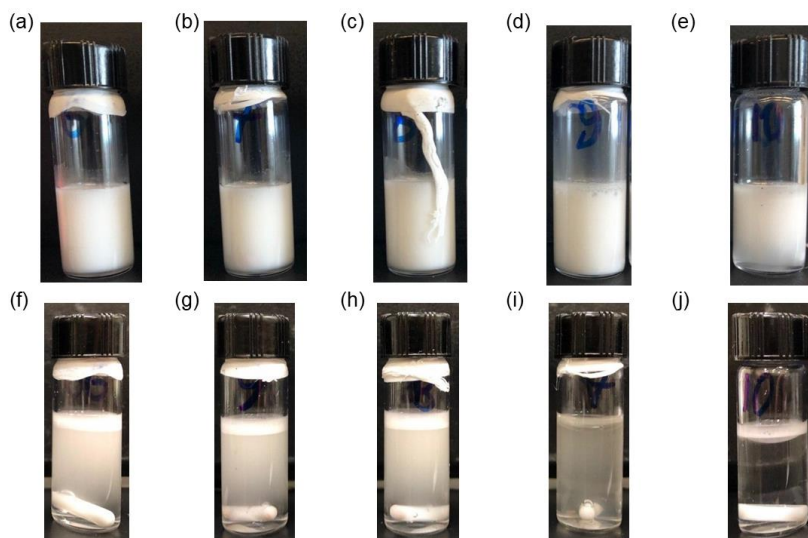


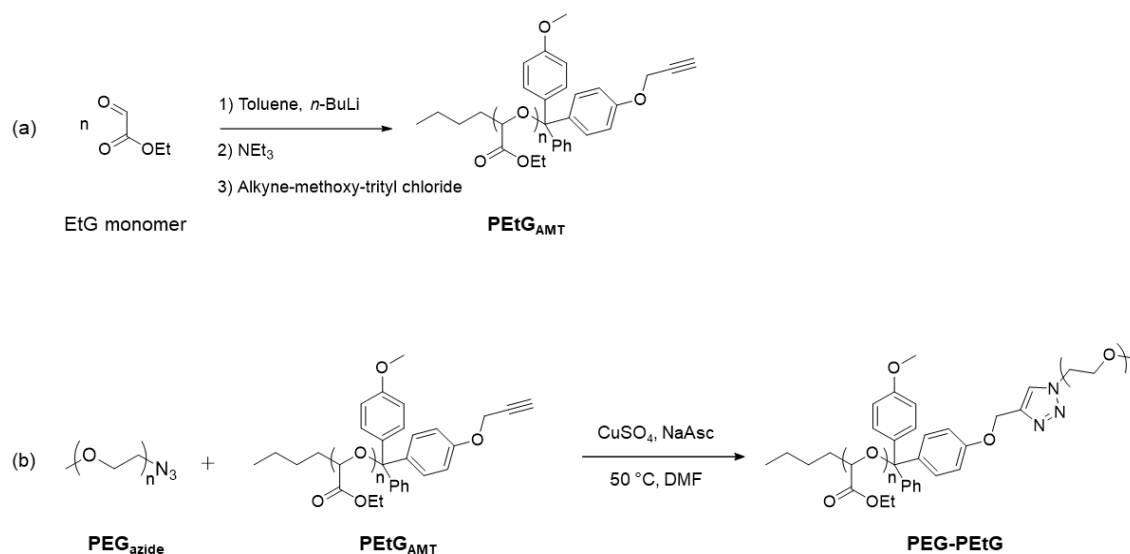
**Figure 2.28** Photos of toluene-in-water emulsions after preparation using (a) **PGAm<sub>control</sub>** (b) **PGAm<sub>UV</sub>** (c) **PGAm<sub>T</sub>** (d) **PGAm<sub>MMT</sub>** (e) without an emulsifier, and after 6 hours (f) **PGAm<sub>control</sub>** (g) **PGAm<sub>UV</sub>** (h) **PGAm<sub>T</sub>** (i) **PGAm<sub>MMT</sub>** (j) without an emulsifier. All the emulsions started to show destabilization after 5-10 hours. The sample without emulsifier and sample using **PGAm<sub>MMT</sub>** showed the first and second destabilization rate as expected.

Thus far, homopolymers have been explored as emulsifiers for oil-in-water and water-in-oil emulsions. The next section was designed to investigate the properties of SIP-based block copolymers as emulsifiers.

### 2.2.9 Synthesis and Characterization of a Poly(ethylene glycol)-poly(ethyl glyoxylate) (PEG-PEtG) Block Copolymer

Amphiphilic properties can also be imparted to self-immolative polyglyoxylates through the preparation of amphiphilic block copolymers, which could also serve as potential degradable surfactants. PEG was selected as the hydrophilic block as it is a highly water-soluble and non-toxic polymer. **PEtG<sub>AMT</sub>** was selected as the hydrophobic block as it has an alkyne group on its end-cap which is suitable for click reaction with the azide group on **PEG<sub>azide</sub>**. **PEtG<sub>AMT</sub>** was synthesized using *n*-BuLi as the initiator and alkyne-methoxytrityl as the end-cap (**Scheme 2.6a**). Its trityl-based end-cap is cleavable in water and its depolymerization proceeds faster in acidic conditions. Both **PEtG<sub>AMT</sub>** (10 kg/mol) and **PEG<sub>azide</sub>** (5 kg/mol) were synthesized as previously reported.<sup>62-63, 141</sup> To synthesize the

**PEG-PEtG** block copolymer, **PEtG<sub>AMT</sub>** was reacted with excess **PEG<sub>azide</sub>** in DMF for 24 hours in the presence of  $\text{CuSO}_4$  and sodium ascorbate (**Scheme 2.6b**).  $^1\text{H}$  NMR spectroscopy of the reaction product confirmed the synthesis of the **PEG-PEtG** block copolymer (**Figure 2.29**). The peaks located at 1.3 and 4.2 ppm correspond to the pendent ethyl groups. The peaks at 5.6 and 3.6 ppm correspond to the hydrogens on the **PEtG<sub>AMT</sub>** backbone and on the **PEG<sub>azide</sub>** block respectively. Further evidence of the formation of **PEG-PEtG** was provided by SEC (**Table 2.10**). SEC analyses also confirmed the synthesis of **PEG-PEtG** as its molar mass was approximately the sum of the molar masses of **PEG-azide** and **PEtG<sub>AMT</sub>**.



**Scheme 2.6** Synthetic approaches for obtaining (a) **PEtG<sub>AMT</sub>** and (b) **PEG-PEtG**.



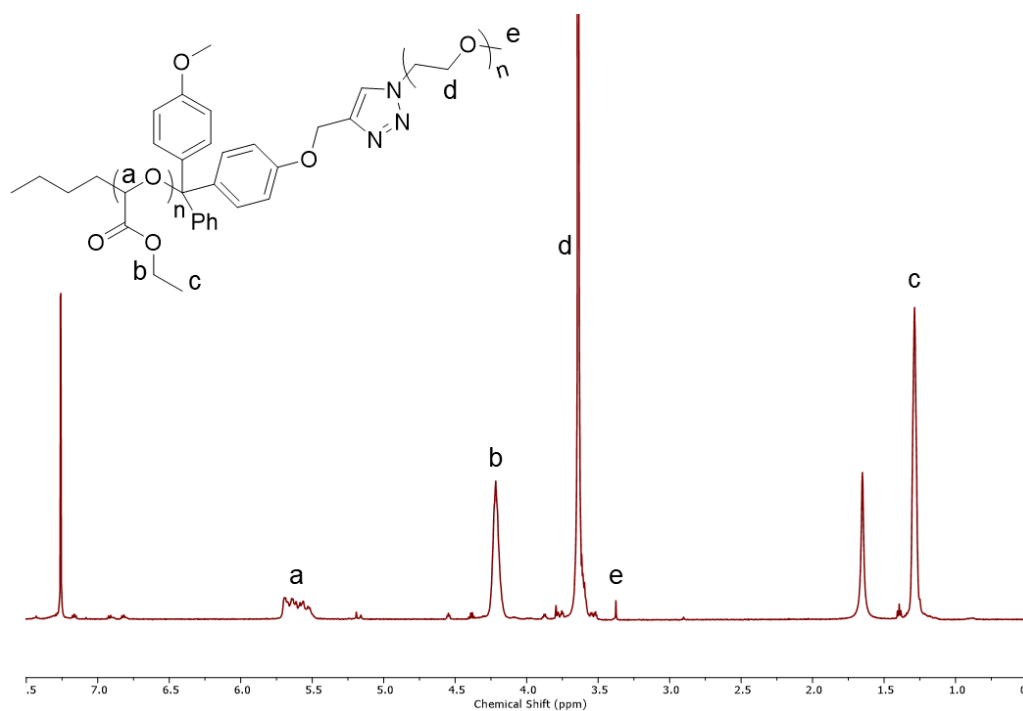


**Figure 2.29**  $^1\text{H}$  NMR spectrum of **PEG-PEtG** (400 MHz,  $\text{CDCl}_3$ ) confirming the synthesis of **PEG-PEtG**.

**Table 2.10** SEC results of **PEG<sub>azide</sub>**, **PEtG<sub>AMT</sub>**, and **PEG-PEtG**. The molar mass of **PEG-PEtG** is approximately the sum of the molar masses of **PEtG<sub>AMT</sub>** and **PEG<sub>azide</sub>** confirming the synthesis of **PEG-PEtG**.

Polymer name	$M_n$ (kg/mol)	$M_w$ (kg/mol)	$\bar{D}$
<b>PEtG<sub>AMT</sub></b>	10.4	14.1	1.4
<b>PEG<sub>azide</sub></b>	5.7	6.7	1.2
<b>PEG-PEtG</b>	14.5	18.1	1.2

To evaluate the properties of the synthesized block copolymers as emulsifiers, **PEG-PEtG** was first used as an emulsifying agent to prepare stable particle emulsions of PEA and PLA. However, **PEG-PEtG** was poorly soluble in water, which made it impossible to emulsify PLA and PEA particles.

The ability of a surfactant to stabilize water-in-oil versus oil-in-water emulsions can be predicted based on its HLB value. While the structure of the PGAm emulsifiers would have made the prediction of their HLB values very difficult, the block copolymer structure of **PEG-PEtG** makes this analysis much simpler. Based on the Griffin method (equation 1-4), the HLB value of synthesized **PEG-PEtG** is approximately 8 which is not in the range of HLB values regarding hydrophilic surfactants.<sup>111</sup> For instance, PVA which was used as a hydrophilic surfactant previously, has an HLB value of 18.<sup>155</sup> Based on the analysis of the HLB values, we focused our studies on water-in-oil emulsions. Toluene was selected as the oil phase as the polymer was soluble in toluene whereas it was not soluble in mineral oil or similar oils. In preliminary experiments, **PEG-PEtG** was dissolved in 1.0 mL of toluene at varying concentrations, followed by the addition of 50  $\mu$ L of water (**Table 2.11**). The resulting mixtures were stirred for 10 minutes and then subjected to sonication for three 30 s intervals with 10 s breaks in between. The sample prepared without emulsifier (experiment 4, **Table 2.11**) was immediately destabilized (**Figure 2.30h** and **l**), while the other samples with different concentrations of the block copolymer stayed milky and turbid for 5 days. The least phase separation and thus, most stable emulsion was observed for the sample prepared at the highest concentration of the block copolymer (**Figure 2.30c, g, and k**), as expected. Qualitative assessment (**Figure 2.30**) indicated the stability of prepared emulsions after days and showing the potential of **PEG-PEtG** as an emulsifier for such systems.

**Table 2.11** Preparation of water-in-toluene emulsions using **PEG-PEtG** as the emulsifier.

Experiment number	Mass of emulsifier (mg)	Water ( $\mu$ L)	Toluene (mL)
1	5.0	50	1.0
2	15	50	1.0
3	25	50	1.0
4	0	50	1.0

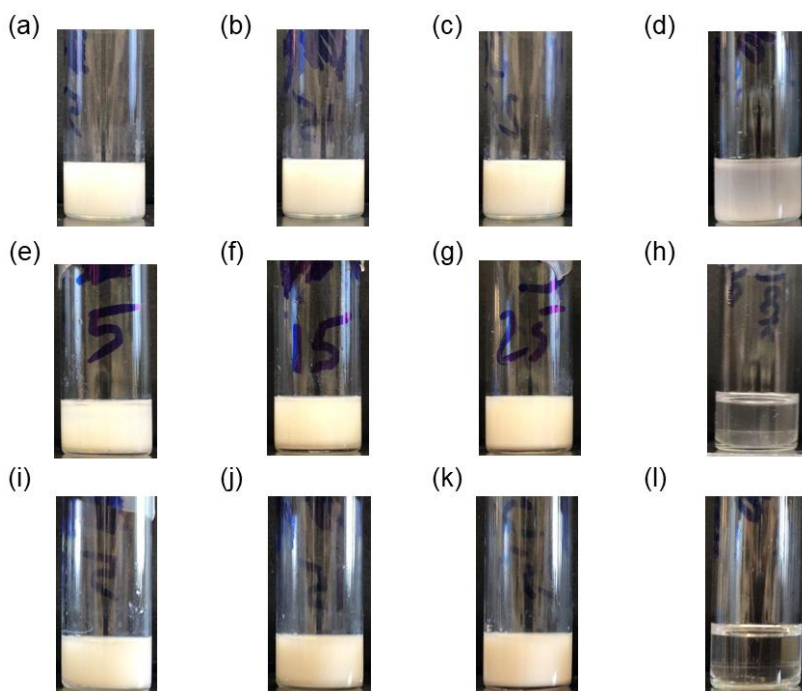


**Figure 2.30** Photos of water-in-toluene emulsions. Experiment 1 after (a) preparation (e) 3 days and (i) 5 days. Experiment 2 after (b) preparation (f) 3 days and (j) 5 days. Experiment 3 after (c) preparation (g) 3 days and (k) 5 days. Experiment 4 after (d) preparation (h) 6 hours and (l) 1 day, indicating the stability of prepared emulsions after days and showing the promise of **PEG-PEtG** as an emulsifier for such systems.

### **Triggered degradation of PEG-PEtG-stabilized water-in-toluene emulsions**

After exploring the promising feature of **PEG-PEtG** to emulsify water-in-toluene emulsions, the behaviour of the stabilized emulsions in response to stimuli was investigated. Eight samples of water-in-toluene emulsions were prepared (**Table 2.12**). Emulsions were prepared as discussed in the previous section. After the preparation, glacial acetic acid was added to the samples to trigger the depolymerization of **PEG-PEtG**. Glacial acetic acid was used as it is soluble in both water and toluene. 18  $\mu\text{L}$  of glacial acetic acid was added to the samples 2, 4, 6, and 8 (**Table 2.12**) to adjust their pH to 3. Based on qualitative assessment (**Figure 2.31**), the addition of glacial acetic acid resulted in the destabilization of the emulsions as a result of the depolymerization of the emulsifiers,

**PEG-PEtG**. In contrast, the emulsions without glacial acetic acid remained stable and turbid after two days as the degradation of **PEG-PEtG** was not triggered.

**Table 2.12** Preparation of water-in-toluene emulsions using **PEG-PEtG** as the emulsifier.

<b>Experiment number</b>	<b>Mass of emulsifier (mg)</b>	<b>Water (<math>\mu\text{L}</math>)</b>	<b>Toluene (mL)</b>
<b>1</b>	25	50	1.0
<b>2</b>	25	50	1.0
<b>3</b>	25	100	1.0
<b>4</b>	25	100	1.0
<b>5</b>	25	200	1.0
<b>6</b>	25	200	1.0
<b>7</b>	0	100	1.0
<b>8</b>	0	100	1.0



**Figure 2.31** Photos of water-in-toluene emulsions. (a) After preparation (b) after 14 hours and (c) after 2 days. In photos, samples are arranged from experiment 1 to 8 (**Table 2.12**) from left to right. The emulsions were destabilized upon the addition of glacial acetic acid, which triggered the depolymerization of the emulsifier, **PEG-PEtG**, while emulsions without glacial acetic acid remained stable and turbid over time.

While the homopolymer PGAMs were not highly effective surfactants for stabilizing either particle suspensions or emulsions, these initial results with the block copolymers show the potential of **PEG-PEtG** to serve as emulsifiers for water-in-oil systems. In addition, qualitative observations suggest that these emulsions can be destabilized on demand upon the application of stimuli. In the future it will be important to follow up these studies with my quantitative assessments of emulsion stability.

## Chapter 3

### 3 Conclusions and Future Work

Surfactants could be categorized among the most important ingredients in cosmetic industry. They play a significant role in cleaning, dispersing, foaming, emulsifying, solubilizing, enhancing penetration, killing microbes and in many other useful applications. Surfactants are also of interest for pharmaceutical applications. They can increase the stability or solubility of a specific drug in its preparation process which can result in enhancing the final dosage of the drug. As excipients, surfactants can boost the chemical and physical properties of the active pharmaceutical ingredients to improve the effectiveness of the final product.

This thesis described the development of SIPs as depolymerizable analogues of widely used surfactants. Aside from studies of block copolymer micelles containing SIP blocks,<sup>156</sup> to the best of our knowledge, the properties and applications of SIPs as potential degradable surfactants have not yet been investigated. They offer the potential to serve as surfactants that can be degraded on demand under specific conditions after their use. They could serve as emulsifiers with potential applications for drug delivery systems or to stabilize hydrophobic ingredients in cosmetic products. Therefore, evaluating their potential for stabilizing particle suspensions and emulsions was the focus of this thesis.

Firstly, to mimic the properties of PVA and obtain a water-soluble surfactant, PGAMs with different end-caps were synthesized via postpolymerization modification from PEtGs. PGAMs were then partially acylated using different acid chlorides to impart amphiphilicity along the polymer backbone. The resulting PGAMs were explored as emulsifying agents to stabilize suspensions of PEA particles. However, partially acylated PGAMs failed to emulsify PEA into stable particles. The main focus was then placed on the non-acylated version of PGAMs, which are more hydrophilic, yet could still exhibit amphiphilic properties due to their hydrophobic backbones and hydrophilic pendent groups. PGAMs were used to emulsify PEA and PLA solutions to form particle suspensions. PGAM-coated particles were exposed to stimuli to trigger the depolymerization of the emulsifier and study the behaviour of particle suspensions after the depolymerization of PGAMs. Nile red was

used as an additional probe to study the behaviour of the particles over time. PGAMs showed acceptable results for preparation of PEA and PLA particle suspensions with short-term stability. **PGAM<sub>MMT</sub>** showed the potential to depolymerize upon application of an acid stimulus, resulting in rapid destabilization of the particle suspension. However, **PGAM<sub>UV</sub>**-coated PEA and PLA did not show any detectable changes after the application of UV light, the stimulus. This result likely arose because **PGAM<sub>UV</sub>** can only degrade to 60% at most, leaving a substantial percentage of the polymer remaining on the particles. Overall, another problem encountered was the poor long-term stability of the PGAM-stabilized particle suspensions. This problem made it difficult to study the triggered destabilization of the suspensions and may also be problematic for applications. The same PGAMs were also investigated as stabilizers of oil-in-water emulsions, but they did not serve as effective surfactants for this application.

To address the limitation of the current work, future work should focus on the preparation of PGAMs with different pendent groups. By introducing different pendent groups, it should be possible to achieve PGAMs with different amphiphilic properties, that may serve as more effective emulsifiers for stabilizing particle suspensions or emulsions.

Next, a **PEG-PEtG** block copolymer containing both hydrophilic and hydrophobic blocks was synthesized to mimic the structure of diblock copolymeric surfactants. The synthesized block copolymer and PGAMs were then investigated as emulsifiers for stabilizing oil-in-water and water-in-oil emulsions. The **PEG-PEtG** block copolymer showed promising results in stabilizing water-in-toluene emulsions. Its depolymerization was triggered by the addition of acid which cleaved off its trityl-based end-cap and resulted in the destabilization of the emulsions. These results showed the promising feature of the **PEG-PEtG** block copolymer as a degradable emulsifier that not only stabilizes the emulsions but also destabilizes the emulsion upon the application of stimuli.

There are a number of aspects that may be addressed in future work. The **PEG-PEtG** was the only block copolymer that was explored, and it showed acceptable results in this regard. Block copolymers of PEG and PEtG with different hydrophobic and hydrophilic chain lengths can be synthesized to explore the effect of hydrophobic and hydrophilic chain

lengths on such systems. Also, a click reaction between hydrophilic SIPs such as PGAMs and hydrophobic blocks can be performed to synthesize other types of SIP-based block copolymers. Thus far, only diblock copolymers containing one SIP-based block were discussed. Block copolymers containing more than one SIP-based block such as a triblock in which two end blocks are SIPs can also be investigated.



## References

1. Nicholson, J. W. *The chemistry of polymers*, 5th ed.; Royal Society of Chemistry: London, UK, 2017.
2. Hosler, D.; Burkett, S. L.; Tarkanian, M. J., Prehistoric polymers: rubber processing in ancient mesoamerica. *Science* **1999**, *284*, 1988–91.
3. Knight, D. K.; Gillies, E. R.; Mequanint, K., Strategies in functional poly (ester amide) syntheses to study human coronary artery smooth muscle cell interactions. *Biomacromolecules* **2011**, *12*, 2475–2487.
4. Crick, F. H. C.; Watson, J. D. The Complementary Structure of Deoxyribonucleic Acid. *Proc. R. Soc. A* **1953**, *223*, 80–96.
5. Namazi, H., Polymers in our daily life. *BioImpacts* **2017**, *7*, 73.
6. McNally, T.; Pötschke, P.; Halley, P.; Murphy, M.; Martin, D.; Bell, S. E. J.; Brennan, G. P.; Bein, D.; Lemoine, P.; Quinn, J. P., Polyethylene multiwalled carbon nanotube composites. *Polymer* **2005**, *46*, 8222–8232.
7. Schellenberg, J.; Leder, H.-J., Syndiotactic polystyrene: Process and applications. *Adv. Polym. Tech.* **2006**, *25*, 141–151.
8. van der Wal, P.; Steiner, U., Super-hydrophobic surfaces made from Teflon. *Soft Matter* **2007**, *3*, 426–429.
9. Geyer, R.; Jambeck, J. R.; Law, K. L., Production, use, and fate of all plastics ever made. *Sci. Adv.* **2017**, *3*, e1700782.
10. Jambeck, J. R.; Geyer, R.; Wilcox, C.; Siegler, T. R.; Perryman, M.; Andrady, A.; Narayan, R.; Law, K. L., Marine pollution. Plastic waste inputs from land into the ocean. *Science* **2015**, *347*, 768–71.
11. Lebreton, L.; Andrady, A., Future scenarios of global plastic waste generation and disposal. *Palgrave. Commun.* **2019**, *5*, 1–11.
12. Stille, J. K., Step-growth polymerization. *J. Chem. Educ.* **1981**, *58*, 862–866.
13. Lodge, T. P., Block copolymers: past successes and future challenges. *Macromol. Chem. Phys.* **2003**, *204*, 265-273.
14. Li, L.; Raghupathi, K.; Song, C.; Prasad, P.; Thayumanavan, S., Self-assembly of random copolymers. *Chem. Commun.* **2014**, *50*, 13417–13432.

15. Bradford, E.; McKeever, L., Block copolymers. *Prog. Polym. Sci.* **1971**, *3*, 109–143.
16. Mark, J. E., *Phys. Prop. Polym. Handb.* Springer: 2007; pp 561–576.
17. Goodman, S. R., An overview of PVC compounds for wire and cable applications. *Wire J. Int.* **2000**, *33*, 214–218.
18. Imazato, S.; KITAGAWA, H.; Tsuboi, R.; Kitagawa, R.; THONGTHAI, P.; Sasaki, J.-i., Non-biodegradable polymer particles for drug delivery: A new technology for “bio-active” restorative materials. *Dent. Mater. J.* **2017**, *36*, 524–532.
19. Albertsson, A. C.; Karlsson, S., Degradable polymers for the future. *Acta Polym.* **1995**, *46*, 114–123.
20. de Gracia Lux, C.; McFearin, C. L.; Joshi-Barr, S.; Sankaranarayanan, J.; Fomina, N.; Almutairi, A., Single UV or near IR triggering event leads to polymer degradation into small molecules. *ACS Macro Lett.* **2012**, *1*, 922–926.
21. Mohajeri, S.; Chen, F.; de Prinse, M.; Phung, T.; Burke-Kleinman, J.; Maurice, D. H.; Amsden, B. G., Liquid degradable poly (trimethylene-carbonate-co-5-hydroxy-trimethylene carbonate): an injectable drug delivery vehicle for acid-sensitive drugs. *Mol. Pharmaceutics* **2020**, *17*, 1363–1376.
22. Wood, K. C.; Boedicker, J. Q.; Lynn, D. M.; Hammond, P. T., Tunable drug release from hydrolytically degradable layer-by-layer thin films. *Langmuir* **2005**, *21*, 1603–1609.
23. Lewis, G. G.; Robbins, J. S.; Phillips, S. T., Phase-switching depolymerizable poly (carbamate) oligomers for signal amplification in quantitative time-based assays. *Macromolecules* **2013**, *46*, 5177–5183.
24. Sagi, A.; Weinstain, R.; Karton, N.; Shabat, D., Self-immolative polymers. *J. Am. Chem. Soc.* **2008**, *130*, 5434–5435.
25. Langer, R.; Vacanti, J., Advances in tissue engineering. *J. Pediatr. Surg.* **2016**, *51*, 8–12.
26. Jambeck, J. R.; Geyer, R.; Wilcox, C.; Siegler, T. R.; Perryman, M.; Andrady, A.; Narayan, R.; Law, K. L., Plastic waste inputs from land into the ocean. *Science* **2015**, *347*, 768–771.

27. Thompson, R. C.; Moore, C. J.; Vom Saal, F. S.; Swan, S. H., Plastics, the environment and human health: current consensus and future trends. *Philos. Trans. R. Soc., B* **2009**, *364*, 2153–2166.
28. Jin, T.; Zhang, H., Biodegradable polylactic acid polymer with nisin for use in antimicrobial food packaging. *J. Food Sci.* **2008**, *73*, M127–M134.
29. Pushpamalar, J.; Veeramachineni, A. K.; Owh, C.; Loh, X. J., Biodegradable polysaccharides for controlled drug delivery. *ChemPlusChem* **2016**, *81*, 504–514.
30. Ulery, B. D.; Nair, L. S.; Laurencin, C. T., Biomedical applications of biodegradable polymers. *J. Polym. Sci., Part B: Polym. Phys.* **2011**, *49*, 832–864.
31. Chourasia, M.; Jain, S., Pharmaceutical approaches to colon targeted drug delivery systems. *J. Pharm. Pharm. Sci.* **2003**, *6*, 33–66.
32. Doppalapudi, S.; Jain, A.; Khan, W.; Domb, A. J., Biodegradable polymers—an overview. *Polym. Adv. Technol.* **2014**, *25*, 427–435.
33. Kamaly, N.; Yameen, B.; Wu, J.; Farokhzad, O. C., Degradable controlled-release polymers and polymeric nanoparticles: mechanisms of controlling drug release. *Chem. Rev.* **2016**, *116*, 2602–2663.
34. Hubbell, J. A., Synthetic biodegradable polymers for tissue engineering and drug delivery. *Curr. Opin. Solid State Mater. Sci.* **1998**, *3*, 246–251.
35. Tian, H.; Tang, Z.; Zhuang, X.; Chen, X.; Jing, X., Biodegradable synthetic polymers: Preparation, functionalization and biomedical application. *Prog. Polym. Sci.* **2012**, *37*, 237–280.
36. Arrieta, M. P.; Samper, M. D.; Aldas, M.; López, J., On the use of PLA-PHB blends for sustainable food packaging applications. *Materials* **2017**, *10*, 1008.
37. Malikmammadov, E.; Tanir, T. E.; Kiziltay, A.; Hasirci, V.; Hasirci, N., PCL and PCL-based materials in biomedical applications. *J. Biomater. Sci., Polym. Ed.* **2018**, *29*, 863–893.
38. Del Nobile, M. A.; Conte, A.; Buonocore, G. G.; Incoronato, A. L.; Massaro, A.; Panza, O., Active packaging by extrusion processing of recyclable and biodegradable polymers. *J. Food Eng.* **2009**, *93*, 1–6.
39. Hoffman, A. S., Stimuli-responsive polymers: Biomedical applications and challenges for clinical translation. *Adv. Drug Delivery Rev.* **2013**, *65*, 10–16.

40. Jeong, B.; Gutowska, A., Lessons from nature: stimuli-responsive polymers and their biomedical applications. *Trends Biotechnol.* **2002**, *20*, 305–311.
41. Wang, D.; Green, M. D.; Chen, K.; Daengngam, C.; Kotsuchibashi, Y., Stimuli-responsive polymers: Design, synthesis, characterization, and applications. *Int. J. Polym. Sci.* **2016**, *2016*.
42. Roth, P. J.; Lowe, A. B., Stimulus-responsive polymers. *Polym. Chem.* **2017**, *8*, 10–11.
43. Meng, F.; Zhong, Z.; Feijen, J., Stimuli-responsive polymersomes for programmed drug delivery. *Biomacromolecules* **2009**, *10*, 197-209.
44. Wells, C. M.; Harris, M.; Choi, L.; Murali, V. P.; Guerra, F. D.; Jennings, J. A., Stimuli-responsive drug release from smart polymers. *J. Funct. Biomater.* **2019**, *10*, 34.
45. Schmaljohann, D., Thermo- and pH-responsive polymers in drug delivery. *Adv. Drug Delivery Rev.* **2006**, *58*, 1655–1670.
46. Fleige, E.; Quadir, M. A.; Haag, R., Stimuli-responsive polymeric nanocarriers for the controlled transport of active compounds: concepts and applications. *Adv. Drug Delivery Rev.* **2012**, *64*, 866–884.
47. Liu, M.; Du, H.; Zhang, W.; Zhai, G., Internal stimuli-responsive nanocarriers for drug delivery: Design strategies and applications. *Mater. Sci. Eng.* **2017**, *71*, 1267–1280.
48. Midoux, P.; Pichon, C.; Yaouanc, J. J.; Jaffrès, P. A., Chemical vectors for gene delivery: a current review on polymers, peptides and lipids containing histidine or imidazole as nucleic acids carriers. *Br. J. Pharmacol.* **2009**, *157*, 166–178.
49. Bajaj, I.; Singhal, R., Poly (glutamic acid)—an emerging biopolymer of commercial interest. *Bioresour. Technol.* **2011**, *102*, 5551–5561.
50. Peterson, G. I.; Larsen, M. B.; Boydston, A. J., Controlled depolymerization: stimuli-responsive self-immolative polymers. *Macromolecules* **2012**, *45*, 7317–7328.
51. Wang, W.; Alexander, C., Self-immolative polymers. *Angew. Chem. Int. Ed. Engl.* **2008**, *47*, 7804–6.
52. Roth, M. E.; Green, O.; Gnaim, S.; Shabat, D., Dendritic, Oligomeric, and Polymeric Self-Immolative Molecular Amplification. *Chem. Rev.* **2016**, *116*, 1309–52.
53. Peterson, G. I.; Church, D. C.; Yakelis, N. A.; Boydston, A. J., 1, 2-oxazine linker as a thermal trigger for self-immolative polymers. *Polymer* **2014**, *55*, 5980–5985.

54. Deng, Z.; Qian, Y.; Yu, Y.; Liu, G.; Hu, J.; Zhang, G.; Liu, S., Engineering intracellular delivery nanocarriers and nanoreactors from oxidation-responsive polymersomes via synchronized bilayer cross-linking and permeabilizing inside live cells. *J. Am. Chem. Soc.* **2016**, *138*, 10452–10466.
55. Dewit, M. A.; Beaton, A.; Gillies, E. R., A reduction sensitive cascade biodegradable linear polymer. *J. Polym. Sci., Part A: Polym. Chem.* **2010**, *48*, 3977–3985.
56. DeWit, M. A.; Gillies, E. R., A cascade biodegradable polymer based on alternating cyclization and elimination reactions. *J. Am. Chem. Soc.* **2009**, *131*, 18327–18334.
57. Liu, G.; Wang, X.; Hu, J.; Zhang, G.; Liu, S., Self-immolative polymersomes for high-efficiency triggered release and programmed enzymatic reactions. *J. Am. Chem. Soc.* **2014**, *136*, 7492–7497.
58. Xiao, Y.; Li, H.; Zhang, B.; Cheng, Z.; Li, Y.; Tan, X.; Zhang, K., Modulating the depolymerization of self-immolative brush polymers with poly (benzyl ether) backbones. *Macromolecules* **2018**, *51*, 2899–2905.
59. Kaitz, J. A.; Diesendruck, C. E.; Moore, J. S., End group characterization of poly (phthalaldehyde): surprising discovery of a reversible, cationic macrocyclization mechanism. *J. Am. Chem. Soc.* **2013**, *135*, 12755–12761.
60. Feinberg, A. M.; Hernandez, H. L.; Plantz, C. L.; Mejia, E. B.; Sottos, N. R.; White, S. R.; Moore, J. S., Cyclic poly (phthalaldehyde): thermoforming a bulk transient material. *ACS Macro Lett.* **2018**, *7*, 47–52.
61. Gnaim, S.; Shabat, D., Self-immolative chemiluminescence polymers: innate assimilation of chemiexcitation in a domino-like depolymerization. *J. Am. Chem. Soc.* **2017**, *139*, 10002–10008.
62. Fan, B.; Salazar, R.; Gillies, E. R., Depolymerization of Trityl End-Capped Poly (Ethyl Glyoxylate): Potential Applications in Smart Packaging. *Macromol. Rapid Commun.* **2018**, *39*, 1800173.
63. Fan, B.; Trant, J. F.; Wong, A. D.; Gillies, E. R., Polyglyoxylates: a versatile class of triggerable self-immolative polymers from readily accessible monomers. *J. Am. Chem. Soc.* **2014**, *136*, 10116–10123.

64. Yardley, R. E.; Kenaree, A. R.; Gillies, E. R., Triggering depolymerization: Progress and opportunities for self-immolative polymers. *Macromolecules* **2019**, *52*, 6342–6360.
65. Penczek, S.; Moad, G., Glossary of terms related to kinetics, thermodynamics, and mechanisms of polymerization (IUPAC Recommendations 2008). *Pure Appl. Chem.* **2008**, *80*, 2163–2193.
66. Olah, M. G.; Robbins, J. S.; Baker, M. S.; Phillips, S. T., End-capped poly (benzyl ethers): Acid and base stable polymers that depolymerize rapidly from head-to-tail in response to specific applied signals. *Macromolecules* **2013**, *46*, 5924–5928.
67. DiLauro, A. M.; Lewis, G. G.; Phillips, S. T., Self-Immolative Poly (4, 5-dichlorophthalaldehyde) and its Applications in Multi-Stimuli-Responsive Macroscopic Plastics. *Angew. Chem.* **2015**, *127*, 6298–6303.
68. Sirianni, Q. E.; Rabiee Kenaree, A.; Gillies, E. R., Polyglyoxylamides: Tuning Structure and Properties of Self-Immolative Polymers. *Macromolecules* **2018**, *52*, 262–270.
69. Fan, B.; Yardley, R. E.; Trant, J. F.; Borecki, A.; Gillies, E. R., Tuning the hydrophobic cores of self-immolative polyglyoxylate assemblies. *Polym. Chem.* **2018**, *9*, 2601–2610.
70. Rabiee Kenaree, A.; Gillies, E. R., Controlled Polymerization of Ethyl Glyoxylate Using Alkylolithium and Alkoxide Initiators. *Macromolecules* **2018**, *51*, 5501–5510.
71. Belloncle, B.; Burel, F.; Oulyadi, H.; Bunel, C., Study of the in vitro degradation of poly (ethyl glyoxylate). *Polym. Degrad. Stab.* **2008**, *93*, 1151–1157.
72. Heuchan, S. M.; Fan, B.; Kowalski, J. J.; Gillies, E. R.; Henry, H. A., Development of Fertilizer Coatings from Polyglyoxylate–Polyester Blends Responsive to Root-Driven pH Change. *J. Agric. Food. Chem.* **2019**, *67*, 12720–12729.
73. Fan, B.; Gillies, E. R., Poly (ethyl glyoxylate)-poly (ethylene oxide) nanoparticles: Stimuli-responsive drug release via end-to-end polyglyoxylate depolymerization. *Mol. Pharmaceutics* **2017**, *14*, 2548–2559.
74. Gambles, M. T.; Fan, B.; Borecki, A.; Gillies, E. R., Hybrid Polyester Self-Immolative Polymer Nanoparticles for Controlled Drug Release. *ACS omega* **2018**, *3*, 5002–5011.

75. Fan, B.; Trant, J. F.; Yardley, R. E.; Pickering, A. J.; Lagugné-Labarthet, F. o.; Gillies, E. R., Photocontrolled degradation of stimuli-responsive poly (ethyl glyoxylate): Differentiating features and traceless ambient depolymerization. *Macromolecules* **2016**, *49*, 7196–7203.
76. Belloncle, B.; Burel, F.; Bunel, C., *Synthesis and Degradation of Poly (ethyl glyoxylate)*. ACS Publications 2009; pp 41–55.
77. Belloncle, B.; Bunel, C.; Menu-Bouaouiche, L.; Lesouhaitier, O.; Burel, F., Study of the degradation of poly (ethyl glyoxylate): Biodegradation, toxicity and ecotoxicity assays. *J. Polym. Environ.* **2012**, *20*, 726–731.
78. Kaitz, J. A.; Diesendruck, C. E.; Moore, J. S., Divergent macrocyclization mechanisms in the cationic initiated polymerization of ethyl glyoxylate. *Macromolecules* **2014**, *47*, 3603–3607.
79. De, S.; Malik, S.; Ghosh, A.; Saha, R.; Saha, B., A review on natural surfactants. *RSC Adv.* **2015**, *5*, 65757–65767.
80. Desai, J. D.; Banat, I. M., Microbial production of surfactants and their commercial potential. *Microbiol. Mol. Biol. Rev.* **1997**, *61*, 47–64.
81. Sachdev, D. P.; Cameotra, S. S., Biosurfactants in agriculture. *Appl. Microbiol. Biotechnol.* **2013**, *97*, 1005–1016.
82. Agredo, P.; Rave, M. C.; Echeverri, J. D.; Romero, D.; Salamanca, C. H., An Evaluation of the Physicochemical Properties of Stabilized Oil-In-Water Emulsions Using Different Cationic Surfactant Blends for Potential Use in the Cosmetic Industry. *Cosmetics* **2019**, *6*, 12.
83. Lawrence, M. J., Surfactant systems: their use in drug delivery. *Chem. Soc. Rev.* **1994**, *23*, 417–424.
84. Singh, P.; Cameotra, S. S., Potential applications of microbial surfactants in biomedical sciences. *Trends Biotechnol.* **2004**, *22*, 142–146.
85. Kralova, I.; Sjöblom, J., Surfactants used in food industry: a review. *J. Dispersion Sci. Technol.* **2009**, *30*, 1363–1383.
86. Banat, I. M., Biosurfactants production and possible uses in microbial enhanced oil recovery and oil pollution remediation: a review. *Bioresour. Technol.* **1995**, *51*, 1–12.

87. Paria, S.; Khilar, K. C., A review on experimental studies of surfactant adsorption at the hydrophilic solid–water interface. *Adv. Colloid Interface Sci.* **2004**, *110*, 75-95.
88. Edmonstone, B.; Craster, R.; Matar, O., Surfactant-induced fingering phenomena beyond the critical micelle concentration. *J. Fluid Mech.* **2006**, *564*, 105.
89. Fuguet, E.; Ràfols, C.; Rosés, M.; Bosch, E., Critical micelle concentration of surfactants in aqueous buffered and unbuffered systems. *Anal. Chim. Acta* **2005**, *548*, 95–100.
90. Shehata, H. A.; Abd El-wahab, A. A.; Hafiz, A.; Aiad, I.; Hegazy, M., Syntheses and characterization of some cationic surfactants. *J. Surfactants Deterg.* **2008**, *11*, 139–144.
91. Holmberg, K., Natural surfactants. *Curr. Opin. Colloid Interface Sci.* **2001**, *6*, 148–159.
92. Amaral, M. H.; das Neves, J.; Oliveira, Â. Z.; Bahia, M. F., Foamability of detergent solutions prepared with different types of surfactants and waters. *J. Surfactants Deterg.* **2008**, *11*, 275–278.
93. Ranjani, I. S.; Ramamurthy, K., Relative assessment of density and stability of foam produced with four synthetic surfactants. *Mater. Struct.* **2010**, *43*, 1317–1325.
94. Wei, X.-f.; Liu, H.-z., Relationship between foaming properties and solution properties of protein/nonionic surfactant mixtures. *J. Surfactants Deterg.* **2000**, *3*, 491–495.
95. Malik, M. A.; Hashim, M. A.; Nabi, F.; Al-Thabaiti, S. A.; Khan, Z., Anti-corrosion ability of surfactants: a review. *Int. J. Electrochem. Sci* **2011**, *6*, 1927–1948.
96. Yokoi, T.; Yoshitake, H.; Tatsumi, T., Synthesis of mesoporous silica by using anionic surfactant. In *Stud. Surf. Sci. Catal.*, Elsevier: 2004; Vol. 154, pp 519–527.
97. Menger, F. M.; Keiper, J. S., Gemini surfactants. *Angew. Chem. Int. Ed.* **2000**, *39*, 1906–1920.
98. Xu, W.; Nikolov, A.; Wasan, D. T.; Gonsalves, A.; Borwankar, R. P., Fat particle structure and stability of food emulsions. *J. Food Sci.* **1998**, *63*, 183–188.
99. Nitschke, M.; Costa, S., Biosurfactants in food industry. *Trends Food Sci. Technol.* **2007**, *18*, 252–259.



100. Sharma, R. K., Surfactants: basics and versatility in food industries. *PharmaTutor* **2014**, *2*, 17–29.
101. Dalgleish, D. G., Food emulsions—their structures and structure-forming properties. *Food hydrocolloids* **2006**, *20*, 415–422.
102. Benichou, A.; Aserin, A.; Garti, N., Double emulsions stabilized with hybrids of natural polymers for entrapment and slow release of active matters. *Adv. Colloid Interface Sci.* **2004**, *108*, 29–41.
103. Tadros, T. F.; Dederen, C.; Taelman, M., A new polymeric emulsifier: An ABA block copolymer surfactant helps make stable water-in-oil emulsions and water-in-oil-in-water multiple emulsions. *Cosmet. Toiletries* **1997**, *112*, 75–86.
104. Yamane, T., Enzyme technology for the lipids industry: an engineering overview. *J. Am. Oil Chem. Soc.* **1987**, *64*, 1657–1662.
105. Brown, M., Biosurfactants for cosmetic applications. *Int. J. Cosmet. Sci.* **1991**, *13*, 61–64.
106. Szűts, A.; Szabó-Révész, P., Sucrose esters as natural surfactants in drug delivery systems—A mini-review. *Int. J. Pharm.* **2012**, *433*, 1–9.
107. Uchegbu, I. F.; Vyas, S. P., Non-ionic surfactant based vesicles (niosomes) in drug delivery. *Int. J. Pharm.* **1998**, *172*, 33–70.
108. Lawrence, M. J., Surfactant systems: microemulsions and vesicles as vehicles for drug delivery. *Eur. J. Drug Metab. Pharmacokinet.* **1994**, *19*, 257–269.
109. Drummond, C. J.; Fong, C., Surfactant self-assembly objects as novel drug delivery vehicles. *Curr. Opin. Colloid Interface Sci.* **1999**, *4*, 449–456.
110. Griffin, W. C., Classification of surface-active agents by "HLB". *J. Soc. Cosmet. Chem.* **1949**, *1*, 311–326.
111. Schramm, L. L., *Emulsions, foams, and suspensions: fundamentals and applications*. John Wiley & Sons. 2006; pp 89–92.
112. Nollet, M.; Boulghobra, H.; Calligaro, E.; Rodier, J. D., An efficient method to determine the Hydrophile-Lipophile Balance of surfactants using the phase inversion temperature deviation of CiEj/n-octane/water emulsions. *Int. J. Cosmet. Sci.* **2019**, *41*, 99–108.

113. Rabaron, A.; Cavé, G.; Puisieux, F.; Seiller, M., Physical methods for measurement of the HLB of ether and ester non-ionic surface-active agents: H-NMR and dielectric constant. *Int. J. Pharm.* **1993**, *99*, 29–36.
114. Griffin, W. C., Calculation of HLB values of non-ionic surfactants. *J. Soc. Cosmet. Chem.* **1954**, *5*, 249–256.
115. Shinoda, K.; Friberg, S., *Emulsions and solubilization*. John Wiley & Sons, New York 1986, pp 174.
116. Rieger, M., *Surfactants in cosmetics*. Routledge: 2017; pp 114–122.
117. Raffa, P.; Wever, D. A. Z.; Picchioni, F.; Broekhuis, A. A., Polymeric surfactants: synthesis, properties, and links to applications. *Chem. Rev.* **2015**, *115*, 8504–8563.
118. Styrkas, D.; Bütün, V.; Lu, J.; Keddie, J.; Armes, S., pH-controlled adsorption of polyelectrolyte diblock copolymers at the solid/liquid interface. *Langmuir* **2000**, *16*, 5980–5986.
119. Sommerdijk, N. A.; Holder, S. J.; Hiorns, R. C.; Jones, R. G.; Nolte, R. J., Self-assembled structures from an amphiphilic multiblock copolymer containing rigid semiconductor segments. *Macromolecules* **2000**, *33*, 8289–8294.
120. Baskar, G.; Landfester, K.; Antonietti, M., Comblike polymers with octadecyl side chain and carboxyl functional sites: scope for efficient use in miniemulsion polymerization. *Macromolecules* **2000**, *33*, 9228–9232.
121. Lewis, R. B.; Corfdir, P.; Li, H.; Herranz, J.; Pfüller, C.; Brandt, O.; Geelhaar, L., Quantum dot self-assembly driven by a surfactant-induced morphological instability. *Phys. Rev. Lett.* **2017**, *119*, 086101.
122. Lee, S. C.; Lee, H. J., pH-Controlled, polymer-mediated assembly of polymer micelle nanoparticles. *Langmuir* **2007**, *23*, 488–495.
123. Bendejacq, D.; Ponsinet, V.; Joanicot, M.; Loo, Y.-L.; Register, R. A., Well-ordered microdomain structures in polydisperse poly (styrene)– poly (acrylic acid) diblock copolymers from controlled radical polymerization. *Macromolecules* **2002**, *35*, 6645–6649.
124. Raffa, P.; Broekhuis, A. A.; Picchioni, F., Polymeric surfactants for enhanced oil recovery: A review. *J. Pet. Sci. Eng.* **2016**, *145*, 723–733.

125. Garnier, S.; Laschewsky, A.; Storsberg, J., Polymeric surfactants: novel agents with exceptional properties. *Tenside, Surfactants, Deterg.* **2006**, *43*, 88–102.
126. Liu, S.; Armes, S. P., Recent advances in the synthesis of polymeric surfactants. *Curr. Opin. Colloid Interface Sci.* **2001**, *6*, 249–256.
127. Torchilin, V. P., Structure and design of polymeric surfactant-based drug delivery systems. *J. Controlled Release* **2001**, *73*, 137–172.
128. Rouzes, C.; Leonard, M.; Durand, A.; Dellacherie, E., Influence of polymeric surfactants on the properties of drug-loaded PLA nanospheres. *Colloids Surf., B* **2003**, *32*, 125–135.
129. Zhou, J.; Wang, L.; Ma, J., Recent research progress in the synthesis and properties of amphiphilic block co-polymers and their applications in emulsion polymerization. *Des. Monomers Polym.* **2009**, *12*, 19–41.
130. Exerowa, D.; Gotchev, G.; Kolarov, T.; Kristov, K.; Levecke, B.; Tadros, T., Oil-in-water emulsion films stabilized by polymeric surfactants based on inulin with different degree of hydrophobic modification. *Colloids Surf., A* **2009**, *334*, 87–91.
131. Baker, M. I.; Walsh, S. P.; Schwartz, Z.; Boyan, B. D., A review of polyvinyl alcohol and its uses in cartilage and orthopedic applications. *J. Biomed. Mater. Res., Part B* **2012**, *100*, 1451–1457.
132. Thong, C.; Teo, D.; Ng, C., Application of polyvinyl alcohol (PVA) in cement-based composite materials: A review of its engineering properties and microstructure behavior. *Constr. Build. Mater.* **2016**, *107*, 172–180.
133. Kumar, A.; Han, S. S., PVA-based hydrogels for tissue engineering: A review. *Int. J. Polym. Mater. Polym. Biomater.* **2017**, *66*, 159–182.
134. Villamagna, I. J.; McRae, D. M.; Borecki, A.; Mei, X.; Lagugn -Labarthe, F.; Beier, F.; Gillies, E. R., GSK3787-Loaded Poly (Ester Amide) Particles for Intra-Articular Drug Delivery. *Polymers* **2020**, *12*, 736.
135. Villamagna, I. J.; Gordon, T. N.; Hurtig, M. B.; Beier, F.; Gillies, E. R., Poly (ester amide) particles for controlled delivery of celecoxib. *J. Biomed. Mater. Res., Part A* **2019**, *107*, 1235–1243.

136. Saadati, R.; Dadashzadeh, S., Marked effects of combined TPGS and PVA emulsifiers in the fabrication of etoposide-loaded PLGA-PEG nanoparticles: in vitro and in vivo evaluation. *Int. J. Pharm.* **2014**, *464*, 135–144.
137. Taylor, P., The effect of an anionic surfactant on the rheology and stability of high volume fraction O/W emulsion stabilized by PVA. *Colloid. Polym. Sci.* **1996**, *274*, 1061–1071.
138. Tadros, T., Polymeric surfactants in disperse systems. *Adv. Colloid Interface Sci.* **2009**, *147*, 281–299.
139. Struijs, J.; Stoltenkamp, J., Testing surfactants for ultimate biodegradability. *Chemosphere* **1994**, *28*, 1503–1523.
140. Scott, M. J.; Jones, M. N., The biodegradation of surfactants in the environment. *Biochim. Biophys. Acta, Biomembr.* **2000**, *1508*, 235–251.
141. Nguyen, P. K.; Snyder, C. G.; Shields, J. D.; Smith, A. W.; Elbert, D. L., Clickable Poly (ethylene glycol)-Microsphere-Based Cell Scaffolds. *Macromol. Chem. Phys.* **2013**, *214*, 948–956.
142. Vogl, O., Addition polymers of aldehydes. *J. Polym. Sci., Part A: Polym. Chem.* **2000**, *38*, 2293–2299.
143. Ma, L.; Baumgartner, R.; Zhang, Y.; Song, Z.; Cai, K.; Cheng, J., UV-responsive degradable polymers derived from 1-(4-aminophenyl) ethane-1, 2-diol. *J. Polym. Sci., Part A: Polym. Chem.* **2015**, *53*, 1161–1168.
144. Fan, B.; Trant, J. F.; Gillies, E. R., End-capping strategies for triggering end-to-end depolymerization of polyglyoxylates. *Macromolecules* **2016**, *49*, 9309–9319.
145. Moustafa, A.; Abd Rabo Moustafa, M. M.; Zilinskas, G. J.; Gillies, E. R., Covalent drug immobilization in poly (ester amide) nanoparticles for controlled release. *Can. J. Chem. Eng.* **2015**, *93*, 2098–2106.
146. Smeraldi, J.; Ganesh, R.; Safarik, J.; Rosso, D., Statistical evaluation of photon count rate data for nanoscale particle measurement in wastewaters. *J. Environ. Monit.* **2012**, *14*, 79–84.
147. Instruments, M., Zetasizer nano series user manual. *MAN0317* **2004**, *1*, 2004.

148. Moncho-Jordá, A.; Martínez-López, F.; Hidalgo-Alvarez, R., The effect of the salt concentration and counterion valence on the aggregation of latex particles at the air/water interface. *J. Colloid Interface Sci.* **2002**, *249*, 405–411.
149. Hawe, A.; Sutter, M.; Jiskoot, W., Extrinsic fluorescent dyes as tools for protein characterization. *Pharm. Res.* **2008**, *25*, 1487–1499.
150. Martínez, V.; Henary, M., Nile red and Nile blue: applications and syntheses of structural analogues. *Chem. - Eur. J.* **2016**, *22*, 13764–13782.
151. Rumin, J.; Bonnefond, H.; Saint-Jean, B.; Rouxel, C.; Sciandra, A.; Bernard, O.; Cadoret, J.-P.; Bougaran, G., The use of fluorescent Nile red and BODIPY for lipid measurement in microalgae. *Biotechnol. Biofuels* **2015**, *8*, 42.
152. Demchenko, A. P., Photobleaching of organic fluorophores: quantitative characterization, mechanisms, protection. *Methods Appl. Fluoresc.* **2020**, *8*, 022001.
153. Tyler, B.; Gullotti, D.; Mangraviti, A.; Utsuki, T.; Brem, H., Polylactic acid (PLA) controlled delivery carriers for biomedical applications. *Adv. Drug Delivery Rev.* **2016**, *107*, 163–175.
154. Rawlings, A.; Lombard, K., A review on the extensive skin benefits of mineral oil. *Int. J. Cosmet. Sci.* **2012**, *34*, 511–518.
155. Xu, Q.; Crossley, A.; Czernuszka, J., Preparation and characterization of negatively charged poly (lactic-co-glycolic acid) microspheres. *J. Pharm. Sci.* **2009**, *98*, 2377–2389.
156. Fan, B.; Gillies, E. R., Poly (ethyl glyoxylate)-poly (ethylene oxide) nanoparticles: Stimuli-responsive drug release via end-to-end polyglyoxylate depolymerization. *Mol. Pharmaceutics* **2017**, *14*, 2548-2559.

## Appendices

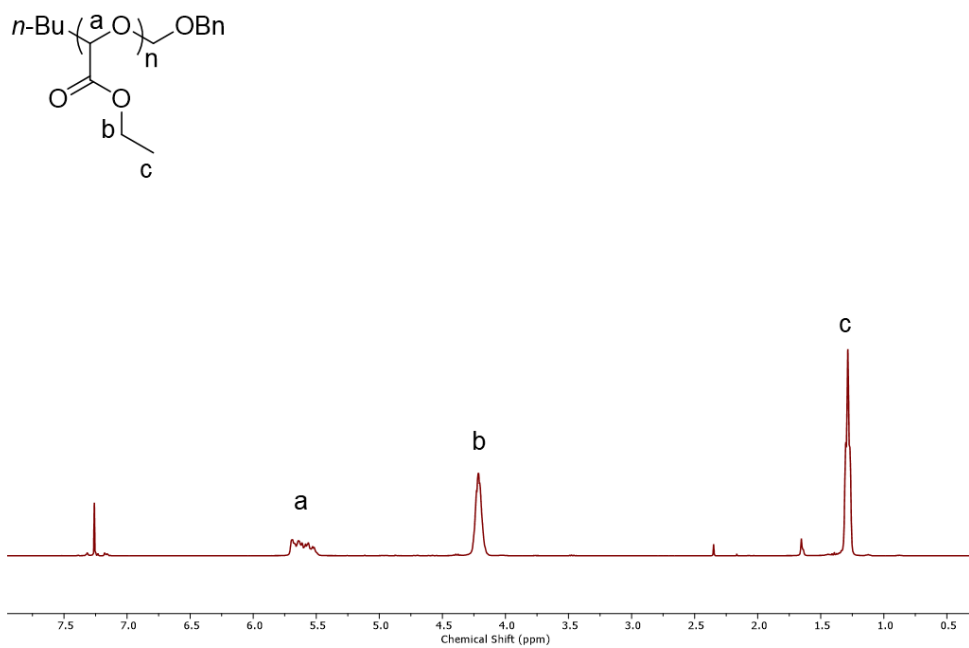


**Figure A1.**  $^1\text{H}$  NMR spectrum of **PEtG<sub>control</sub>** (400 MHz,  $\text{CDCl}_3$ ).

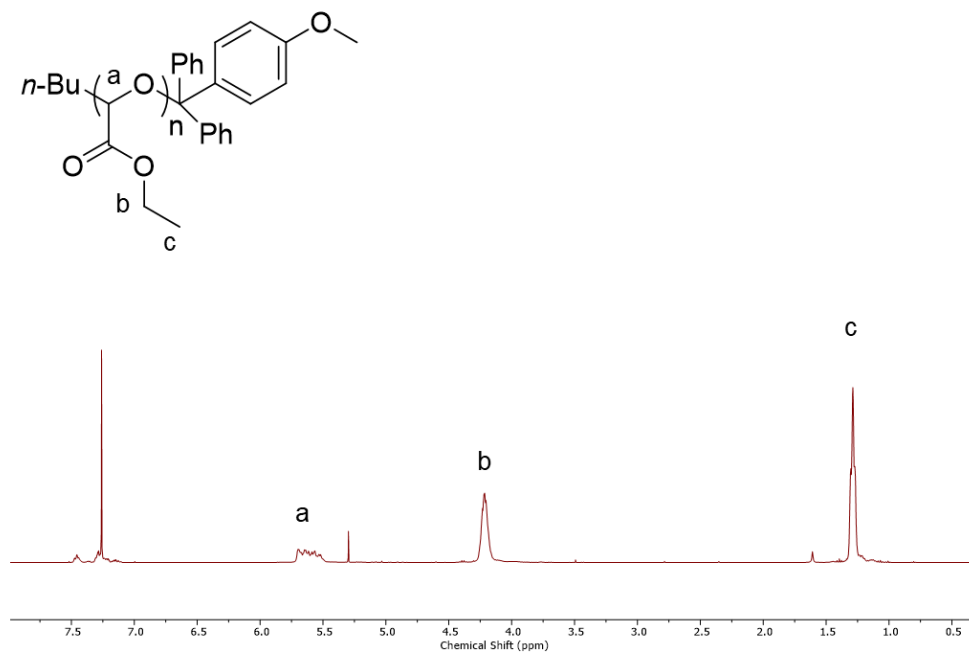


**Figure A2.**  $^1\text{H}$  NMR spectrum of **PEtG<sub>MMT</sub>** (400 MHz,  $\text{CDCl}_3$ ).

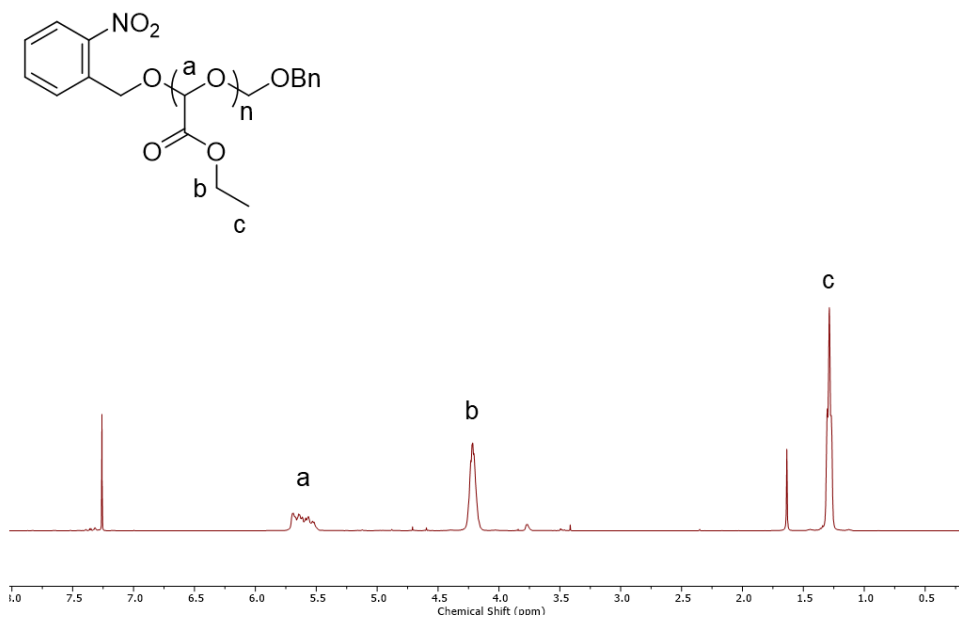


**Figure A3.** <sup>1</sup>H NMR spectrum of **PETG<sub>uv</sub>** (400 MHz, CDCl<sub>3</sub>).

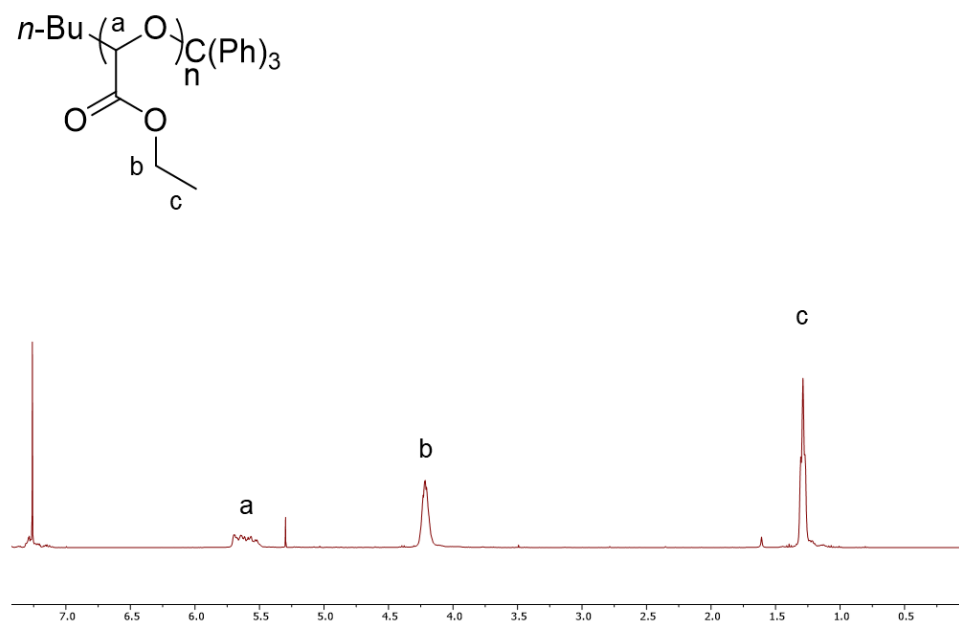


**Figure A4.** <sup>1</sup>H NMR spectrum of **PETG<sub>T</sub>** (400 MHz, CDCl<sub>3</sub>).

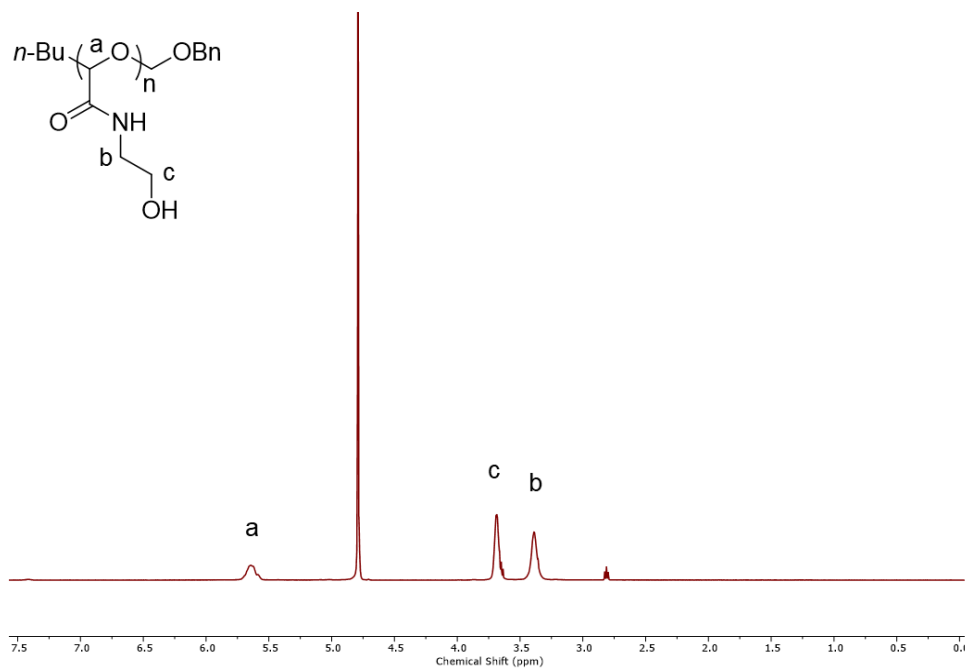


**Figure A5.**  $^1\text{H}$  NMR spectrum of  $\text{PGAm}_{\text{control}}$  (400 MHz,  $\text{D}_2\text{O}$ ).

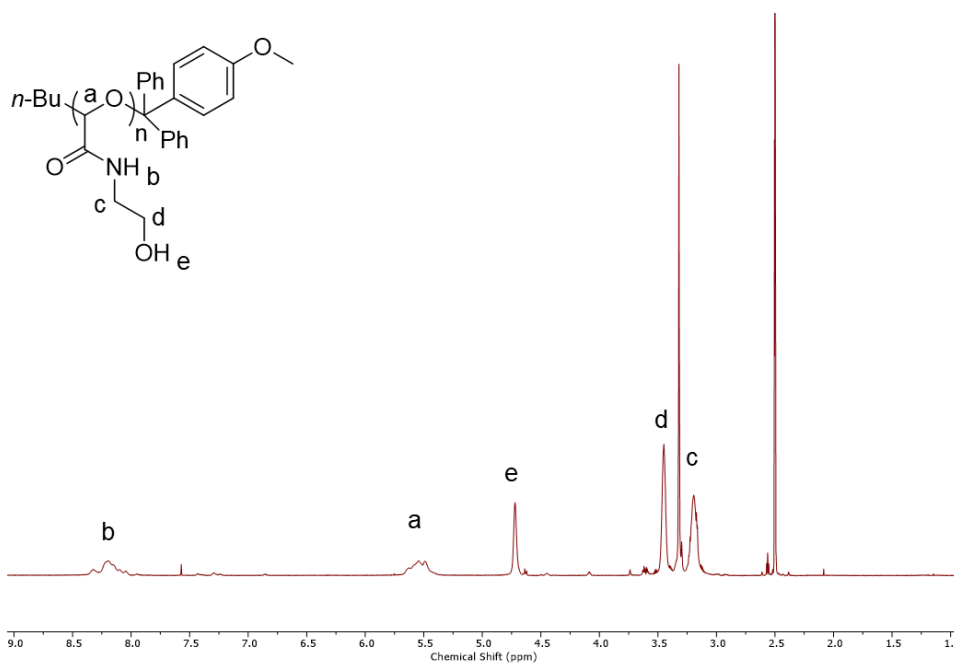


**Figure A6.**  $^1\text{H}$  NMR spectrum of  $\text{PGAm}_{\text{MMT}}$  (400 MHz, DMSO).



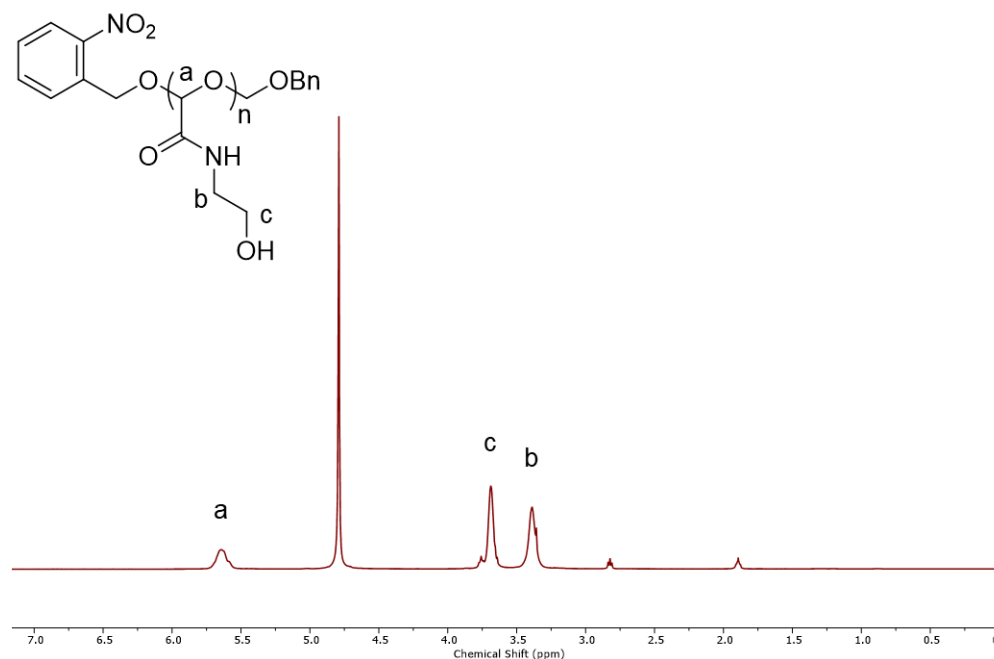


**Figure A7.** <sup>1</sup>H NMR spectrum of **PGAmuv** (400 MHz, D<sub>2</sub>O).

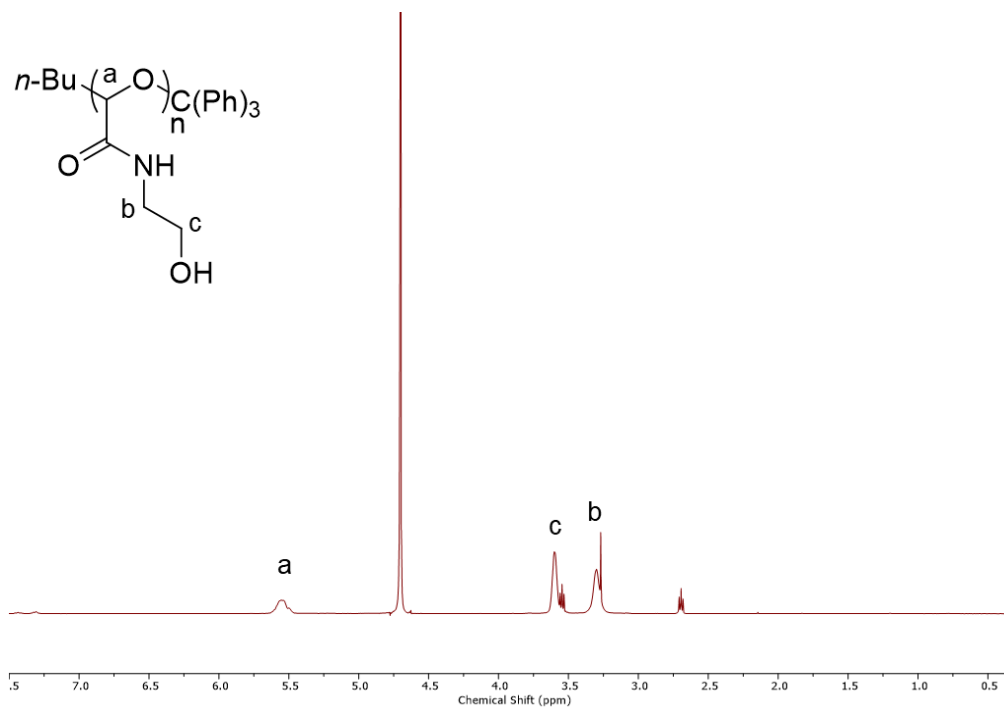


**Figure A8.** <sup>1</sup>H NMR spectrum of **PGAmT** (400 MHz, D<sub>2</sub>O). Extra peaks at 3.3, 2.7, and 3.6 ppm denote residual methanol and ethanolamine signals.

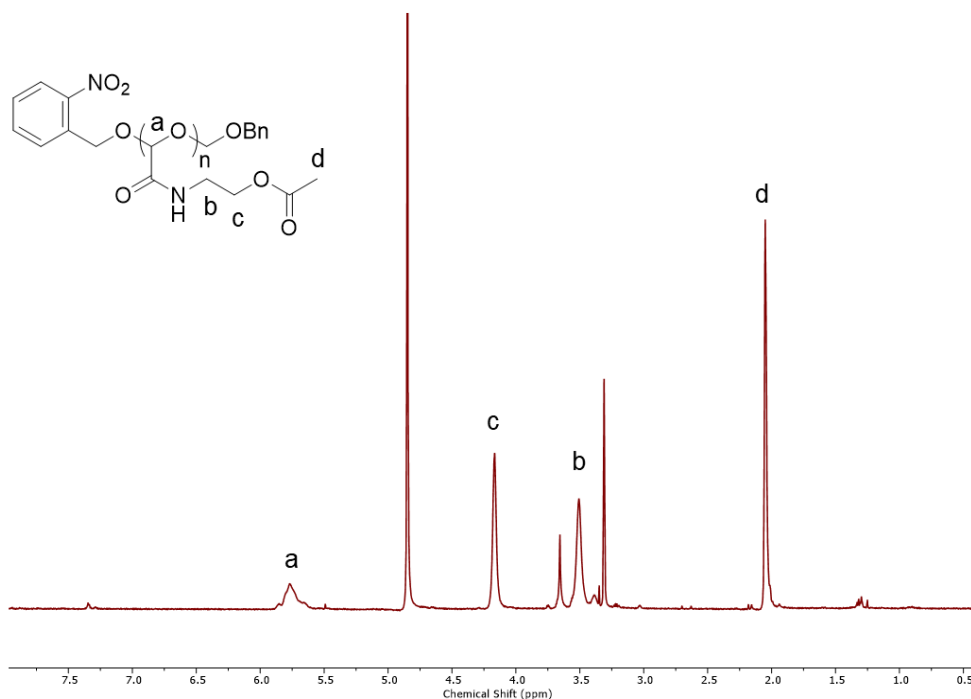


**Figure A9.** <sup>1</sup>H NMR spectrum of **PGAmac-100** (400 MHz, D<sub>2</sub>O). Extra peak at 3.3 ppm denotes residual methanol signal.

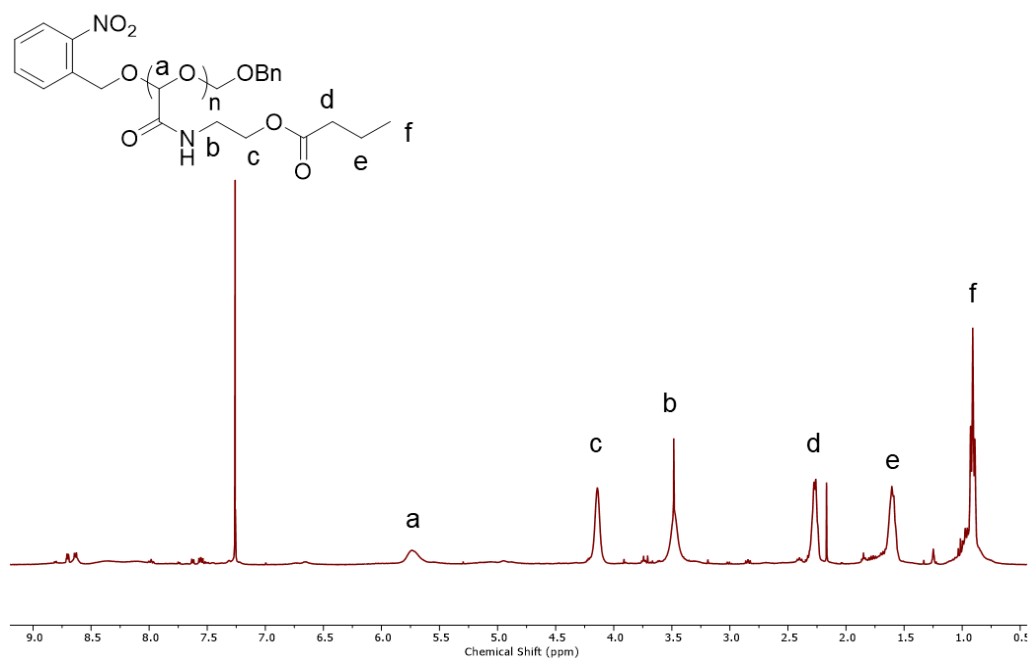


**Figure A10.** <sup>1</sup>H NMR spectrum of **PGAmbuty-100** (400 MHz, D<sub>2</sub>O). Extra peak at 2.2 ppm denotes residual acetone signal.

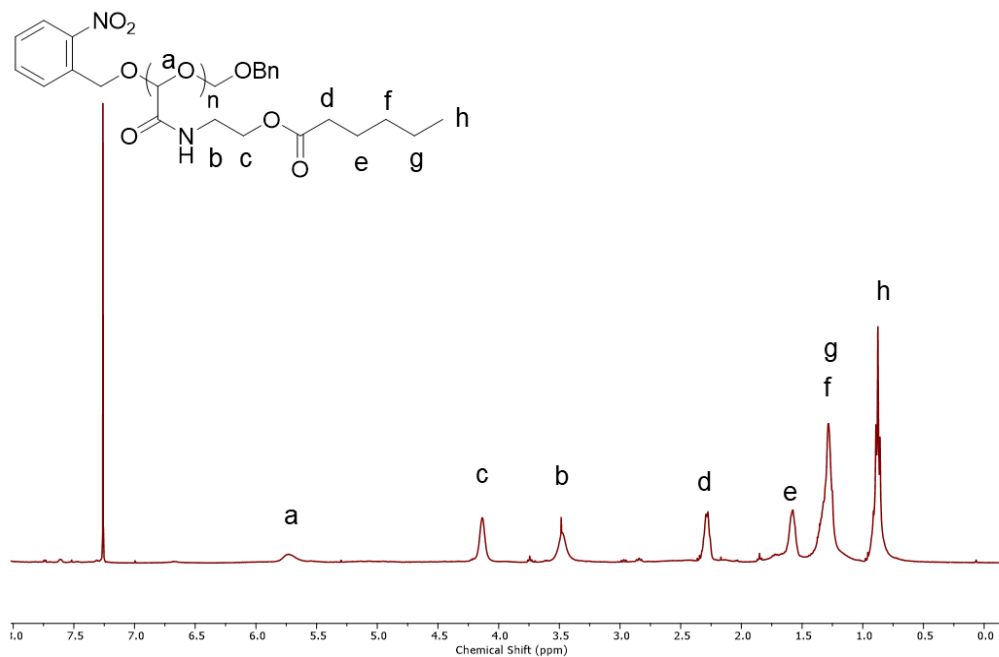


**Figure A11.** <sup>1</sup>H NMR spectrum of PGAm<sub>hex</sub>-100 (400 MHz, D<sub>2</sub>O).

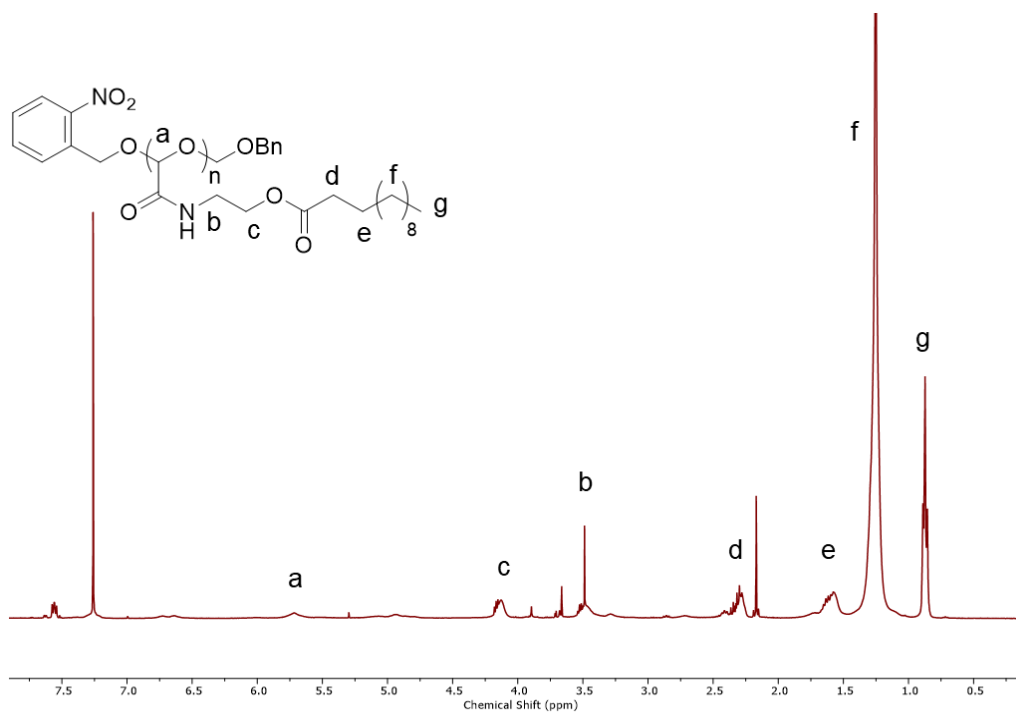


**Figure A12.** <sup>1</sup>H NMR spectrum of PGAm<sub>1au</sub>-100 (400 MHz, D<sub>2</sub>O). Extra peak at 2.2 ppm denotes residual acetone signal.

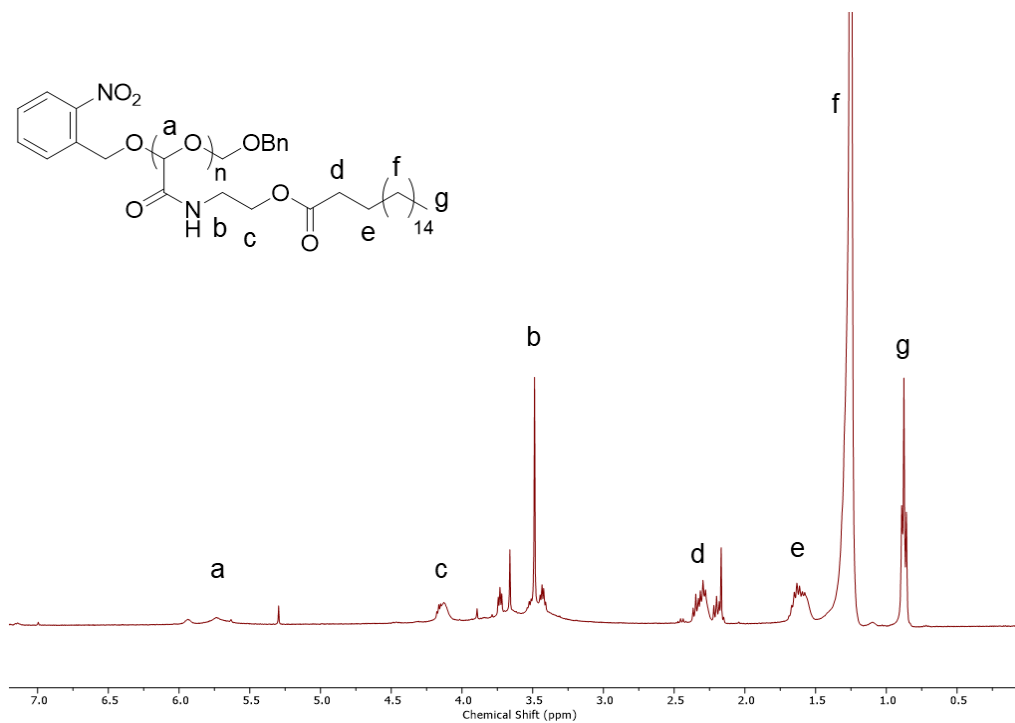


**Figure A13.**  $^1\text{H}$  NMR spectrum of  $\text{PGAm}_{\text{ste-100}}$  (400 MHz,  $\text{D}_2\text{O}$ ).

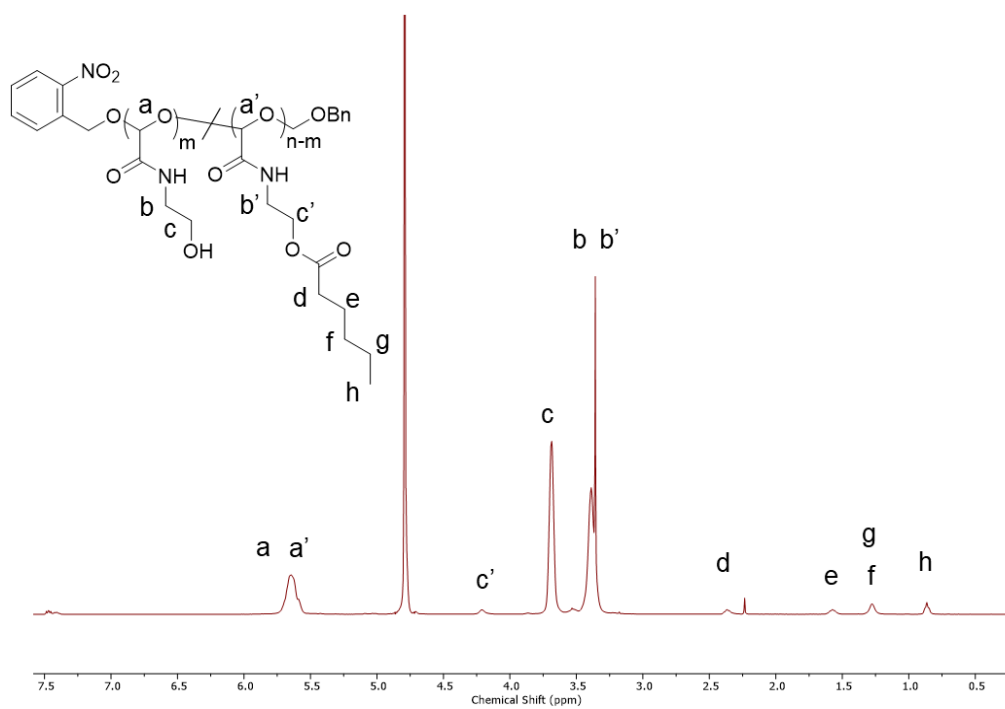


**Figure A14.**  $^1\text{H}$  NMR spectrum of  $\text{PGAm}_{\text{hex-5}}$  (400 MHz,  $\text{D}_2\text{O}$ ). Extra peaks at 2.2 and 3.3 ppm denote residual acetone and methanol signals.

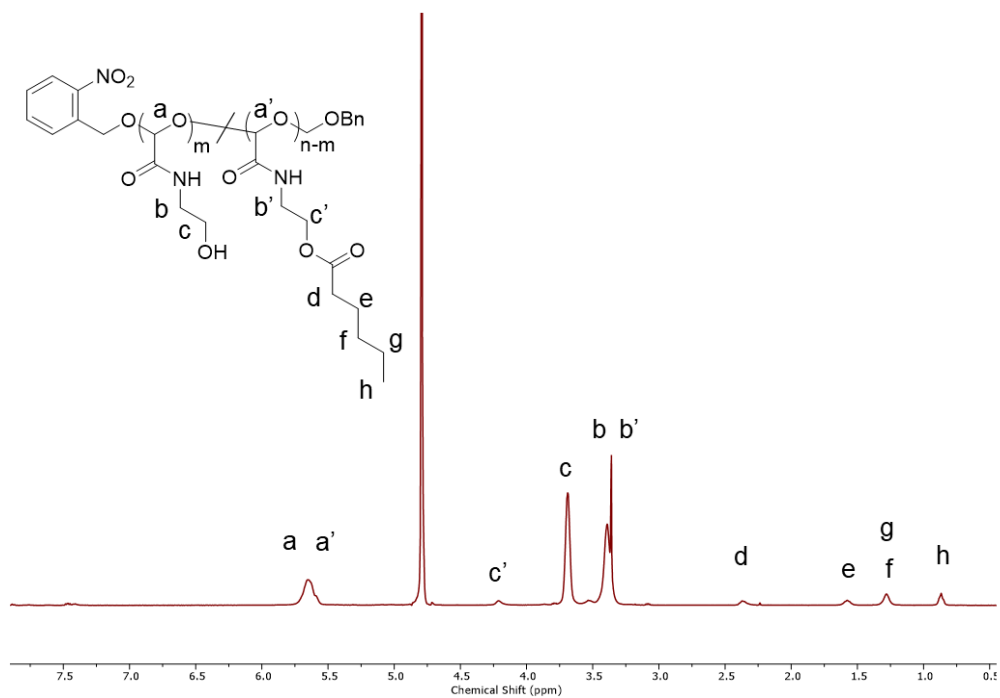


**Figure A15.** <sup>1</sup>H NMR spectrum of PGAm<sub>hex-10</sub> (400 MHz, D<sub>2</sub>O). Extra peak at 3.3 ppm denotes residual methanol signal.

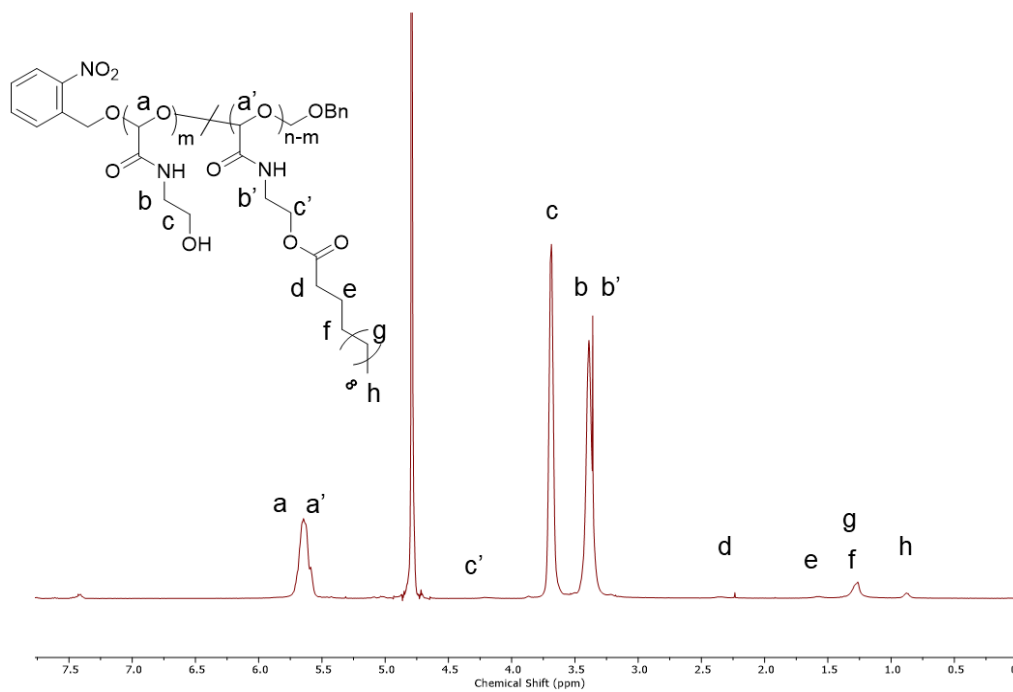


**Figure A16.** <sup>1</sup>H NMR spectrum of PGAm<sub>1au-5</sub> (400 MHz, D<sub>2</sub>O). Extra peak at 3.3 ppm denotes residual methanol signal.

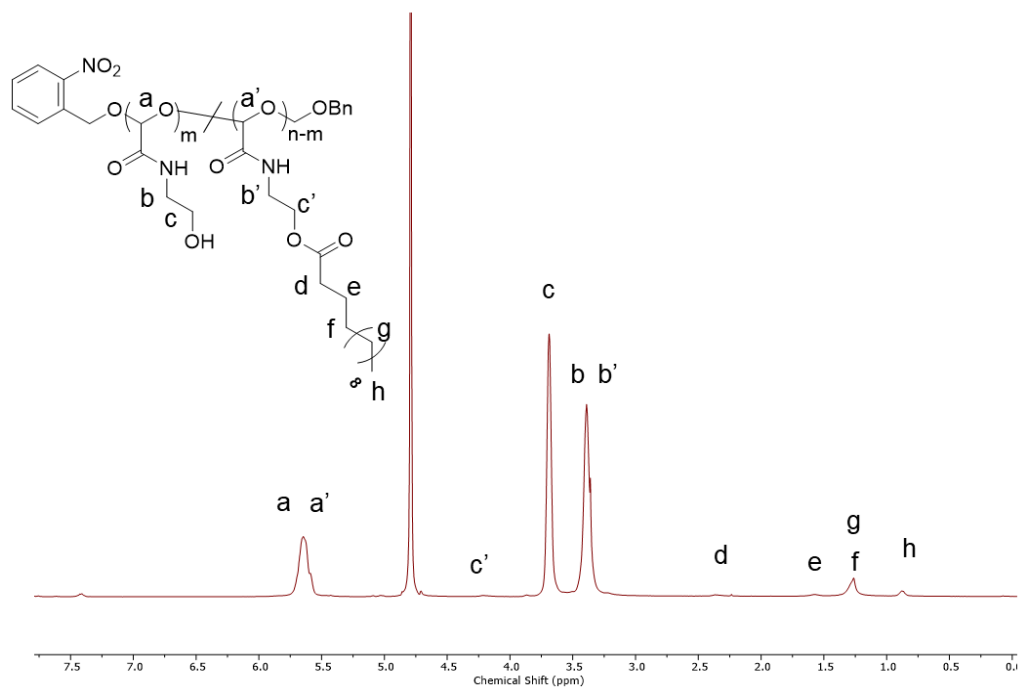


**Figure A17.**  $^1\text{H}$  NMR spectrum of **PGAm<sub>1au-10</sub>** (400 MHz,  $\text{D}_2\text{O}$ ).

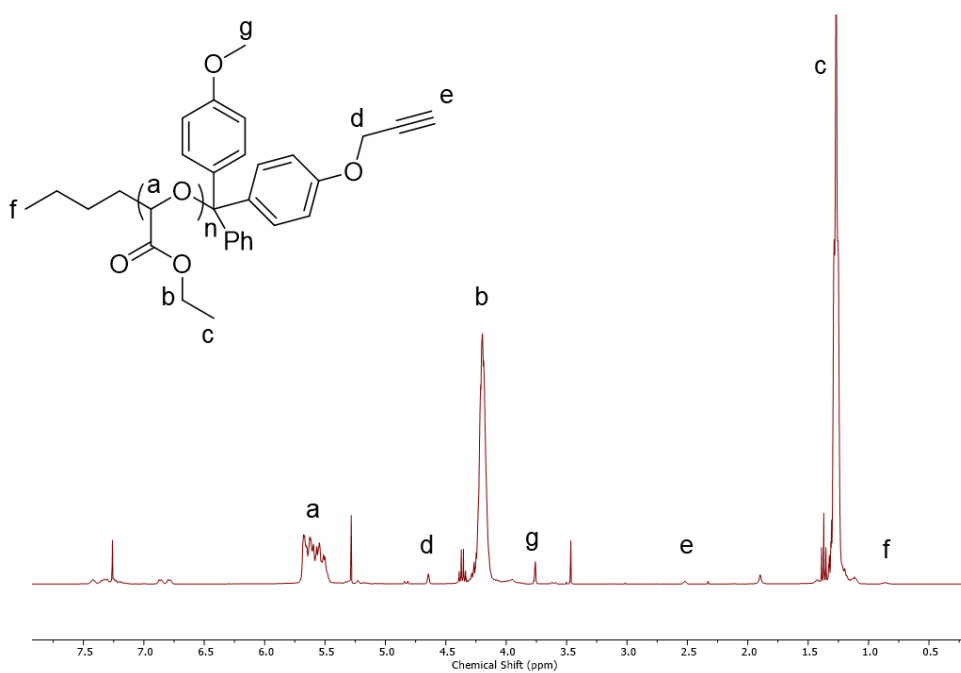


**Figure A18.**  $^1\text{H}$  NMR spectrum of **PEtGAMT** (400 MHz,  $\text{CDCl}_3$ ). Extra peaks at 3.5 and 5.3 ppm denote residual methanol and dichloromethane signals.

## Curriculum Vitae

- Name:** Siamak Keshtpour
- Post-secondary Education and Degrees:** Sharif University of Technology  
Tehran, Iran  
2013-2018 B.Sc. (Chemistry)
- The University of Western Ontario  
London, Ontario, Canada  
2018-2020 M.Sc. (Chemistry)
- Honours and Awards:** Western Graduate Research Scholarship (WGRS)  
2018-2020
- Silver Medal in Iranian National Chemistry Olympiad  
Tehran, Iran  
Sept 2012
- Related Work Experience** Teaching Assistant – 2213b and 2223b  
The University of Western Ontario  
2018-2020
- Conferences:**
1. **S. Keshtpour**, Q. E. A. Sirianni, E. R. Gillies “Self-immolative Polymers as a Degradable and Triggerable Class of Surfactants.” Accepted for an oral presentation at the 103<sup>rd</sup> Canadian Chemistry Conference and Exhibition, Winnipeg, MB, May 2020 (the conference was cancelled due to Covid-19).